Summer 9-1-2014

Regulation and inhibition of pro-tumorigenic microenvironments

Elise Oster Alspach
Washington University in St. Louis

WASHINGTON UNIVERSITY IN ST. LOUIS

Division of Biology and Biomedical Sciences

Molecular Genetics and Genomics

Dissertation Examination Committee

Sheila A. Stewart, Chairperson
Nicholas Davidson
Fanxin Long
Joshua Rubin
Michael Tomasson
Jason Weber

Regulation and Inhibition of Pro-Tumorigenic Microenvironments

by

Elise Julia Oster Alspach

A dissertation presented to the
Graduate School of Arts & Sciences
of Washington University in
partial fulfillment of the
requirements for the degree
of Doctor of Philosophy

August 2014

St. Louis, Missouri

TABLE OF CONTENTS

LIST OF FIGURES

CHAPTER 1: INTRODUCTION AND SIGNIFICANCE

CHAPTER 2: CHROMATIN REMODELING UNDERLIES THE SENESCENCE-ASSOCIATED SECRETORY PHENOTYPE OF TUMOR STROMAL FIBROBLASTS THAT SUPPORTS CANCER PROGRESSION

CHAPTER 3: THE TRANSCRIPTON FACTOR C-MYB IS A NOVEL REGULATOR OR SASP EXPRESSION

CHAPTER 4: P38MAPK PLAYS A CRUCIAL ROLE IN STROMAL MEDIATED TUMORIGENESIS

APPENDIX 1: THE SMALL HEAT SHOCK PROTEIN HSP27 REGULATES SASP mRNA STABILITY

ACKNOWLEDGMENTS

My rotation with the Stewart laboratory was my first, and I knew almost instantly that I had found my home within the Washington University community. I looked at the senior graduate students that were part of the Stewart laboratory and felt that they represented what I wanted to become: a strong, independent scientist adept at critical thinking and problem solving. I figured that the best way to become that kind of scientist was to do my training in the environment that produced people with those qualities. Through Sheila Stewart's mentorship, I feel that I have indeed achieved what I set out to do, but I've also achieved so much more than I thought I was capable of. I thank Sheila for challenging me to become better than I thought I could be.

I thank the NIH Cellular Biochemical and Molecular Sciences Pre-doctoral Training Grant (T32 GM007067) for funding my work.

I have had the absolute pleasure of working with an amazing group of people. I thank Julien Duxin for guiding me through my rotation, and being the personification of determination and perseverance. I thank Mira Pazolli for being such a wonderful and encouraging mentor, both during and after her time in the Stewart laboratory. Daniel Teasley has been a constant sounding board for both scientific ideas and venting about the trials and tribulations of graduate school. I thank Megan Ruhland and Hayley Moore for being my partners in crime, and providing endless comedic relief during some of my most trying times. Kevin Flanagan has been an amazing source of assistance and support as we have struggled and triumphed together to figure out c-myb. Finally, I thank Shankar Parajuli and Bhavna Murali for providing fresh sets of eyes at the end of my graduate work.

Not only did I get a Ph.D. in St. Louis, I met my husband. Jake never gave up on the idea of me graduating even during the times when I had. I would not have been able to make it through this without his endless love and support. This thesis is just as much his as it is mine. Along with Jake came the most supportive group of in-laws that anyone could hope for: Scott, Sue and Lauren. I thank you all for accepting me in to your family, and supporting Jake and me through this graduate school process. We definitely could not have done it without you.

Finally, I thank my family. My twin sister Jennifer has been my constant source of encouragement. My parents, Phil and Julie, while unable to be with me in person, have been with me in spirit through it all. My father taught me the importance of having a job that you truly love. And my mother, a victim of lung cancer, has made me aware of how truly appreciated every small step toward a cure is. They are my source of inspiration, and who drove me to keep pushing.

I dedicate my thesis work to the memory of my parents, Phillip and Julia Oster, who have been with me throughout this entire journey

ABSTRACT OF THE DISSERTATION

Regulation and Inhibition of Pro-Tumorigenic Microenvironments

by

Elise Julia Oster Alspach

Doctor of Philosophy in Biology and Biomedical Sciences

(Molecular Genetics and Genomics)

Washington University in St. Louis, 2014

Dr. Sheila A. Stewart, Chairperson

Age is the number one risk factor for the development of cancer. While accumulation of epithelial cell mutations is a driving factor for this risk, the role that the tumor microenvironment plays in this process is now well established. Indeed, seminal work has shown that tumorigenic cells unable to grow in xenografts can form tumors when supportive stromal cells are present. Work by many laboratories has demonstrated that a wide variety of cells including endothelial cells, immune cells, the extracellular matrix and fibroblasts can all assume a pro-tumorigenic phenotype.

Like cancer-associated fibroblasts (CAFs), senescent cells promote all stages of tumor development and progression. We and others have demonstrated that senescent fibroblasts have an altered expression profile known as the senescence-associated secretory phenotype (SASP). The SASP is composed of pro-angiogenic, pro-inflammatory, pro-growth and extracellular matrix remodeling proteins. Through the

SASP, senescent cells promote all stages of tumorigenesis. Interestingly, senescent fibroblasts accumulate in human tissues with age, making them potential players in increasing cancer incidences.

Given the profound impact the SASP has on nearly every step in the tumorigenic process I investigated how it is regulated. Furthermore, identification of SASP regulatory pathways will identify targets for anti-cancer therapies aimed at inhibiting the pro-tumorigenic microenvironment. I have investigated the regulation of the SASP on several different levels. My work has uncovered a novel transcriptional regulator of SASP factor expression, c-myb. I have also identified a post-transcriptional regulatory network composed of p38MAPK and the RNA-binding protein AUF1, which regulates SASP mRNA stability and sustains SASP expression after the induction of senescence. Finally, I have demonstrated that p38MAPK is a viable stromal-specific therapeutic target for the inhibition of tumor-promoting microenvironments in general, not just those containing senescent fibroblasts. Indeed, cancer-associated fibroblasts (CAFs), which promote tumor growth through an altered gene expression profile similar to the SASP, are dependent upon p38MAPK activity. Inactivation of p38MAPK using an orally administered small molecule inhibitor results in significant blunting of both senescent fibroblast-driven and CAF-driven epithelial cell growth.

CHAPTER 1

INTRODUCTION AND SIGNIFICANCE

Portions of this chapter were published in 2013 in *Critical Reviews in Oncogenesis* 18(6): 549-58

Tumors as organs: the importance of the tumor microenvironment

The different cellular compartments that comprise normal tissues are constantly in communication with one another. The same is true for cancerous lesions, where the surrounding normal tissue (the microenvironment) plays a role in cancer progression. The first indication of the importance of the microenvironment to tumor development came from the observation that tumors in a xenograft setting could not grow in the absence of cancer-derived stromal tissue (1, 2).

Different cell types within the microenvironment as well as the extra cellular matrix can influence every step of tumorigenesis. Cancer cells promote the growth and generation of new blood vessels (3-5), a process known as angiogenesis, which provides the growing tumor with oxygen and nutrients from circulating blood. The extracellular matrix provides migrating cancer cells with structure upon which to migrate. Furthermore, cancer cells activate proteases embedded in the extracellular matrix, which enables the remodeling of the extracellular matrix to aid in cancer cell invasion (6). Immune cells infiltrating into the tumor microenvironment create chronic inflammation, which correlates with increased cancer risk in a wide variety of tissues including the stomach and intestines (7, 8). Indeed, the role of the immune system in tumorigenesis is the topic of much investigation in recent years. It has been shown that tumors can reprogram anti-tumorigenic infiltrating immune cells to pro-tumorigenic immune cells capable of inhibiting antitumor immunity and facilitating the escape of tumor detection by the immune system (9). Finally, stromal fibroblasts promote the growth of epithelial cells by

secreting factors that promote extracellular matrix remodeling, angiogenesis and reprogramming of the immune system (1, 10, 11). The role of stromal fibroblasts in tumorigenesis and how these cells promote all aspects of cancer growth and development will be discussed in detail in the following sections.

Stromal fibroblasts in tumorigenesis: two flavors with similar functions

Senescent fibroblasts increase the risk for cancer with age

Age is the number one risk factor for the development of cancer (12). While traditionally this has been thought to occur because of the accumulation of mutations within the epithelial compartment, age-related changes in the microenvironment are now considered a contributor to this age-related risk factor.

Specifically, the presence of senescent fibroblasts in the stroma is hypothesized to drive changes in the microenvironment that enable the growth and progression of cancer lesions.

A primer on cellular senescence

Cellular senescence was first described *in vitro* with the observation that primary cells have a finite replicative lifespan. When cells reach the end of their replicative lifespan they are unable to reenter the cell cycle, yet remain metabolically active (13). Investigation into the mechanisms governing this finite replicative lifespan revealed that telomeres, the nucleo-protein structures located at the ends of the chromosomes, controlled replicative lifespan.

Senescent fibroblasts have several characteristics that distinguish them from actively dividing and quiescent cells (**Fig 1.1**). Growth arrest is the most readily observed characteristic of senescent cells. Senescent cells typically arrest with a G_1 DNA content (14) and display an enlarged and flattened morphology. The growth arrest is permanent and senescent cells do not respond to strong mitogenic stimuli (15). Growth arrest in senescent cells is mediated through activation of the senescence effector proteins Rb and p53 and results in the upregulation of cell-cycle inhibitors, including p21 and p16 (16-18). In contrast to quiescent cells, senescent cells are generally resistant to apoptosis (19).

As alluded to earlier, senescence was originally characterized as being mediated by telomere dysfunction. In addition to this telomere dysfunction, it is now well accepted that senescence can be induced by a wide variety of stimuli. Oxidative stress that arises from mitochondrial dysfunction and subsequent accumulation of reactive oxygen species (ROS) induces cellular senescence (20, 21). Overexpression of oncogenes can also result in cellular senescence due to persistent DNA damage caused by over replication of the genome and uncontrolled cellular division (22, 23). Other forms of DNA damage, including those induced by chemotherapy drugs (24-26) and irradiation (27) also result in cellular senescence. Indeed, persistent DNA damage is a reoccurring theme in senescence-inducing stimuli, and one marker of senescent cells is the appearance of large, unresolved DNA-damage foci (28). Interestingly, several groups have recently shown that these persistent damage foci are localized to telomeres,

regardless of whether the senescence-inducing stimulus was specific to telomeres or affected the whole genome (29, 30). How these foci form and what function they play in the maintenance of the senescent phenotype is unclear.

Senescent cells accumulate in tissues with age

The accumulation of senescent cells within tissues is hypothesized to contribute to age-related diseases and degeneration, possibly through the depletion of stem cell populations or through alterations of the tissue architecture through an altered secretory profile. The putative importance of these cells in the degeneration of tissue was shown when they were selectively removed from mice. Indeed, removal of senescent cells in these mouse models abrogated the development of a wide variety of age-related phenotypes, including sarcopenia and loss of adipose tissue (31). The presence of senescent cells in human tissues has been documented in a variety of human tissues including kidney, prostate, skin, and liver (32-37). Evidence that senescent cells accumulate in tissues with age comes from observational studies of primate and human tissue. Indeed, skin biopsies from human donors revealed that in the skin dermal layer, very few senescent fibroblasts (identified by senescence-associated β-galactosidase staining) are present in donors under the age of 40, while readily detectable senescent fibroblasts were identified in donors over age 60 (32). Perhaps the most stunning data was derived from baboons where senescent cells were found to increase over the life span of individual animals (38). Together these data clearly demonstrated an age

related increase in senescent cells in primates and humans and suggests that they contribute to a wide variety of pathologies.

Senescent cells promote tumorigenesis through the senescence-associated secretory phenotype

The description of a limited replicative lifespan in the 1960's provided the basis for the hypothesis that senescence was a potent tumor suppressive mechanism (13). The argument that was proposed was that because cancer cells were immortal, senescence represented a hurdle that would need to be overcome if an incipient tumor cell was going to progress to a fully neoplastic cell. This original hypothesis was validated decades later by investigators examining human tissues and animal models. Indeed, senescent cells were found in premalignant melanocytic naevi in humans that arose as a result of a mutation in the BRAF gene ($BRAF^{E600}$) that created a constitutively active protein (39). Importantly, progression to neoplastic disease was associated with loss of senescent cells. In addition, senescent cells were found in a mouse prostate model. In this model, analysis of premalignant lesions of the prostate generated by loss of the tumor suppressor *Pten* (40) demonstrated that the lesions harbored senescent cells. Importantly, senescent cells were lost upon progression to malignancy (40, 41). Furthermore, inactivation of senescence-inducing pathways, either through inactivation of p53 or through inactivation of the DNA damage response (a critical driver of senescence induction) in the *Pten* model as well as others, results in a more rapid progression from premalignancy to malignancy and larger tumor size (40, 41). Finally,

restoration of p53 activity in sarcomas results in senescence induction and regression of the tumor (42).

In contrast to the tumor-inhibiting effects that senescence mediates in transformed cells, senescence of normal cells in the surrounding microenvironment is tumor-promoting. Senescent human prostate fibroblasts stimulate the growth of epithelial cells harboring mutations that create preneoplastic cells in co-culture experiments while they have no effect on normal checkpoint competent cells (43). Furthermore, senescent human lung fibroblasts stimulate preneoplastic epithelial cell growth in xenograft experiments in both the mammary fat pad and subcutaneous skin (44). Senescent fibroblasts also promote epithelial-to-mesenchymal transition and invasion in preneoplastic breast cells (45), indicating the ability of senescent fibroblasts to promote not only the growth of pre-neoplastic cells, but also the progression from pre-cancerous to cancerous lesions. Thus, it is important to place senescence into the tissue context where it arises. When senescence arises in an incipient tumor cell that has begun its journey toward neoplasia, it is a potent tumor suppressor mechanism. However, when senescence occurs in surrounding cells it can stimulate tumorigenesis (**Fig 1.2**).

How do senescent cells within the microenvironment promote tumorigenesis? Work from Campisi and colleagues demonstrated that senescent cells promote tumorigenesis through the upregulation and secretion of a wide variety of pro-tumorigenic proteins into the microenvironment ((44) (reviewed in (46)). These proteins are collectively referred

to as the senescence-associated secretory phenotype (SASP) (24). SASP is enriched in proteins involved in inflammation (e.g. interleukins, cytokines and chemokines), alteration of the extracellular matrix (e.g. matrix metalloproteinases), and cell division (e.g. growth factors) (24, 43, 47).

The SASP's pro-tumorigenic nature has been demonstrated extensively both *in vitro* and *in vivo*. Senescent fibroblasts stimulate the invasiveness of human umbilical vascular endothelial cells (HUVECs) *in vitro* and increase vascularization of tumors in xenograft experiments through secretion of vascular endothelial growth factor (VEGF) (48). Osteopontin (OPN) expression level is elevated in senescent fibroblasts and is necessary for the stimulation of pre-neoplastic cell growth induced by senescent fibroblasts *in vivo* (47). Down-regulation of OPN in senescent mammary fibroblasts also inhibits the invasion and migration of associated epithelial cells *in vitro* (49). Interleukins IL6 and IL8 promote breast cancer epithelial cell growth. Indeed, treatment of co-cultures of senescent cells and preneoplastic epithelial cells with neutralizing antibodies against IL6 and IL8 results in decreased growth-promotion (24). Furthermore, treatment of breast cancer epithelial cells with recombinant IL6 and IL8 is sufficient to promote growth (24). Finally, matrix metalloproteinase 3 (MMP3) from senescent cells promotes branching and proliferation of breast epithelial cell organoids as well as the growth of breast cancer epithelial cells in xenograft experiments (45, 50). These results demonstrate that senescent cells promote the establishment of primary tumors through the expression of SASP factors.

In addition to promoting primary tumors, senescent cells have been hypothesized to promote later stages of tumor progression through expression of SASP. Indeed, senescent cells can promote epithelial-to-mesenchymal transition (EMT) (24), a crucial step in tumor cell metastasis. It has been shown that treatment of human breast cancer cell lines with conditioned medium from senescent fibroblasts resulted in decreased expression of cytokeratin and E-cadherin, hallmarks of EMT (24). This promotion of EMT by senescent cells was mediated by MMP3 (45). Recent work has also focused on identifying and elucidating the mechanisms that drive the emergence of cancer initiating cells or cancer stem cells (CSC), which appear to be responsible for forming distant metastasis (51). While the identification of surface markers that precisely define CSCs has remained elusive, emerging data suggests that the tumor microenvironment can influence their prevalence (52, 53). Intriguingly, chemokines secreted by senescent cells select for CSCs (52). IL6, one of the most highly expressed SASP factors, can play an important role in regulating breast CSC self-renewal (54).

Cancer cells activate cancer-associated fibroblasts to aid in tumor progression

In addition to fibroblast senescence, non-senescent fibroblasts also promote the growth and progression of tumor cells. The presence of these “activated”, cancer-associated fibroblasts or CAFs was first made in the 1990’s. Indeed, genetically normal fibroblasts isolated from prostate lesions promote preneoplastic prostate epithelial cell growth and invasive characteristics both in co-culture and in *in vivo* settings (1). CAFs have been

shown to be instrumental in other tissues as well, including breast and endometrial cancers.

Unlike senescent fibroblasts, which accumulate in the microenvironment through cell-intrinsic processes, CAFs are generated by the tumor through paracrine signaling (**Fig 1.2**). Work to elucidate that factors secreted by cancer cells to activate CAFs uncovered transforming growth factor β (TGFβ) as a primary player. For example, co-cultures of pancreas carcinoma cells made to over express TGFβ and fibroblasts resulted in increased growth and increased expression of growth factors and matrix proteins in the fibroblasts (55). Furthermore, activation of an inducible TGFβ in a mouse skin papilloma model resulted in increased expression of MMP2 and MMP9 within the tumor stroma (56). More recent work has implicated granulin from cancer cells in the activation of CAFs. Indeed, treatment of breast fibroblasts with granulin resulted in upregulation of many inflammatory cytokines including IL6, IL8, CXCLs and CCLs (57). These granulin-treated fibroblasts were capable of promoting breast cancer cell growth in a xenograft model (57).

Like senescent fibroblasts, CAFs promote tumorigenesis through an altered gene expression profile, which is very reminiscent of the SASP (**Fig 1.2**). Indeed, cancer-associated stromal cells isolated by laser-capture micro-dissection and subjected to microarray analysis revealed an expression profile enriched in many SASP factors, including IL6, IL8, CXCLs and MMPs (58-60). The important role that the factors

secreted by CAFs play in tumorigenesis has been demonstrated experimentally. For example, inhibition of CAF-secreted CXCL12 prevented CAF-driven growth of breast epithelial cells (10). The similarities between the expression profiles of senescent fibroblasts and CAFs raises the intriguing question of whether the regulatory mechanisms elucidated for these shared factors in one pro-tumorigenic cell type could be applicable in the other. If true, the therapeutic targets identified for one tumor-promoting fibroblast could be applicable to a wide variety of tumor-promoting stroma. Furthermore, I suggest that SASP expression is a trait of tumor-promoting microenvironments in general, and is not restricted to cells that have undergone senescence.

SASP expression is subject to complex regulation

In an attempt to identify potential therapeutic targets for the inhibition of pro-tumorigenic microenvironments, many laboratories have worked at elucidating how the SASP is initiated and maintained. As discussed previously, persistent activation of the DNA-damage response is an important inducer of senescence, and ATM activity is required for expression of a wide variety of SASP factors (61). Indeed, shRNA directed depletion of ATM from cells inhibits expression of the vast majority of SASP factors in senescent cells (61). However, not all SASP factors are dependent on ATM for their expression; ATM-dependency is predominantly a characteristic of the inflammatory SASP factors (61). The SASP is also transcriptionally regulated by NFκB and C/EBPβ (62-64). Interestingly, NFκB activity in senescent cells is decreased in response to ATM

depletion, suggesting that ATM and NFκB function within the same signaling pathway (62). Similar to ATM depletion, inhibition of NFκB or C/EBPβ results in an inability of senescent cells to activate a subset of SASP factors (62, 64).

In addition to DNA-damage response signaling, mitogen-activated protein kinase (MAPK) signaling is also an important regulator of SASP factor activation (62). p38MAPK inhibition, either through expression of shRNA directed at p38MAPKα or through treatment with small molecule inhibitors of p38MAPK, results in decreased expression of SASP in response to senescence (62). Similar to the effects of ATM depletion, inhibition of p38MAPK activity reduces the activity of NFκB (62). Furthermore, constitutive activation of the p38MAPK-signaling pathway results in SASP activation even in the absence of ATM. ATM, however, is not required for p38MAPK activation in response to senescence, suggesting that p38MAPK and ATM function in parallel pathways, both of which end in NFκB activation and SASP factor expression (62). As with ATM and NFκB, p38MAPK is predominantly involved in the activation of the inflammatory SASP components. How p38MAPK is activated in response to senescence is not understood, but the slow kinetics of its activation suggests a non-canonical mechanism. As indicated previously, many of the SASP regulatory pathways elucidated thus far do not control the expression of all SASP factors, and p38MAPK is no exception. There remains much to be uncovered regarding the regulation of non-inflammatory SASP factors. Furthermore, no central SASP regulator capable of

coordinating upregulation of this diverse array of pro-tumorigenic factors has been identified.

Finally, it is important to note that SASP does not require activation of senescence for expression. Cells defective in the p53 and pRb pathways, both central regulators of the senescent phenotype, either singularly or in combination retain the ability to express SASP factors in response to stress and persistent DNA damage signaling (24, 65). This uncoupling of SASP expression and the senescent phenotype is further demonstrated by cells induced to senesce through over-expression of the cell cycle inhibitors p16 and p21 (66). Senescence induced by ectopic expression of p16 or p21 fails to activate the SASP despite these cells displaying the hallmark cell cycle arrest and cellular morphologies of senescence (66). Thus, senescence represents merely one way to achieve expression of SASP factors. This concept parallels closely with our suggestion that SASP is a characteristic of tumor-promoting stromal cells in general regardless of whether they are senescent. Therefore, further characterization of SASP regulatory pathways in senescent cells and CAFs is critical to our understanding of these mechanisms and to future therapeutic approaches. Indeed, NFκB, a central transcriptional regulator of SASP expression in senescent cells, is also the mediator of expression of pro-inflammatory factors expressed by CAFs (67). This observation suggests that therapeutic targets identified in SASP factor expression will be applicable to wide variety of cancer-promoting microenvironments.

My thesis work has focused on further elucidating unique SASP regulatory mechanisms. I have investigated SASP regulation at multiple levels including chromatin-based regulation, transcription and post-transcriptional stabilization of SASP mRNA. My work has uncovered a central role for p38MAPK in SASP factor regulation in not only senescent fibroblasts but also in the tumor-promoting activity of CAFs.

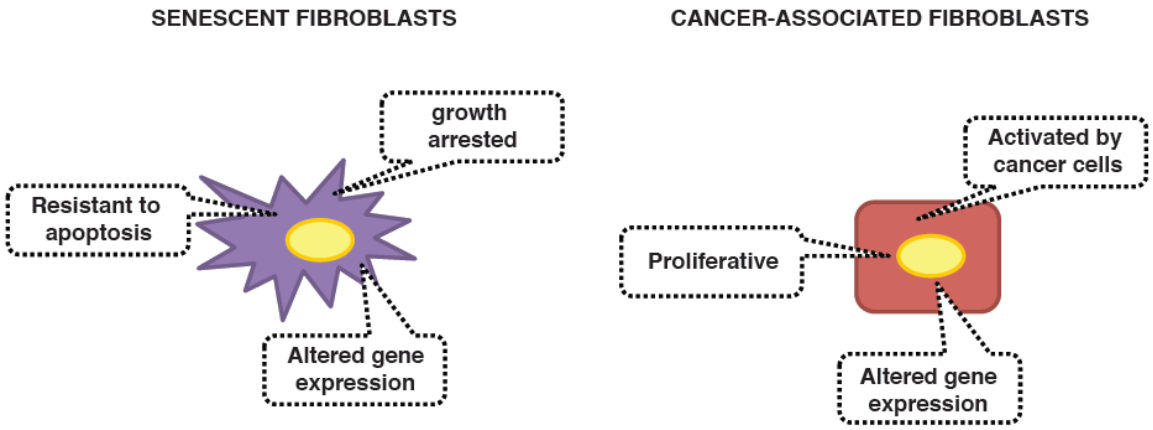

Fig 1.1: Characteristics of tumor-promoting fibroblasts. While differences exist between them, senescent and cancer-associated fibroblasts both promote tumorigenesis through similar altered gene expression profiles.

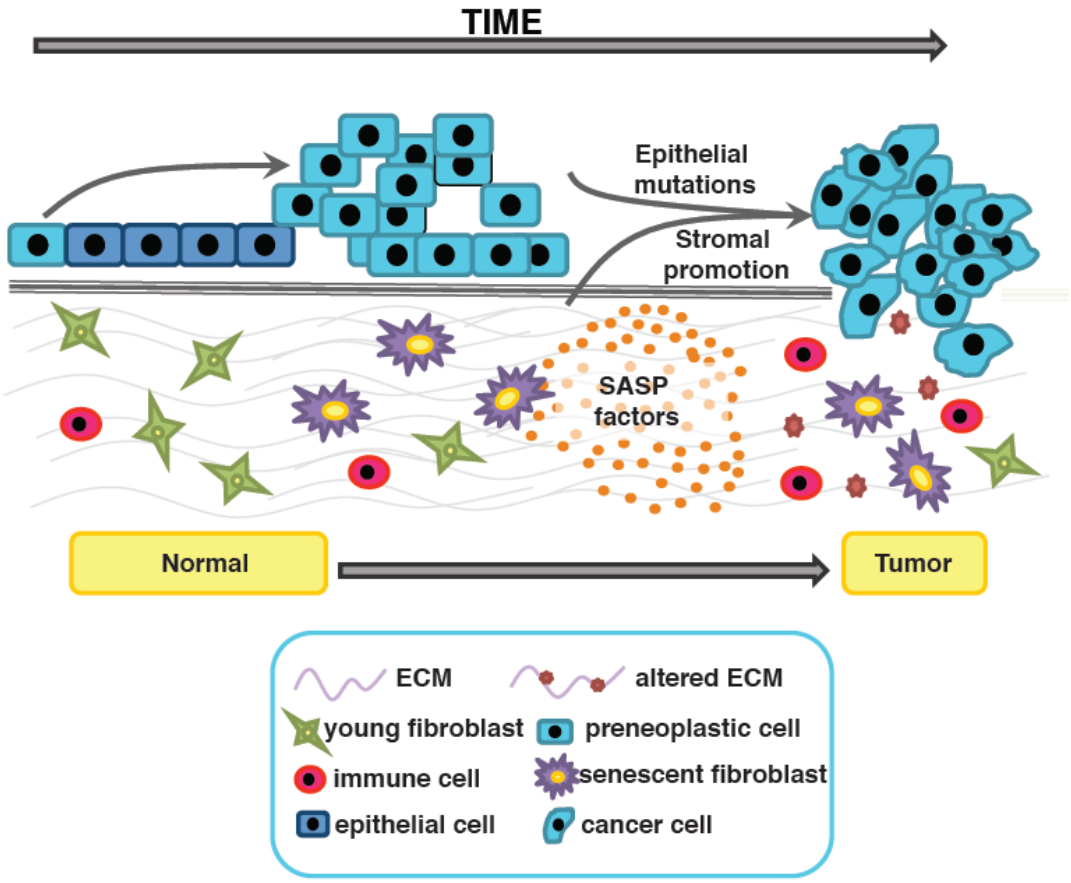

Fig 1.2: the presence of senescent fibroblasts within the tumor microenvironment promotes tumorigenesis. The accumulation of senescent fibroblasts within the tumor microenvironment promotes tumor progression through secretion of SASP components that mediate alteration of the ECM, recruitment of inflammatory cells and growth of epithelial cells. Adapted from E. Pazolli et al., *Curr Opin Genet Dev,* 2008, 18(1):42-7.

REFERENCES

1. Olumi AF, Grossfeld GD, Hayward SW, Carroll PR, Tlsty TD, Cunha GR. Carcinoma-associated fibroblasts direct tumor progression of initiated human prostatic epithelium. Cancer research. 1999;59(19):5002-11.

2. Kuperwasser C, Chavarria T, Wu M, Magrane G, Gray JW, Carey L, Richardson A, Weinberg RA. Reconstruction of functionally normal and malignant human breast tissues in mice. Proceedings of the National Academy of Sciences of the United States of America. 2004;101(14):4966-71.

3. Hanahan D, Folkman J. Patterns and emerging mechanisms of the angiogenic switch during tumorigenesis. Cell. 1996;86(3):353-64. Epub 1996/08/09.

4. Vajkoczy P, Farhadi M, Gaumann A, Heidenreich R, Erber R, Wunder A, Tonn JC, Menger MD, Breier G. Microtumor growth initiates angiogenic sprouting with simultaneous expression of VEGF, VEGF receptor-2, and angiopoietin-2. The Journal of clinical investigation. 2002;109(6):777-85. Epub 2002/03/20.

5. Holash J, Wiegand SJ, Yancopoulos GD. New model of tumor angiogenesis: dynamic balance between vessel regression and growth mediated by angiopoietins and VEGF. Oncogene. 1999;18(38):5356-62. Epub 1999/09/28.

6. Noel A, Maillard C, Rocks N, Jost M, Chabottaux V, Sounni NE, Maquoi E, Cataldo D, Foidart JM. Membrane associated proteases and their inhibitors in tumour angiogenesis. Journal of clinical pathology. 2004;57(6):577-84. Epub 2004/05/29.

7. Kornfeld D, Ekbom A, Ihre T. Is there an excess risk for colorectal cancer in patients with ulcerative colitis and concomitant primary sclerosing cholangitis? A population based study. Gut. 1997;41(4):522-5. Epub 1997/12/10.

8. Blaser MJ, Perez-Perez GI, Kleanthous H, Cover TL, Peek RM, Chyou PH, Stemmermann GN, Nomura A. Infection with Helicobacter pylori strains possessing cagA is associated with an increased risk of developing adenocarcinoma of the stomach. Cancer research. 1995;55(10):2111-5. Epub 1995/05/15.

9. Ruffell B, Affara NI, Coussens LM. Differential macrophage programming in the tumor microenvironment. Trends in immunology. 2012;33(3):119-26. Epub 2012/01/27.

10. Orimo A, Gupta PB, Sgroi DC, Arenzana-Seisdedos F, Delaunay T, Naeem R, Carey VJ, Richardson AL, Weinberg RA. Stromal fibroblasts present in invasive human breast carcinomas promote tumor growth and angiogenesis through elevated SDF-1/CXCL12 secretion. Cell. 2005;121(3):335-48. Epub 2005/05/11.

11. Sato T, Sakai T, Noguchi Y, Takita M, Hirakawa S, Ito A. Tumor-stromal cell contact promotes invasion of human uterine cervical carcinoma cells by augmenting the expression and activation of stromal matrix metalloproteinases. Gynecologic oncology. 2004;92(1):47-56. Epub 2004/01/31.

12. DePinho RA. The age of cancer. Nature. 2000;408(6809):248-54.

13. Hayflick L. The Limited in Vitro Lifetime of Human Diploid Cell Strains. Experimental cell research. 1965;37:614-36.

14. Di Leonardo A, Linke SP, Clarkin K, Wahl GM. DNA damage triggers a prolonged p53-dependent G1 arrest and long-term induction of Cip1 in normal human fibroblasts. Genes & development. 1994;8(21):2540-51.

15. Stein GH, Drullinger LF, Robetorye RS, Pereira-Smith OM, Smith JR. Senescent cells fail to express cdc2, cycA, and cycB in response to mitogen stimulation. Proceedings of the National Academy of Sciences of the United States of America. 1991;88(24):11012-6. Epub 1991/12/15.

16. Noda A, Ning Y, Venable SF, Pereira-Smith OM, Smith JR. Cloning of senescent cell-derived inhibitors of DNA synthesis using an expression screen. Experimental cell research. 1994;211(1):90-8. Epub 1994/03/01.

17. Alcorta DA, Xiong Y, Phelps D, Hannon G, Beach D, Barrett JC. Involvement of the cyclin-dependent kinase inhibitor p16 (INK4a) in replicative senescence of normal human fibroblasts. Proceedings of the National Academy of Sciences of the United States of America. 1996;93(24):13742-7. Epub 1996/11/26.

18. Atadja P, Wong H, Garkavtsev I, Veillette C, Riabowol K. Increased activity of p53 in senescing fibroblasts. Proceedings of the National Academy of Sciences of the United States of America. 1995;92(18):8348-52. Epub 1995/08/29.

19. Wang E. Senescent human fibroblasts resist programmed cell death, and failure to suppress bcl2 is involved. Cancer research. 1995;55(11):2284-92. Epub 1995/06/01.

20. von Zglinicki T, Saretzki G, Docke W, Lotze C. Mild hyperoxia shortens telomeres and inhibits proliferation of fibroblasts: a model for senescence? Experimental cell research. 1995;220(1):186-93.

21. von Zglinicki T. Role of oxidative stress in telomere length regulation and replicative senescence. Ann N Y Acad Sci. 2000;908:99-110.

22. Di Micco R, Fumagalli M, Cicalese A, Piccinin S, Gasparini P, Luise C, Schurra C, Garre M, Nuciforo PG, Bensimon A, Maestro R, Pelicci PG, d'Adda di Fagagna F. Oncogene-induced senescence is a DNA damage response triggered by DNA hyper-replication. Nature. 2006;444(7119):638-42.

23. Mallette FA, Gaumont-Leclerc MF, Ferbeyre G. The DNA damage signaling pathway is a critical mediator of oncogene-induced senescence. Genes & development. 2007;21(1):43-8. Epub 2007/01/11.

24. Coppe JP, Patil CK, Rodier F, Sun Y, Munoz DP, Goldstein J, Nelson PS, Desprez PY, Campisi J. Senescence-associated secretory phenotypes reveal cell-nonautonomous functions of oncogenic RAS and the p53 tumor suppressor. PLoS biology. 2008;6(12):2853-68.

25. te Poele RH, Okorokov AL, Jardine L, Cummings J, Joel SP. DNA damage is able to induce senescence in tumor cells in vitro and in vivo. Cancer research. 2002;62(6):1876-83. Epub 2002/03/26.

26. Roninson IB, Broude EV, Chang BD. If not apoptosis, then what? Treatment-induced senescence and mitotic catastrophe in tumor cells. Drug resistance updates : reviews and commentaries in antimicrobial and anticancer chemotherapy. 2001;4(5):303-13. Epub 2002/05/07.

27. Suzuki K, Mori I, Nakayama Y, Miyakoda M, Kodama S, Watanabe M. Radiation-induced senescence-like growth arrest requires TP53 function but not telomere shortening. Radiation research. 2001;155(1 Pt 2):248-53.

28. Narita M, Nunez S, Heard E, Narita M, Lin AW, Hearn SA, Spector DL, Hannon GJ, Lowe SW. Rb-mediated heterochromatin formation and silencing of E2F target genes during cellular senescence. Cell. 2003;113(6):703-16.

29. Hewitt G, Jurk D, Marques FD, Correia-Melo C, Hardy T, Gackowska A, Anderson R, Taschuk M, Mann J, Passos JF. Telomeres are favoured targets of a persistent DNA damage response in ageing and stress-induced senescence. Nature communications. 2012;3:708. Epub 2012/03/20.

30. Fumagalli M, Rossiello F, Clerici M, Barozzi S, Cittaro D, Kaplunov JM, Bucci G, Dobreva M, Matti V, Beausejour CM, Herbig U, Longhese MP, d'Adda di Fagagna F. Telomeric DNA damage is irreparable and causes persistent DNA-damage-response activation. Nature cell biology. 2012;14(4):355-65. Epub 2012/03/20.

31. Baker DJ, Wijshake T, Tchkonia T, LeBrasseur NK, Childs BG, van de Sluis B, Kirkland JL, van Deursen JM. Clearance of p16Ink4a-positive senescent cells delays ageing-associated disorders. Nature. 2011;479(7372):232-6. Epub 2011/11/04.

32. Dimri GP, Lee X, Basile G, Acosta M, Scott G, Roskelley C, Medrano EE, Linskens M, Rubelj I, Pereira-Smith O, et al. A biomarker that identifies senescent human cells in culture and in aging skin in vivo. Proceedings of the National Academy of Sciences of the United States of America. 1995;92(20):9363-7.

33. Melk A, Schmidt BM, Takeuchi O, Sawitzki B, Rayner DC, Halloran PF. Expression of p16INK4a and other cell cycle regulator and senescence associated genes in aging human kidney. Kidney international. 2004;65(2):510-20.

34. Chkhotua AB, Gabusi E, Altimari A, D'Errico A, Yakubovich M, Vienken J, Stefoni S, Chieco P, Yussim A, Grigioni WF. Increased expression of p16(INK4a) and p27(Kip1) cyclin-dependent kinase inhibitor genes in aging human kidney and chronic allograft nephropathy. American journal of kidney diseases : the official journal of the National Kidney Foundation. 2003;41(6):1303-13. Epub 2003/05/31.

35. Choi J, Shendrik I, Peacocke M, Peehl D, Buttyan R, Ikeguchi EF, Katz AE, Benson MC. Expression of senescence-associated beta-galactosidase in enlarged prostates from men with benign prostatic hyperplasia. Urology. 2000;56(1):160-6.

36. Lee CT, Capodieci P, Osman I, Fazzari M, Ferrara J, Scher HI, Cordon-Cardo C. Overexpression of the cyclin-dependent kinase inhibitor p16 is associated with tumor recurrence in human prostate cancer. Clinical cancer research : an official journal of the American Association for Cancer Research. 1999;5(5):977-83. Epub 1999/06/03.

37. Wiemann SU, Satyanarayana A, Tsahuridu M, Tillmann HL, Zender L, Klempnauer J, Flemming P, Franco S, Blasco MA, Manns MP, Rudolph KL. Hepatocyte telomere shortening and senescence are general markers of human liver cirrhosis. FASEB journal : official publication of the Federation of American Societies for Experimental Biology. 2002;16(9):935-42. Epub 2002/06/28.

38. Herbig U, Ferreira M, Condel L, Carey D, Sedivy JM. Cellular senescence in aging primates. Science. 2006;311(5765):1257.

39. Michaloglou C, Vredeveld LC, Soengas MS, Denoyelle C, Kuilman T, van der Horst CM, Majoor DM, Shay JW, Mooi WJ, Peeper DS. BRAFE600-associated senescence-like cell cycle arrest of human naevi. Nature. 2005;436(7051):720-4.

40. Chen Z, Trotman LC, Shaffer D, Lin HK, Dotan ZA, Niki M, Koutcher JA, Scher HI, Ludwig T, Gerald W, Cordon-Cardo C, Pandolfi PP. Crucial role of p53-dependent cellular senescence in suppression of Pten-deficient tumorigenesis. Nature. 2005;436(7051):725-30.

41. Bartkova J, Rezaei N, Liontos M, Karakaidos P, Kletsas D, Issaeva N, Vassiliou LV, Kolettas E, Niforou K, Zoumpourlis VC, Takaoka M, Nakagawa H, Tort F, Fugger K, Johansson F, Sehested M, Andersen CL, Dyrskjot L, Orntoft T, Lukas J, Kittas C, Helleday T, Halazonetis TD, Bartek J, Gorgoulis VG. Oncogene-induced senescence is part of the tumorigenesis barrier imposed by DNA damage checkpoints. Nature. 2006;444(7119):633-7.

42. Ventura A, Kirsch DG, McLaughlin ME, Tuveson DA, Grimm J, Lintault L, Newman J, Reczek EE, Weissleder R, Jacks T. Restoration of p53 function leads to tumour regression in vivo. Nature. 2007;445(7128):661-5.

43. Bavik C, Coleman I, Dean JP, Knudsen B, Plymate S, Nelson PS. The gene expression program of prostate fibroblast senescence modulates neoplastic epithelial cell proliferation through paracrine mechanisms. Cancer research. 2006;66(2):794-802.

44. Krtolica A, Parrinello S, Lockett S, Desprez PY, Campisi J. Senescent fibroblasts promote epithelial cell growth and tumorigenesis: a link between cancer and aging.

Proceedings of the National Academy of Sciences of the United States of America. 2001;98(21):12072-7.

45. Parrinello S, Coppe JP, Krtolica A, Campisi J. Stromal-epithelial interactions in aging and cancer: senescent fibroblasts alter epithelial cell differentiation. Journal of cell science. 2005;118(Pt 3):485-96.

46. Copperman AB, DeCherney AH. Turn, turn, turn. Fertility and sterility. 2006;85(1):12-3. Epub 2006/01/18.

47. Pazolli E, Luo X, Brehm S, Carbery K, Chung JJ, Prior JL, Doherty J, Demehri S, Salavaggione L, Piwnica-Worms D, Stewart SA. Senescent Stromal-Derived Osteopontin Promotes Preneoplastic Cell Growth. Cancer research. 2009.

48. Coppe JP, Kauser K, Campisi J, Beausejour CM. Secretion of vascular endothelial growth factor by primary human fibroblasts at senescence. The Journal of biological chemistry. 2006;281(40):29568-74.

49. Yang L, Shang X, Zhao X, Lin Y, Liu J. [Correlation study between OPN, CD44v6, MMP-9 and distant metastasis in laryngeal squamous cell carcinoma]. Lin chuang er bi yan hou tou jing wai ke za zhi = Journal of clinical otorhinolaryngology, head, and neck surgery. 2012;26(21):989-92. Epub 2013/02/05.

50. Liu D, Hornsby PJ. Senescent human fibroblasts increase the early growth of xenograft tumors via matrix metalloproteinase secretion. Cancer research. 2007;67(7):3117-26.

51. Simos G, Segref A, Fasiolo F, Hellmuth K, Shevchenko A, Mann M, Hurt EC. The yeast protein Arc1p binds to tRNA and functions as a cofactor for the methionyl- and glutamyl-tRNA synthetases. The EMBO journal. 1996;15(19):5437-48.

52. Cahu J, Bustany S, Sola B. Senescence-associated secretory phenotype favors the emergence of cancer stem-like cells. Cell death & disease. 2012;3:e446. Epub 2012/12/21.

53. Tsuyada A, Chow A, Wu J, Somlo G, Chu P, Loera S, Luu T, Li AX, Wu X, Ye W, Chen S, Zhou W, Yu Y, Wang YZ, Ren X, Li H, Scherle P, Kuroki Y, Wang SE. CCL2 mediates cross-talk between cancer cells and stromal fibroblasts that regulates breast cancer stem cells. Cancer research. 2012;72(11):2768-79. Epub 2012/04/05.

54. Korkaya H, Liu S, Wicha MS. Breast cancer stem cells, cytokine networks, and the tumor microenvironment. The Journal of clinical investigation. 2011;121(10):3804-9. Epub 2011/10/04.

55. Lohr M, Schmidt C, Ringel J, Kluth M, Muller P, Nizze H, Jesnowski R. Transforming growth factor-beta1 induces desmoplasia in an experimental model of human pancreatic carcinoma. Cancer research. 2001;61(2):550-5. Epub 2001/02/24.

56. Weeks BH, He W, Olson KL, Wang XJ. Inducible expression of transforming growth factor beta1 in papillomas causes rapid metastasis. Cancer research. 2001;61(20):7435-43. Epub 2001/10/19.

57. Elkabets M, Gifford AM, Scheel C, Nilsson B, Reinhardt F, Bray MA, Carpenter AE, Jirstrom K, Magnusson K, Ebert BL, Ponten F, Weinberg RA, McAllister SS. Human tumors instigate granulin-expressing hematopoietic cells that promote malignancy by

activating stromal fibroblasts in mice. The Journal of clinical investigation. 2011;121(2):784-99. Epub 2011/01/27.

58. Finak G, Bertos N, Pepin F, Sadekova S, Souleimanova M, Zhao H, Chen H, Omeroglu G, Meterissian S, Omeroglu A, Hallett M, Park M. Stromal gene expression predicts clinical outcome in breast cancer. Nat Med. 2008;14(5):518-27.

59. Karnoub AE, Dash AB, Vo AP, Sullivan A, Brooks MW, Bell GW, Richardson AL, Polyak K, Tubo R, Weinberg RA. Mesenchymal stem cells within tumour stroma promote breast cancer metastasis. Nature. 2007;449(7162):557-63. Epub 2007/10/05.

60. Ma XJ, Dahiya S, Richardson E, Erlander M, Sgroi DC. Gene expression profiling of the tumor microenvironment during breast cancer progression. Breast Cancer Res. 2009;11(1):R7.

61. Rodier F, Coppe JP, Patil CK, Hoeijmakers WA, Munoz DP, Raza SR, Freund A, Campeau E, Davalos AR, Campisi J. Persistent DNA damage signalling triggers senescence-associated inflammatory cytokine secretion. Nature cell biology. 2009;11(8):973-9.

62. Freund A, Patil CK, Campisi J. p38MAPK is a novel DNA damage response-independent regulator of the senescence-associated secretory phenotype. The EMBO journal. 2011;30(8):1536-48. Epub 2011/03/15.

63. Chien Y, Scuoppo C, Wang X, Fang X, Balgley B, Bolden JE, Premsrirut P, Luo W, Chicas A, Lee CS, Kogan SC, Lowe SW. Control of the senescence-associated secretory phenotype by NF-kappaB promotes senescence and enhances chemosensitivity. Genes & development. 2011;25(20):2125-36. Epub 2011/10/08.

64. Kuilman T, Michaloglou C, Vredeveld LC, Douma S, van Doorn R, Desmet CJ, Aarden LA, Mooi WJ, Peeper DS. Oncogene-induced senescence relayed by an interleukin-dependent inflammatory network. Cell. 2008;133(6):1019-31.

65. Pazolli E, Alspach E, Milczarek A, Prior J, Piwnica-Worms D, Stewart SA. Chromatin remodeling underlies the senescence-associated secretory phenotype of tumor stromal fibroblasts that supports cancer progression. Cancer research. 2012;72(9):2251-61. Epub 2012/03/17.

66. Coppe JP, Rodier F, Patil CK, Freund A, Desprez PY, Campisi J. Tumor suppressor and aging biomarker p16(INK4a) induces cellular senescence without the associated inflammatory secretory phenotype. The Journal of biological chemistry. 2011;286(42):36396-403. Epub 2011/09/02.

67. Erez N, Truitt M, Olson P, Arron ST, Hanahan D. Cancer-Associated Fibroblasts Are Activated in Incipient Neoplasia to Orchestrate Tumor-Promoting Inflammation in an NF-kappaB-Dependent Manner. Cancer cell. 2010;17(2):135-47. Epub 2010/02/09.

CHAPTER 2

Chromatin remodeling underlies the senescence-associated secretory phenotype of tumor stromal fibroblasts that supports cancer progression

Ermira Pazolli, Elise Alspach, Agnieszka Milczarek, Julie Prior, David Piwnica-Worms, and Sheila A. Stewart

E. Alspach was a contributing author to this work

This chapter was published in 2012 in *Cancer Research* 72(9): 2251-61

INTRODUCTION

Senescent cells promote tumorigenesis through expression of the senescence-associate secretory phenotype (SASP). Investigation into the cellular signaling pathways that activate the SASP has revealed that a persistent DNA damage response (DDR) is sufficient to activate some SASP factors. Indeed, signaling downstream of ATM (including NBS1 and Chk2) controls a subset of SASP factors, including IL6 and IL8 (1). The mechanisms linking DDR to SASP activation remain unclear but it is known that DDR leads to chromatin alterations that impact numerous transcription pathways. Therefore, transcriptional changes observed in senescent cells may result from specific chromatin modulations. Mounting evidence implicates chromatin remodeling in the establishment of the senescent state. Several studies have reported the appearance of SAHFs in senescent cells and have shown that they occur at E2F promoters and functionally repress cellular proliferation (2). Conversely, senescence is associated with transcriptional activation generally attributed to chromatin decondensation. For example, loss of heterochromatin is associated with aging in yeast (3) and other model organisms (4), and is observed in cells from patients with premature aging syndromes such as Hutchinson–Gilford Progeria Syndrome (HGPS) (5). In replicative senescence, histone deacetylase (HDAC) activity diminishes (6) corresponding with an increase in histone acetylation. Additionally, a decline in global DNA methylation has been reported ((7) and references therein). Interestingly, treatment with HDAC inhibitors including sodium butyrate (NaB) or trichostatin A (TSA) induces senescence, further supporting the hypothesis that chromatin relaxation plays a causative role in senescence (6, 8).

A role for transcriptional control in the regulation of SASP factors has also been suggested by recent work, particularly for inflammation-related members of the SASP including IL6, IL8 and CXCR2. Transcriptional regulation of such chemokines in other biological settings by NF-κB and C/EBPβ applies to senescence as well. In fact, these transcription factors occupy the promoters of several cytokines in senescent cells (9, 10). However, it is unknown how these factors are activated in response to senescence-inducing stimuli and subsequently direct transcriptional changes in senescence.

Osteopontin (OPN), also known as secreted phosphoprotein 1 (SPP1), is a multifunctional signaling molecule (11). Originally identified in cancer cells (12), the physiological function of OPN is linked to matrix integrity and bone maintenance (13). Since its initial identification, OPN has been implicated in every stage of tumorigenesis and is a prognostic factor for several malignancies (14). We previously reported that OPN levels increase in senescent cells and showed that it is a critical mediator of stromal-epithelial interactions in tumorigenesis (15). In addition, OPN expression in the stromal compartment of human skin coincides with senescent markers, raising the possibility that it plays an important role in the early stages of tumorigenesis (16). Despite the importance of senescence-derived OPN, its regulation in senescent cells remains unknown. Here we report that following senescence-inducing stimuli, OPN upregulation occurs independent of the senescence effector pathways p53 and Rb, similar to what has been shown for other SASP members including IL6 and IL8 (17).

This finding demonstrates that SASP activation occurs in response to cellular stress insults and that senescence-inducing stimuli produce sufficient stress to induce SASP. Further investigation revealed that contrary to the signature SASP members, IL6 and IL8, OPN expression is insensitive to NF-κB and ATM signaling. Together our results indicate that SASP is controlled by at least two independent transcription programs. Importantly, agents capable of directly perturbing chromatin structure without inducing DNA breaks were potent inducers of SASP including OPN expression. Specifically, ectopic expression of a dominant negative form of HDAC1 leads to OPN mRNA upregulation. Furthermore, treatment of fibroblasts with HDAC inhibitors led to a significant paracrine stimulation of tumor growth, which suggests that these inhibitors may adversely impact the stromal compartment in the therapeutic setting.

METHODS

Cell lines and treatments

Human foreskin BJ fibroblasts and 293T cells were grown as previously described (15). These cell lines were originally obtained from Dr. Robert Weinberg's laboratory and were not recently reauthenticated. Human AT fibroblasts (GM09607) were purchased from Coriell Institute (Camden, NJ), used within six months of receipt and grown in MEM media supplemented with 15% non-heat inactivated FBS (Sigma, St. Louis, MO). WI38 fetal lung fibroblasts were grown in DME media supplemented with 10% heat-inactivated FBS (Sigma, St. Louis, MO) and transduced with telomerase (pBabe vector with hygromycin selection) and human papilloma virus 16 proteins E6 and E7

(expressed from the LXSN vector (18)). Fibroblasts were mock- or bleomycin sulfate-treated (100 µg/ml, Sigma, St. Louis, MO) for 24 hrs. After 72 hr serum-starvation, RNA was collected using TRI Reagent (Ambion/Applied Biosystems, Foster City, CA). Cells were incubated with two fresh changes of 4 mM sodium butyrate (Sigma) for 72 or 144 hr, 6 µM MS-275 (Santa Cruz Biotechnologies, Santa Cruz, CA) for 6 days, 3 µM of suberoylanilide hydroxamic acid (SAHA) or vorinostat (Selleck, Houston, TX) for 6 days, or 1 mM TSA (Sigma, St. Louis, MO) for 3 days.

Plasmids

The IκBα-mut in a pBabe construct (19) was purchased from Addgene (Boston, MA plasmid 15291). The NF-κB promoter luciferase construct, pκB$_5$-Fluc (Stratagene, La Jolla, CA) and pRL-CMV (Promega, Madison, WI) were used in transient transfections. Two shRNA sequences targeting the human ATM gene (shATM-1:CCTTTCATTCAGCCTTTAGAA; shATM-2: TGATGGTCTTAAGGAACATCT) were provided in the pLKO.1 plasmid by the Washington University in St. Louis Children's Discovery Institute and the RNAi Consortium. The p53-DD and DK constructs (18) were kindly provided by Robert Weinberg (Whitehead Institute, Boston, MA). The HDAC1-H140A cDNA in pBabe-puro (20) was kindly provided by Tso-Pang Yao (Duke University, Durham, NC). The HDAC3mut (HDAC3 1-401) cDNA (21) was kindly provided by Edward Seto (Moffit Cancer Center, Tampa, FL) and was subcloned into the *Eco*RI/*Pac*I sites of pBabe-hygro-3xFLAG vector.

Quantitative PCR (qPCR)

Standard protocol was followed for cDNA and quantitative PCR (as previously reported in (15)) using the following primers (IDT, Coralville, IA):

OPN, F 5′-TTGCAGCCTTCTCAGCCAA-3′, R 5′-CAAAAGCAAATCACTGCAATTCTC-3′; GAPDH, F 5′-GCATGGCCTTCCGTGTCC-3′, R 5′-AATGCCAGCCCCAGCGTCAAA-3′; IL6, F 5′-ACATCCTCGACGGCATCTCA-3′, R 5′-TCACCAGGCAAGTCTCCTCA-3′; IL8, F 5′-GCTCTGTGTGAAGGTGCAGT-3′, R 5′-TGCACCCAGTTTTCCTTGGG-3′; ATM (Taqman, Applied Biosystems, Carlsbad, CA cat.# Hs01112317-g1). All qPCR results were analyzed using the method reported in Livak et al., (22).

Western Blot Analysis

Fibroblast cell pellets were lysed in 100 µl of lysis buffer (50 mM HEPES pH 7.4, 150 mM NaCl, 1% Triton X-100, 1 M EDTA, 10% (v/v) glycerol) and protein was quantified by the Bradford Protein Assay (Bio-Rad, Hercules, CA). The following primary antibodies were used: p421, a p53 hybridoma supernatant kindly provided by Robert Weinberg (Whitehead Institute, Cambridge, MA) at 1:100; Cdk4 (Santa Cruz Biotechnologies, Santa Cruz, CA) at 1:200; β-actin (Sigma, St. Louis, MO) at 1:10,000; γ-actin (Novus, St. Louis, MO) at 1:5000; γH2AX (Millipore/Upstate, Billerica, MA) at 1:1000; FLAG (Sigma, St. Louis, MO) at 1:1000. All primary antibodies were detected by the appropriate HRP-conjugated secondary antibodies (Sigma, St. Louis, MO).

Virus production and retroviral infections

Virus was produced and target cells transduced as previously described (15).

Senescence-associated β-galactosidase (SA-βgal) staining

SA-βgal staining on cells was performed as previously described (4).

Xenograft model

All animal procedures were approved by the Washington University School of Medicine Animal Studies Committee. $5x10^5$ BJ fibroblasts treated as described above and $5x10^5$ $HaCaT_{CBR}$ were injected subcutaneously into the flanks of female NOD/SCID mice (NCI-Fredrick). *In vivo* imaging was performed on days 10 and 12 on an IVIS50 (Caliper; Living Image 3.2, 60 s exposure, binning 8, FOV 12cm, f/stop 1, open filter). For analysis, total photon flux (photons/sec) was measured from a fixed region of interest over the xenografts using Living Image 2.6.

HDAC1 IP and deacetylase assay

Vehicle and bleomycin-treated fibroblasts were lysed as described (5) and 2 mg of protein was immunoprecipitated with an antibody against HDAC1 (ab7028, Abcam, Cambridge, MA or a negative control antibody (β-galactosidase, ab616, Abcam, Cambridge, MA) as described (5). HDAC activity was measured with the Fluor-de-Lys HDAC Activity Assay Kit (Enzo Life Sciences, Farmingdale, NY) per manufacturer's recommendations.

Expression Analysis

Comparison of HDAC1 mRNA levels in normal vs. invasive breast cancer-associated stroma was exported from Oncomine (23) as extracted from the Finak *et al.* study (24). Expression values are log-transformed and median-centered per array. Differential

expression is identified by a permutation test and p-values are calculated by t-test and corrected for multiple comparisons by the method of false discovery rates (23).

Statistical analysis

Data are presented as the mean ± STDEV or SEM. Statistical significance was calculated using Student's t-test. Values of $p < 0.05$ were considered significant.

RESULTS

The senescence effector pathways p53 and Rb are not required to activate OPN

Activation of senescence is accompanied by upregulation of pro-tumorigenic factors collectively referred to as SASP (17). Our previous work revealed that one member of this group, OPN, stimulates preneoplastic keratinocyte growth and is a critical stromal-derived pro-tumorigenic factor in a xenograft model (15). Given the significance of OPN in this model and the importance of the other senescent secreted proteins, we investigated OPN's regulation in senescence. We initially turned our attention to the senescence effector and tumor-suppressor proteins p53 and Rb. Importantly, in human cells, inhibition of the p53 or Rb pathways alone is insufficient to bypass senescence while concomitant abrogation of these pathways allows cells to bypass senescence (25). However, previous work has shown that p53 and Rb actively suppress the activation of some SASP factors including IL6 and IL8 (17). However, p53 regulates OPN expression in mouse embryonic fibroblasts, raising the possibility that it plays a role in the regulation of OPN in senescence (26). To investigate the requirement for p53 and Rb activity in senescence-associated OPN regulation, we ectopically

expressed a well-characterized dominant negative p53 cDNA (p53-DD) (18) or a cDNA expressing a fusion protein consisting of a mutant form of cyclin dependent kinase 4^{R24C} (Cdk4) and cyclin D1 (DK) that inhibits Rb (18) (**Fig 2.1A**). Abrogation of the p53 or Rb pathway alone had no impact on the induction of senescence. Indeed, exposure of control cells or cells expressing p53-DD or DK to bleomycin induced robust senescence as evidenced by growth inhibition, the appearance of large flattened cells and the induction of senescence associated β-galactosidase (SA-βgal) (data not shown and **Fig 2.1B**). We found that neither abrogation of p53 nor Rb reduced OPN transcripts upon activation of senescence (**Fig 2.2C**). On the contrary, in the absence of p53 or Rb, OPN basal levels in vehicle-treated cells increased (**Fig S2.1B** and **C**) and they were further augmented upon bleomycin treatment and the induction of senescence, arguing that p53 and Rb are not only dispensable for the senescence-associated stimulation of OPN expression, but that they suppress it. As previously reported, IL6 and IL8 levels were also increased in senescent cells when p53 and Rb function was compromised (**Fig S2.1A** and (17)), indicating that the p53 and Rb pathways actively suppress a wide range of SASP members.

Previous work had indicated that while SASP factors are robustly activated in senescent cells, the induction of senescence was dispensable for SASP activation (1, 17). We next wished to address whether OPN expression was dependent on senescence activation or if it was instead the cellular stress associated with senescence that activated SASP. To address this question, we treated immortalized WI38 fibroblasts

expressing the papilloma virus E6 and E7 proteins, which abrogate p53 and Rb, respectively with bleomycin. As expected, bleomycin treatment of E6/E7-expressing cells did not induce senescence (**Fig S2.1D**). We found that these cells continued to divide and failed to acquire the flattened cellular morphology of senescent cells and did not stain positive for SA-βgal (**Fig S2.1D)**. Despite the fact that E6/E7 cells failed to enter senescence, analysis of OPN, IL6, and IL8 revealed that these cells retained the ability to activate SASP (**Fig S2.1E**), indicating that SASP expression does not require the activation of the senescence effector proteins p53 and Rb nor entry into senescence. Thus, cellular stresses capable of inducing senescence activate SASP, regardless of the status of the senescence effector proteins or the induction of senescence itself.

SASP is controlled by distinct regulatory mechanisms

NF-κB is a master regulator of cytokine production in inflammatory responses (27) and was recently invoked in the transcriptional control of some SASP members, including IL6 and IL8 (10, 28). Like IL6, OPN can participate in cellular responses characterized by chronic inflammation (11) and NF-κB can directly activate OPN transcription under certain conditions (29). Therefore, we investigated whether NF-κB activates OPN transcription in senescent cells. NF-κB canonically resides in a complex with IκBα, which sequesters it in the cytoplasm. Upon stimulation, IκBα is phosphorylated and subsequently degraded, allowing NF-κB to translocate to the nucleus where it activates target gene transcription (27). We successfully blocked NF-κB signaling by stably

expressing a mutant of IκBα that cannot be phosphorylated (IκBα-mut), thus trapping NF-κB in the cytoplasm (19). To confirm that the mutant was active, we examined its impact on an NF-κB reporter plasmid containing five tandem NF-κB binding elements. BJ fibroblasts were transduced with the NF-κB reporter plasmid or a vector alone. As expected, we found that expression of the reporter plasmid was inhibited in IκBα-mut cells compared to cells expressing a vector control (**Fig. 2.2A**).

To determine whether NF-κB activity was required to activate OPN in senescent cells, BJ fibroblasts expressing a control vector or the IκBα mutant (IκBα-mut) were treated with bleomycin. We found that bleomycin treatment induced robust senescence in the control and IκBα mutant-expressing cells as evidenced by the induction of a flattened morphology and the induction of SA-βGal (**Fig 2.2B**), indicating that this mode of NF-κB inhibition does not abrogate the induction of senescence in these cells. In agreement with previous reports (10), we found that NF-κB activation is essential for the upregulation of IL6 and IL8 in senescence (**Fig 2.2C**). Indeed, we found that IκBα-mut cells treated with bleomycin failed to upregulate IL6 and IL8. In contrast, OPN levels remained unperturbed in IκBα-mut cells treated with bleomycin (**Fig 2.2C**). Because the expression of the IκBα mutant precedes the exposure to bleomycin, our findings indicate that NF-κB signaling is neither required for the initiation nor maintenance of OPN levels in response to DNA damage. Together these findings also indicate that SASP is regulated by at least two distinct transcriptional pathways.

Having established that neither the p53 or Rb pathways nor activation of NF-κB plays a role in OPN regulation following bleomycin treatment and SASP activation, we next turned our attention to the putative role of the DNA damage response (DDR). Senescence is characterized by a robust and persistent DNA damage response (30) that includes the activation of the ATM kinase, which has been implicated in SASP activation (1). To address whether ATM activation was required for OPN upregulation in senescent cells, we utilized ATM-specific short hairpin (shRNA) constructs to deplete cells of ATM to greater than 80% (**Fig 2.2D**). As expected (1), ATM depletion had no impact on the induction of senescence (**Fig 2.2E)** but resulted in a significant reduction in IL6 and IL8 levels (**Fig 2.2F**). In contrast, ATM depletion had no impact on OPN expression following bleomycin treatment (**Fig 2.2F**). These results indicate that OPN expression, unlike IL6 and IL8, is not controlled by DDR or NF-κB signaling in senescence, but instead is regulated by a distinct mechanism.

Histone deacetylase (HDAC) inhibition induces SASP

Cellular senescence can be induced by a wide variety of cellular stresses. Previous work demonstrated agents that impact histone deacetylase (HDAC) activity, including sodium butyrate (NaB) and trichostatin A (TSA), induce senescence or a senescence-like state, which is typically characterized by growth arrest but a lack of SA-βgal activity (6, 8). These findings raised the possibility that chromatin modulation rather than *bona fide* DNA breaks were responsible for the activation of SASP. Therefore, we examined whether *bona fide* double strand DNA breaks were required for SASP expression. BJ

fibroblasts were treated with NaB, which resulted in a robust cell cycle arrest and a flattened cellular morphology but failed to activate SA-βgal activity, consistent with a senescence-like state (**Fig S2.2**). Given the morphology of the cells and the growth arrest observed, we ext examined whether these treatments induced DNA double strand breaks. To assess the presence of DNA double strand breaks, we evaluated levels of γH2AX, a phosphorylated form of the histone variant H2AX that is widely recognized as a marker of double strand breaks and active DDR (31). As a control for γH2AX induction we analyzed irradiated cells by western blot analysis and found robust increase in γH2AX as expected. In contrast, NaB treatment did not increase γH2AX levels compared to vehicle-treated cells (**Fig 2.3A**). The comet assay, a sensitive technique utilized to detect DNA breaks in individual cells (32), corroborated these results (data not shown) in agreement with previous findings (8). Next, we examined OPN mRNA levels and observed robust induction despite the lack of detectable DNA damage (**Fig 2.3B**). In agreement with previous findings, both IL6 and IL8 also increased in NaB-treated cells (28). Together these findings indicate that DNA breaks are not required for SASP induction.

HDAC inhibition in tumor cells results in reduced cell growth and tumor cell death. Thus, recent work in xenografts and human clinical trials has focused on the therapeutic potential of HDAC inhibition (33). These findings have led to the approval of one such compound, suberoylanilide hydroxamic acid (SAHA) or vorinostat, for the treatment of cutaneous T-cell lymphoma, with several other classes of HDAC inhibitors currently in

clinical trials (34). Given the putative clinical importance of these inhibitors and our findings with NaB, we tested whether other HDAC inhibitors activated SASP. Indeed, we found that other HDAC inhibitors including TSA, MS275 and vorinostat similarly increased OPN, IL6, and IL8 levels (**Fig 2.3B**). We obtained identical results when we treated primary breast fibroblasts with NaB and vorinostat (**Fig S2.3**), indicating that HDAC inhibition also elicits a SASP response in primary stromal cells. Together, these findings raise concern that HDAC inhibitors may impact the tumor microenvironment.

Above we show that the SASP is induced in the absence of DNA double strand breaks; however, ATM is activated in cells treated with chromatin relaxers (35), raising the possibility that the DDR required to activate IL6 and IL8 is initiated by a more general mechanism such as chromatin modulation independently of physical damage. Given that in bleomycin-induced senescence, ATM and NF-κB are required for IL6 and IL8 upregulation (**Fig. 2.2**), we next investigated whether both ATM and NF-κB were also required to regulate IL6 and IL8 in NaB-treated cells. We treated cells that express the IκBα-mut or AT cells (genetically deficient in ATM activity) with NaB as above. Although NaB does not induce DNA double strand breaks ((8) and data not shown), we found that IL6 and IL8 upregulation retained the requirement for both NF-κB and ATM (**Fig 2.3C and D**). In contrast, we observed a robust upregulation of OPN in IκBα-mut expressing fibroblasts and AT cells following NaB treatment (data not shown). Together these findings indicate that the DNA damage signaling required for the upregulation of IL6 and

IL8 does not emanate from physical DNA breaks (28) and suggest instead that chromatin modulation is central to the regulation of SASP factors.

HDAC inhibition creates a pro-tumorigenic microenvironment

Our finding that HDAC inhibition stimulates the tumor-promoting SASP (**Fig 2.3B**) led us to investigate their impact *in vivo*. To investigate this we treated BJ fibroblasts with NaB, which led to the robust upregulation of OPN, IL6, and IL8 (**Fig S2.4A**) and examined whether these fibroblasts promoted tumor growth *in vivo*. Similar to our previous report, we found that bleomycin-treated fibroblasts significantly promote preneoplastic $HaCaT_{CBR}$ cell growth when co-injected in xenografts (**Fig 2.4A** and **B**). When cells were injected in combination with vehicle-treated fibroblasts, there was minimal growth. Significantly, the presence of fibroblasts treated with NaB also led to a substantial enhancement of $HaCAT_{CBR}$ cell growth compared to cells injected with vehicle, non-promoting fibroblasts (**Fig 2.4A** and **B**), arguing that HDAC inhibition is a potent SASP inducer *in vivo*. To further corroborate our findings, we tested the only HDAC inhibitor currently used in the clinic – vorinostat. Upon treatment with vorinostat, BJ fibroblasts activated SASP (**Fig S2.4B**) and promoted $HaCAT_{CBR}$ cell growth compared to their vehicle counterparts (**Fig 2.4C** and **D**). Together, our results indicate that HDAC inhibition in the stroma activates a protumorigenic profile and leads to increased tumor growth *in vivo*.

HDAC1 inhibition activates OPN

There are three major groups of HDACs (excluding sirtuins) and 18 HDACs are present in the human genome. Most HDAC inhibitors target multiple HDACs; therefore, we next examined whether a specific HDAC was critical for OPN activation. A recent study analyzing stromal changes in breast cancer identified OPN as a key component of a stroma-derived prognostic predictor (SDPP) that successfully clustered tumors by clinical outcome (24). Oncomine-based interrogation of the same dataset revealed that HDAC1 levels were significantly ($p < 0.05$) lower in breast cancer-associated stroma compared to normal stroma (**Fig 2.5A**). Given that the SASP is reminiscent of the expression profile observed in cancer-associated fibroblasts and that the HDAC inhibitors used in our study target HDAC1, we examined whether HDAC1 played an important role in OPN activation.

To determine whether HDAC1 levels changed in vehicle versus bleomycin-treated cells, we examined HDAC1 mRNA levels by quantitative PCR (qPCR). In agreement with our previous microarray data (15), we observed a decrease in HDAC1 mRNA levels in bleomycin-treated fibroblasts compared to vehicle-treated cells (**Fig 2.5B**). When we immunoprecipitated HDAC1 from vehicle and bleomycin-treated fibroblasts and assayed for deacetylase activity, we observed a consistent decrease in cells treated with bleomycin (**Fig 2.5C**), raising the possibility that loss of HDAC1 activity specifically contributes to OPN activation following bleomycin treatment.

To directly test whether HDAC1 activity was important for the increase in OPN expression, we ectopically expressed a dominant-negative mutant of HDAC1 (HDAC1-DN) (20) in fibroblasts (**Fig S2.5A**). While overexpression of HDAC1-DN significantly reduced cell proliferation it did not result in growth arrest or SA-βgal expression ((36) and **Fig S2.5B**). However, we observed that ectopic expression of HDAC1-DN was sufficient to induce significant upregulation in OPN mRNA levels (**Fig 2.5D**), mirroring the response to treatments with HDAC inhibitors (**Fig 2.3B**). This finding further demonstrates that the induction of SASP can be decoupled from the induction of senescence. Importantly, this is an HDAC1-specific effect, because ectopic expression of an HDAC3 mutant (**Fig S2.4C**) did not alter OPN levels (**Fig 2.5D**). Analysis of IL6 and IL8 expression in HDAC1-DN expressing cells revealed that loss of HDAC1 activity was also sufficient to increase IL8 and to a lesser extent IL6 while HDAC3-DN had no impact on either IL6 or IL8. Together, these findings suggest that chromatin alterations via manipulation of HDAC1 activity impact the regulation of SASP independent of the activation of senescence.

DISCUSSION

Senescent fibroblasts promote tumorigenesis in multiple models (15, 37). In efforts to understand how this is accomplished, several groups have examined the expression profile of senescent cells and uncovered a signature secretory program enriched in growth factors, cytokines, and proteases termed the senescence-associated secretory phenotype (SASP) (9, 10, 15, 17). Specific SASP components have been directly

implicated in senescent stromal-promoted tumorigenesis (9, 15, 28, 38). However, it is still unclear how SASP is activated. Initial findings demonstrated that the transcription factors NF-κB and C/EBPβ directly bind the promoters of some of the inflammatory cytokines expressed in senescent cells (9, 10, 28). Additionally, the DNA damage response (DDR) was identified as an upstream SASP inducer (1). Indeed, the above-mentioned transcription factors can be activated in response to DNA damage (39, 40), although the mechanism of activation in senescence is not known. Utilizing osteopontin (OPN) as a surrogate for SASP regulation, we found that the SASP is not characterized by a single transcriptional axis, but is instead controlled by at least two independent signaling cascades both of which may be activated in response to chromatin changes.

OPN impacts a vast array of signaling pathways, hence its transcription is governed by multiple mechanisms in a tissue- and context-dependent manner (11). We demonstrate that following a senescence-inducing dose of bleomycin, OPN expression is not controlled by p53, Rb, or NF-κB, although p53 and NF-κB binding sites are present in the OPN promoter and are used in some biological settings (26, 29). The lack of p53 and Rb involvement is in agreement with previous work showing that these essential senescence effector pathways are dispensable for activation of the SASP factors IL6 and IL8 (17). Furthermore, our work demonstrates that OPN, like other SASP factors including IL6 and IL8, is expressed in cells that are unable to senesce due to abrogation of the p53 and Rb pathways. This finding is significant because it demonstrates that while senescent cells express SASP factors, the induction of senescence is not required

to activate SASP. Thus, SASP activation may occur in a wide variety of stromal cells undergoing cellular stress. It is interesting to note that the SASP is highly reminiscent of the expression profile observed in cancer associated fibroblasts (CAFs), which like senescent cells stimulate tumor formation in xenograft models (41).

This work and that of others demonstrates p53 and Rb are uniformly dispensable for SASP expression, yet it is clear that SASP regulation is complex and several distinct mechanisms drive expression of specific SASP factors. Indeed, we show that while NF-κB directly activates IL6 and IL8 (**Fig 2.2** and data not shown), it is not required for OPN upregulation in senescence (**Fig 2.2** and data not shown). Similarly, ATM knockdown has a profound effect on IL6 and IL8 expression, yet OPN increases to the same levels as in control cells (**Fig 2.2**). Together, these results indicate that IL6 and IL8 are activated by the DDR and NF-κB as has been demonstrated (1, 28), and OPN is not. Therefore, it is reasonable to speculate that subsets of SASP are regulated by discrete signaling pathways. In fact, SASP is defined by distinct classes of proteins such as growth factors, mitogens, and extracellular remodeling enzymes (15) whose activation may be governed by several mechanisms. Indeed, our work demonstrates that OPN regulation is distinct from the inflammatory cytokines IL6 and IL8 (9, 10). Discovery of putative activators of OPN and whether they control the expression of other proteins belonging to the extracellular matrix core of the SASP is the subject of ongoing work (15).

Despite the fact that IL6 and IL8 are regulated independently of OPN, following the induction of senescence, all three factors increase at the mRNA level, arguing that there must be a common inducer of SASP. Our work shows that ATM and NF-κB are not the sole SASP regulators, raising the possibility that an upstream stimulus initiates multiple signaling cascades. Our experiments with histone deacetylase inhibitors demonstrate that in the absence of DNA breaks (as measured by H2AX phosphorylation and comet assays (see **Fig 2.3** and (8)), SASP is still activated. Interestingly, ATM and NF-κB are still required for the upregulation of IL6 and IL8 (**Fig 2.3**) in HDAC inhibitor-induced SASP, thus lending additional support to the argument that DNA damage signaling, but not breaks per se, activates SASP. HDAC inhibition modifies the chromatin by inducing hyperacetylation of histone and non-histone proteins (42), resulting in sustained transcriptional changes (42). The data presented here fit a model wherein ATM activation upon bleomycin and NaB treatment occurs in response to chromatin alteration. It is known that DNA breaks induce changes in the surrounding chromatin, which facilitates signaling and repair; conversely, chromatin modifications trigger the DNA damage checkpoint (43). Indeed, because treatment with an HDAC inhibitor activates ATM (35), it is plausible that chromatin relaxation in senescence induces ATM activation and subsequent IL6 and IL8 expression.

While it is unclear how chromatin changes are instituted and maintained in senescence, there is ample evidence for their presence (2, 44). It is conceivable that widespread chromatin modifications impact promoter activity globally. However, only two percent of

the genes are differentially regulated in senescence (15) making this unlikely. Furthermore, specific transcription factors (e.g., NF-κB and C/EBPβ) are required for expression of some SASP factors, pointing to a regulated mechanism of expression. Finally, our results demonstrate that only specific chromatin modifiers impact OPN expression. Specifically, inhibition of HDAC1 but not HDAC3, upregulates OPN, IL6, and IL8 mRNA levels. Furthermore, we observe a reduction in HDAC1 levels and activity in senescent cells compared to their vehicle-treated counterparts. Together these data argue that HDAC1 containing complexes drive chromatin alterations that then drive OPN expression. HDACs role in transcriptional regulation is not limited to SASP. Indeed, HDAC1 inhibition results in an altered transcriptional profile in HGPS cells (5). Additionally, HDAC1 is decreased in breast cancer stroma (**Fig 2.5A** and (24)), which also undergoes profound transcriptional changes that alter the microenvironment and contribute to tumorigenesis. What initiates the changes in chromatin in these different biological settings is currently unknown and the triggers are likely to vary depending on the biological context. It is known that HDAC1 binds Rb (45) and interestingly, individual inhibition of either Rb or HDAC1 leads to marked upregulation of OPN mRNA levels (**Figs 2.1** and **2.5**), raising the possibility that in non-senescent cells HDAC1 complexes occupy SASP promoters and actively repress transcription, but upon senescence induction, they translocate preferentially to E2F targets (45). It remains to be determined if the Rb-HDAC1 complex is targeted to the promoters of OPN and other SASP members or whether it controls upstream regulators.

Our results add an additional layer of complexity to HDACs and their putative involvement in the tumor microenvironment. Recently, significant effort has been invested in designing HDAC inhibitors as anticancer agents leading to the approval of one compound, vorinostat (also known as SAHA), for the treatment of cutaneous T-cell lymphoma (46) and several others currently in clinical trials (47). Most studies focus on the antiproliferative or apoptotic effects of these reagents on tumor cells and report a minimal impact on normal cells (46, 48, 49). Indeed, we and others demonstrate that normal cells, including fibroblasts, are relatively resistant to apoptosis (50) but can assume a senescence-like state following HDAC inhibitor treatment (8). Moreover, regardless of the effect on cell cycle progression, all the HDAC inhibitors we tested (**Fig 2.3B**) robustly upregulate SASP expression and promote tumor growth *in vivo* in a paracrine fashion (**Fig 2.4)**. The half-life of the HDAC inhibitors used in the clinic is relatively short (50), limiting the therapeutic window for solid malignancies (51). However, the molecular responses as measured by overall hyperacetylation are sustained following treatment with HDAC inhibitors. Our results indicate that the transcriptional changes associated with HDAC inhibitor treatment are maintained in normal fibroblasts, and previous studies have demonstrated that the SASP is a chronic response (1). Therefore, it will be important to assess sustained molecular changes in the stroma that may lead to increased tumor formation following HDAC therapy. Our work underscores the importance of examining the tumor microenvironment when analyzing the profile of therapeutic agents.

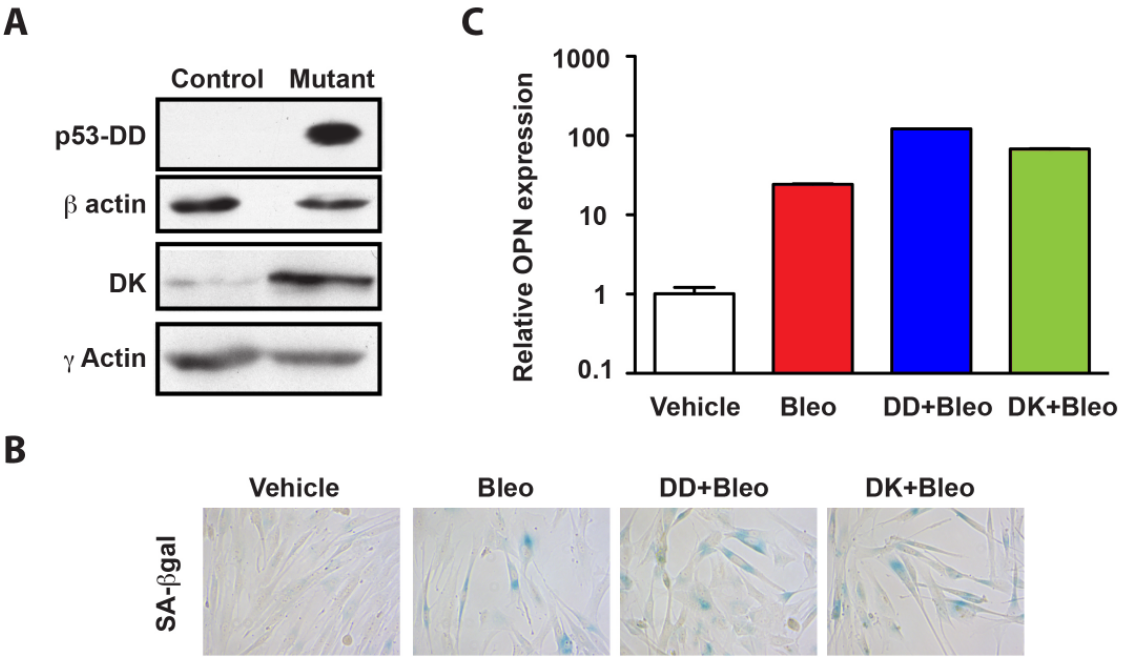

Fig 2.1: The senescence effector pathways p53 and Rb are not required to activate OPN. A) Western blot analysis of BJ fibroblasts transduced with a p53 mutant (DD) or CDK4/DK fusion construct that inhibits p53 and Rb respectively. B) SA-βgal staining of BJ fibroblasts transduced with vector control, DD or DK treated with vehicle alone or bleomycin (bleo). C) qPCR analysis of OPN mRNA levels in cells described in A following treatment with vehicle or bleomycin. Data represent mean + SD, n=3.

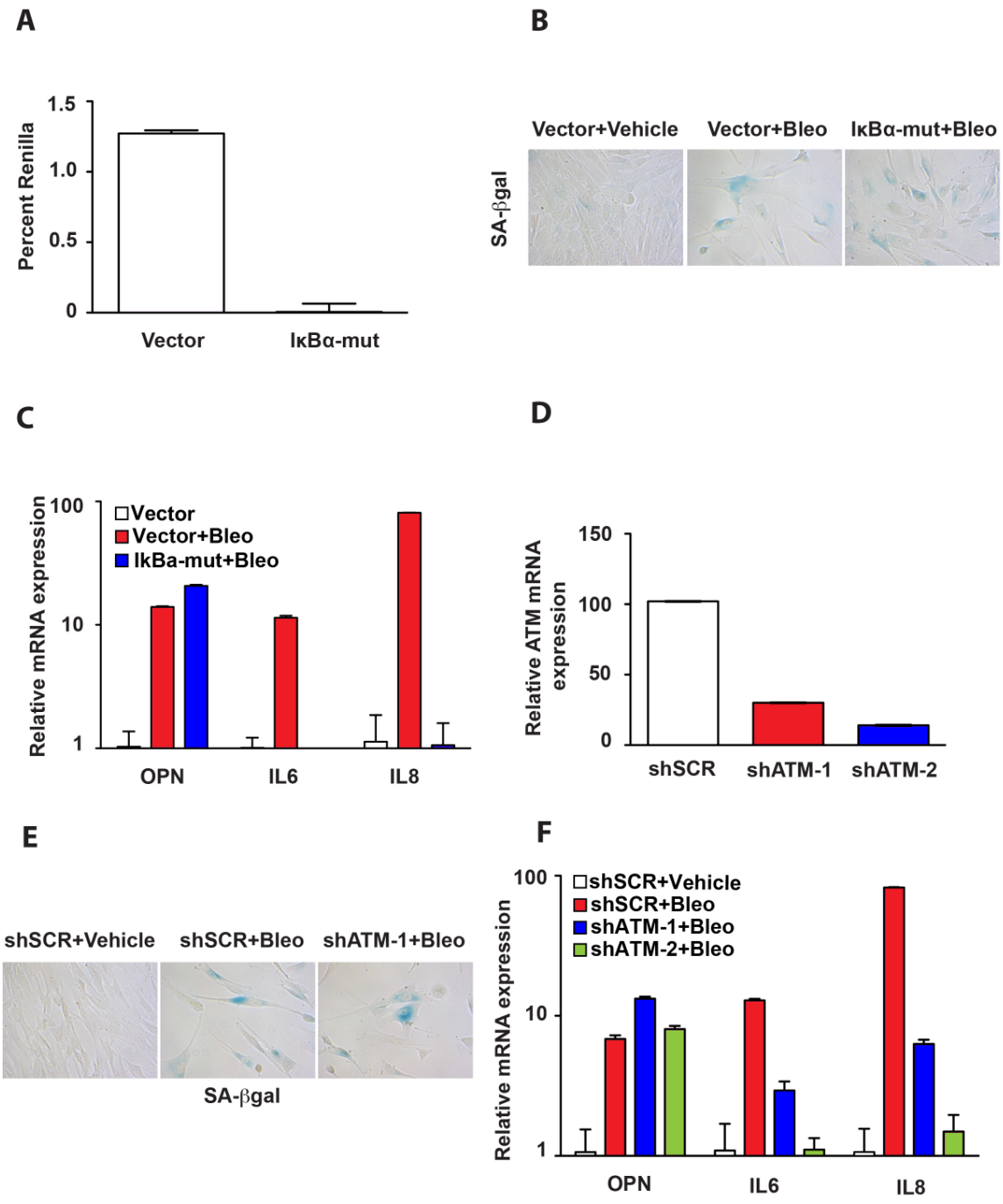

Fig 2.2: SASP is controlled by distinct regulatory mechanisms. A) BJ fibroblasts were transduced with a control vector or IκBα-mut. Inhibiton of NFκB was analyzed by transfection with an NFκB luciferase reporter plasmid. Data represent mean + SEM,

n=3. B) SA-βgal staining of BJ fibroblasts transduced with either a vector control or IκBα-mut. Cells were treated with either vehicle or bleomycin. C) qPCR was used to analyzed mRNA levels of IL6, IL8 and OPN in vehicle or bleomycin-treated BJ fibroblasts transduced with vector control and bleomycin-treated BJ fibroblasts transduced with IκBα-mut. Data represent mean + SD, n=3. D) qPCR was used to analyze ATM depletion in BJ fibroblasts transduced with either two independent shRNA targeting ATM or a control shRNA (shSCR). E) SA-βgal staining of vehicle or bleomycin-treated BJ fibroblasts transduced with shSCR and bleomycin-treated BJ fibroblasts transduced with shATM-1. F) qPCR was used to measure OPN, IL6 and IL8 mRNA levels in vehicle or bleomycin-treated BJ fibroblasts transduced with shSCR and bleomycin-treated BJ fibroblasts transduced with shATM-1 or shATM-2. Data represent mean + SD, n=3.

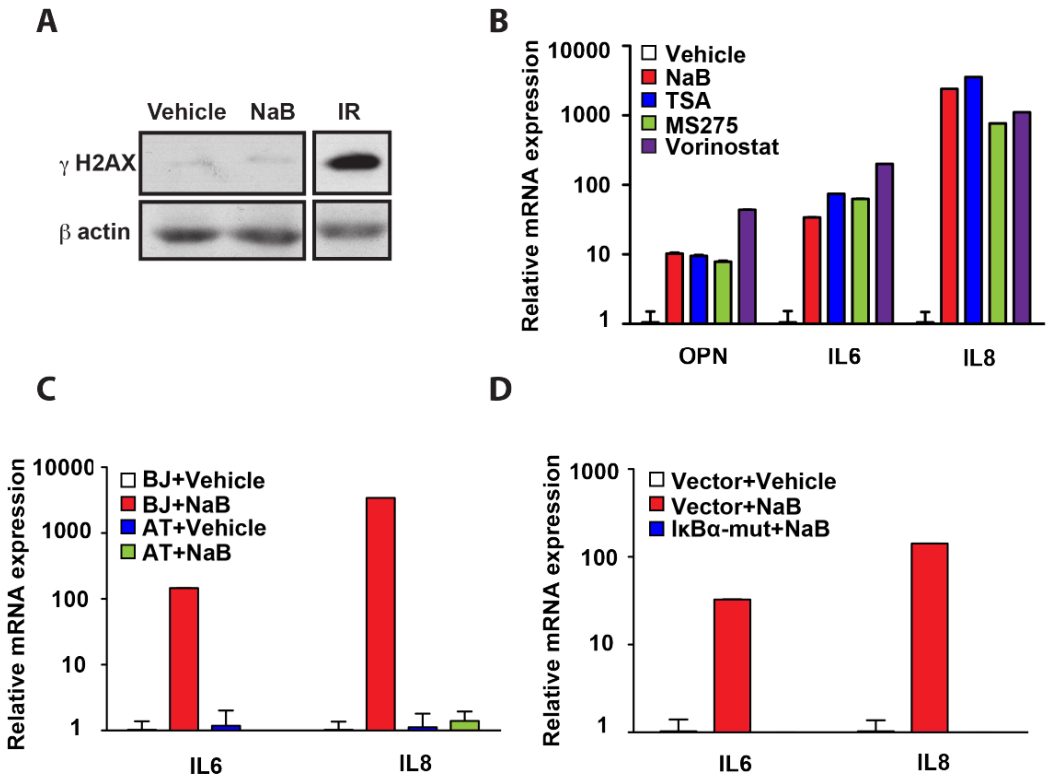

Fig 2.3: Histone deacetylase (HDAC) inhibition induces SASP. A) Western blot for γH2AX in vehicle or NaB-treated BJ fibroblasts. Cells were irradiated with 10 Gy (IR) to serve as a positive control. B) qPCR was used to measure the mRNA levels of OPN, IL6 and IL8 in BJ fibroblasts treated with vehicle or a variety of HDAC inhibitors. Data represent mean + SD, n=3. C) qPCR was used to measure IL6 and IL8 mRNA levels in BJ fibroblasts and AT fibroblasts treated with vehicle or NaB. Data represent mean + SD, n=3. D) qPCR was used to measure IL6 and IL8 mRNA levels in vehicle or NaB-treated BJ fibroblasts transduced with vector control and NaB-treated BJ fibroblasts transduced with IκBα-mut. Data represent mean + SD, n=3.

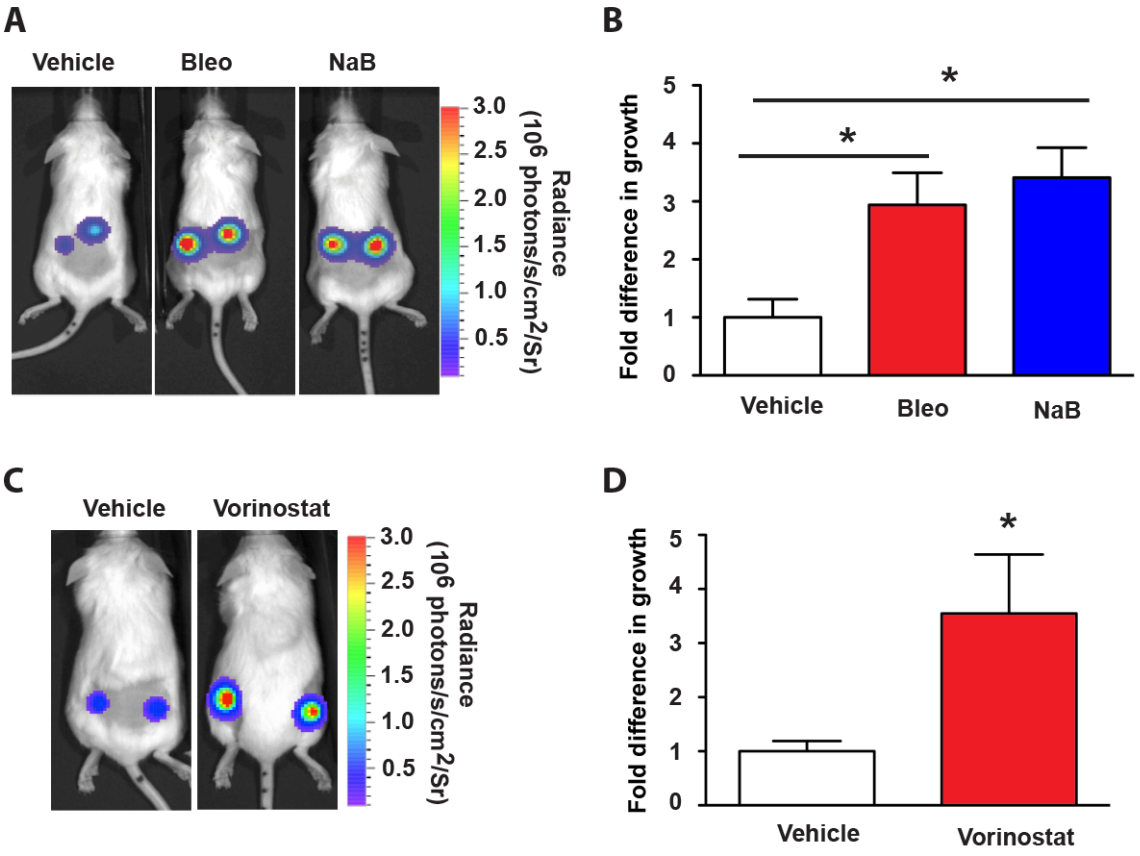

Fig 2.4: HDAC inhibition creates a pro-tumorigenic microenvironment. A) bioluminescent images (day 10) of representative mice injected in the flanks with $HaCaT_{CBR}$ cells in combination with vehicle-treated (vehicle), bleomycin-treated (Bleo), or NaB-treated (NaB) fibroblasts. B) Quantification of the luminescence in A [measured as photons/second/cm^2/steradian (photons/s/cm^2/Sr)]. Data represent mean + SEM, n=8. *, $P < 0.05$. C) Bioluminescent images (day 12) of representative mice injected in the flanks with a mixture of $HaCaT_{CBR}$ cells with either vehicle-treated BJ fibroblasts or vorinostat-treated BJ fibroblasts D) Quantification of the luminescence in the groups described in C. Data represent mean + SEM, n=8. *, $P < 0.05$.

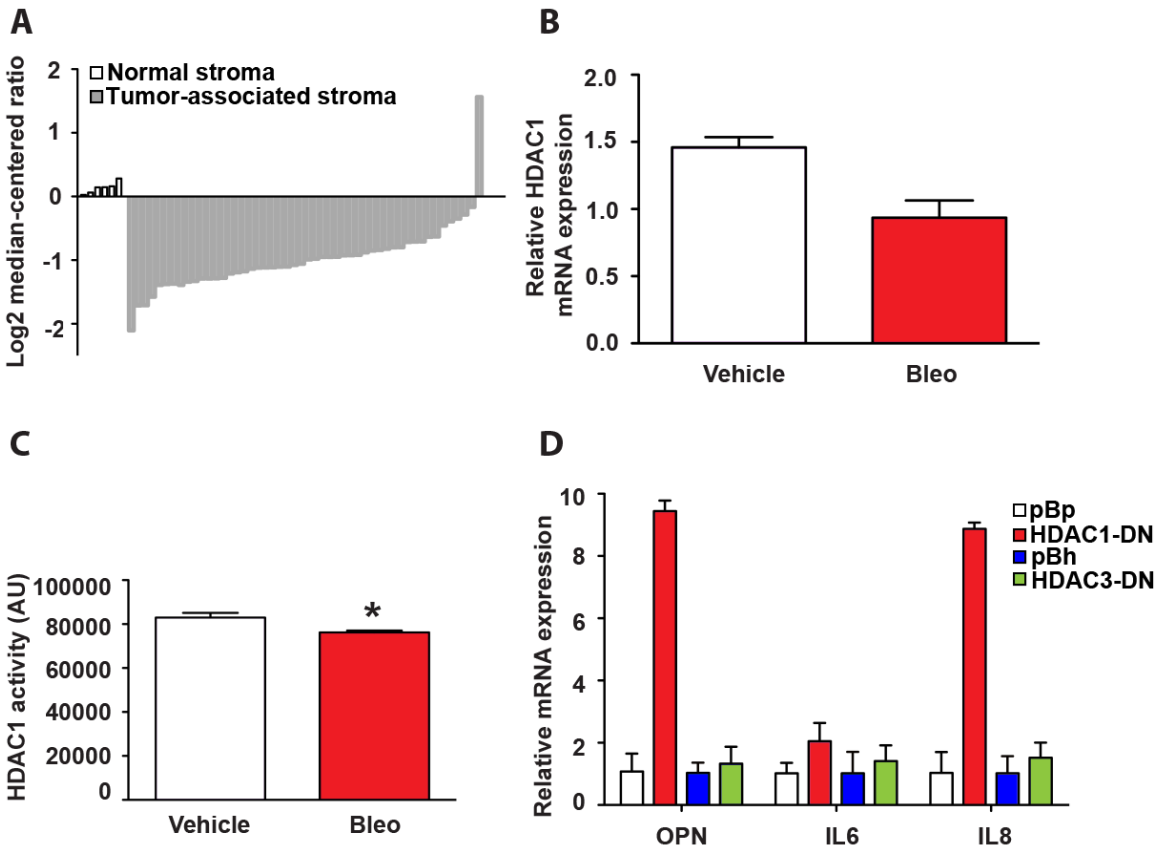

Fig 2.5: HDAC1 inhibition activates OPN. A) Oncomine expression analysis of HDAC1 levels between normal stroma and invasive breast cancer-associated stroma extracted from the study of Finak and colleagues. Expression values are log transformed and median centered per array (see Materials and Methods). B) qPCR was used to measure HDAC1 mRNA levels in vehicle and bleomycin-treated BJ fibroblasts. Data represent mean + SD, n=3. C) HDAC1 activity was measured in lysates from vehicle or bleomycin-treated cells after immunoprecipitation of HDAC1 with an HDAC1 antibody. Data represent mean + SEM, n=3. *, $P < 0.05$. D) qPCR was used to measure OPN, IL6 and IL8 mRNA levels in BJ fibroblasts transduced with vector control (pBp or pBh), HDAC1-DN or HDAC3-DN. Data represent mean + SD, n=3.

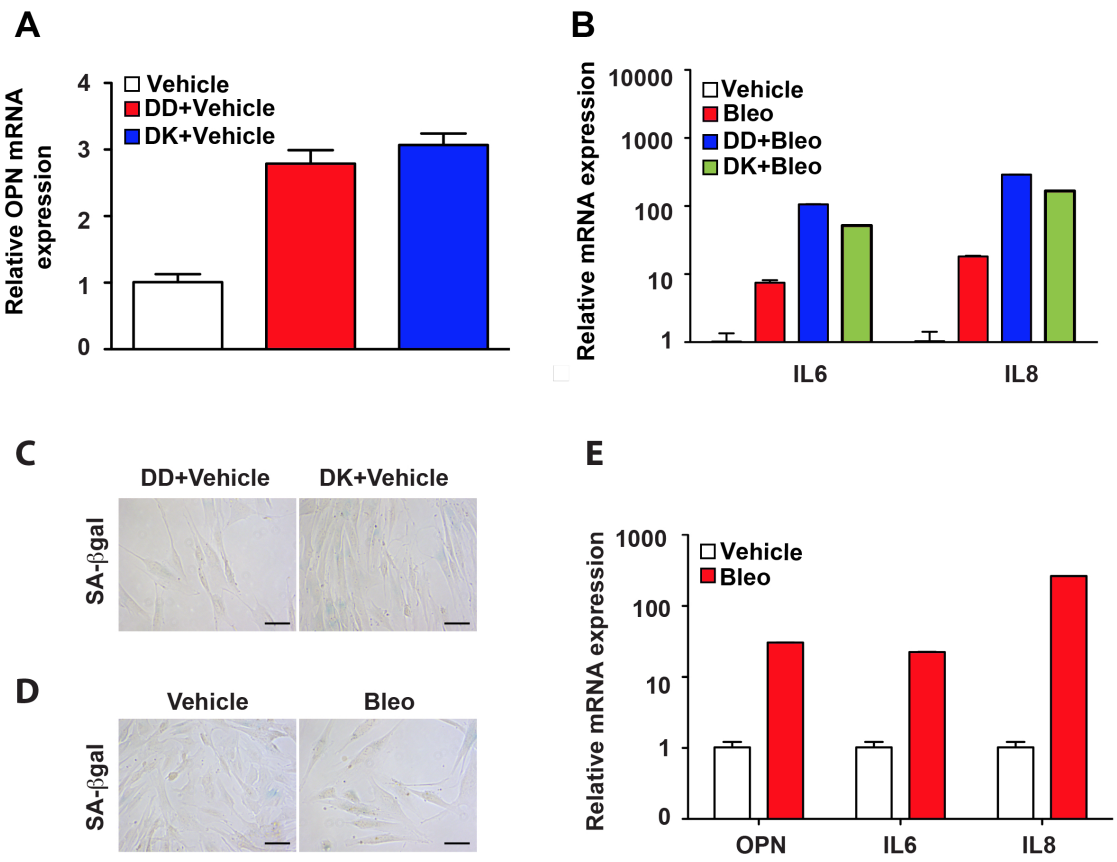

Fig S2.1: The senescence effectors are dispensable for SASP activation. A) qPCR was used to measure OPN mRNA levels in vehicle-treated BJ fibroblasts transduced with vector control, DD or DK. Data represent mean + SD, n=3. B) qPCR was used to measure IL6 and IL8 mRNA levels in vehicle or bleomycin (bleo)-treated BJ fibroblasts transduced with vector control and bleo-treated BJ fibroblasts transduced with DD or DK. Data represent mean + SD, n=3. C) SA-βgal staining of BJ fibroblasts transduced with DD or DK. D) SA-βgal staining of WI38tert-E6/7 fibroblasts treated with bleomycin (bleo). E) qPCR was used to measure OPN, IL6 and IL8 mRNA levels in WI38TH-E6E7 fibroblasts treated with vehicle or bleomycin (bleo). Data represent mean + SD, n=3.

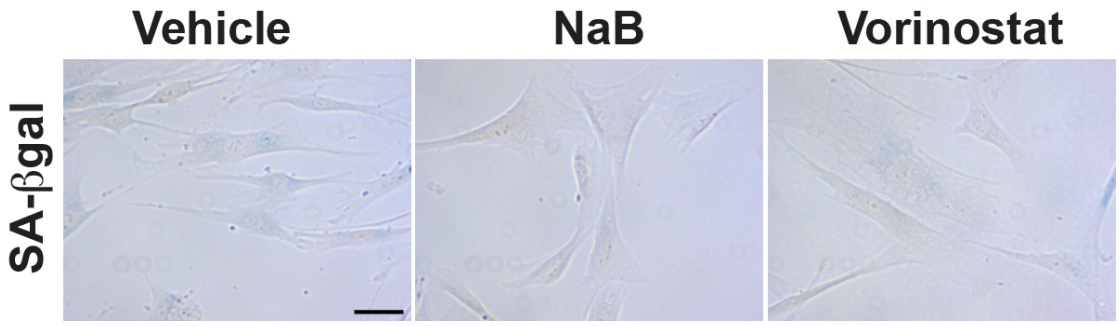

Fig S2.2: SA-βgal staining of BJ fibroblasts treated with vehicle, NaB or vorinostat.

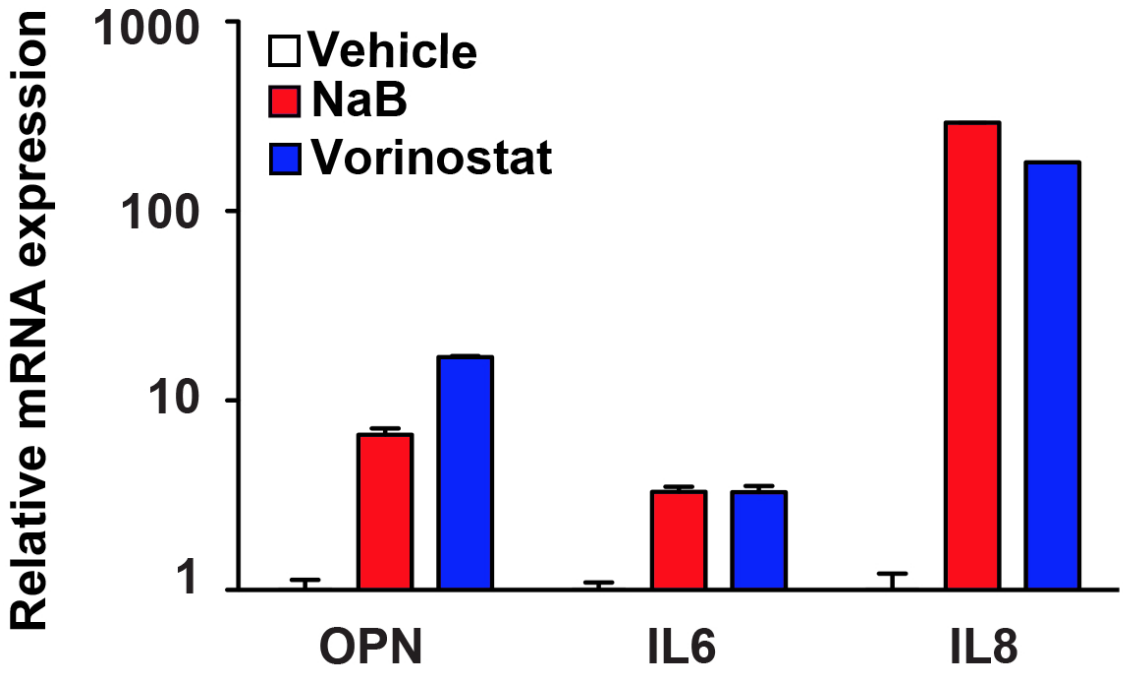

Fig S2.3: SASP activation in primary breast fibroblasts. qPCR was used to measure mRNA levels of OPN, IL6 and IL8 in breast fibroblasts treated with vehicle, NaB or vorinostat.

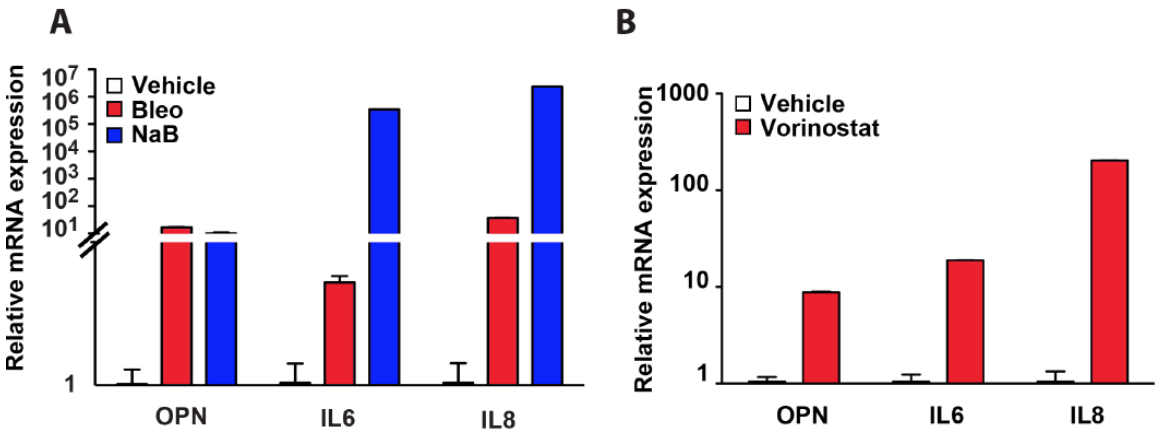

Fig S2.4: SASP activation in cells used in xenografts. A) qPCR was used to measure OPN, IL6 and IL8 mRNA levels in BJ fibroblasts treated with vehicle, bleomycin (bleo) or NaB. B) qPCR was used to measure OPN, IL6 and IL8 mRNA levels in BJ fibroblasts treated with vehicle or vorinostat.

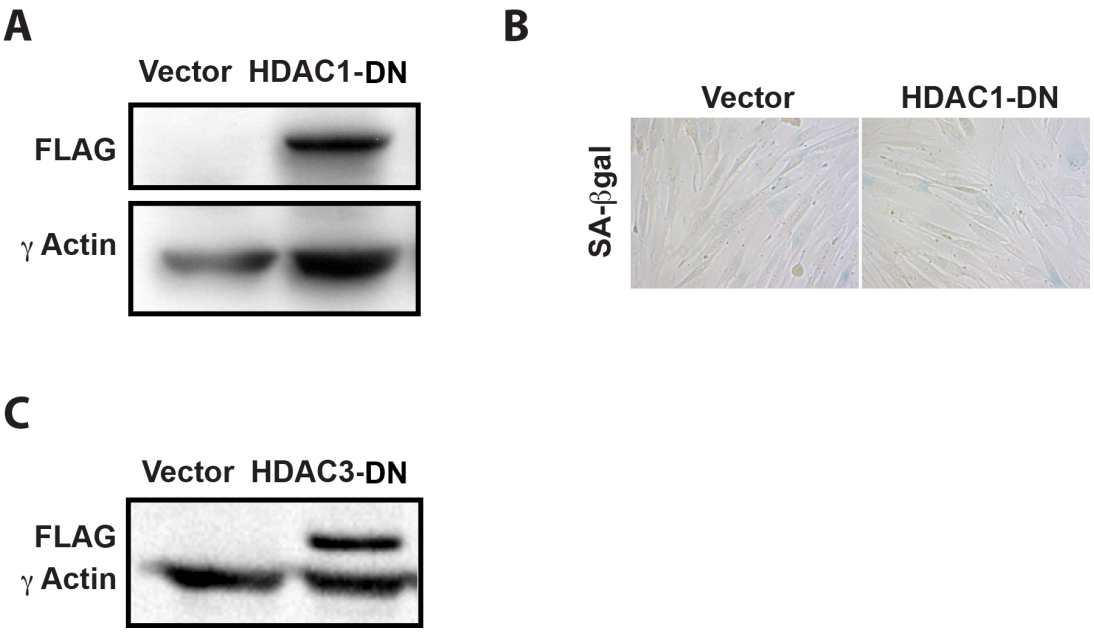

Fig S2.5: Ectopic expression of dominant negative HDAC1 and HDAC3 constructs. A) Western blot analysis of BJ fibroblasts transduced with vector or FLAG-tagged HDAC1-DN. B) SA-βgal staining of BJ fibroblasts transduced with vector or HDAC1-DN. C) Western blot analysis of BJ fibroblasts transduced with vector or FLAG-tagged HDAC3-DN

REFERENCES

1. Rodier F, Coppe JP, Patil CK, Hoeijmakers WA, Munoz DP, Raza SR, Freund A, Campeau E, Davalos AR, Campisi J. Persistent DNA damage signalling triggers senescence-associated inflammatory cytokine secretion. Nature cell biology. 2009;11(8):973-9.

2. Narita M, Nunez S, Heard E, Lin AW, Hearn SA, Spector DL, Hannon GJ, Lowe SW. Rb-mediated heterochromatin formation and silencing of E2F target genes during cellular senescence. Cell. 2003;113(6):703-16.

3. Oberdoerffer P, Sinclair DA. The role of nuclear architecture in genomic instability and ageing. Nature reviews Molecular cell biology. 2007;8(9):692-702. Epub 2007/08/19.

4. Haithcock E, Dayani Y, Neufeld E, Zahand AJ, Feinstein N, Mattout A, Gruenbaum Y, Liu J. Age-related changes of nuclear architecture in Caenorhabditis elegans. Proceedings of the National Academy of Sciences of the United States of America. 2005;102(46):16690-5. Epub 2005/11/05.

5. Pegoraro G, Kubben N, Wickert U, Gohler H, Hoffmann K, Misteli T. Ageing-related chromatin defects through loss of the NURD complex. Nature cell biology. 2009;11(10):1261-7.

6. Place RF, Noonan EJ, Giardina C. HDACs and the senescent phenotype of WI-38 cells. BMC Cell Biol. 2005;6:37.

7. Calvanese V, Lara E, Kahn A, Fraga MF. The role of epigenetics in aging and age-related diseases. Ageing Res Rev. 2009;8(4):268-76.

8. Pospelova TV, Demidenko ZN, Bukreeva EI, Pospelov VA, Gudkov AV, Blagosklonny MV. Pseudo-DNA damage response in senescent cells. Cell Cycle. 2009;8(24):4112-8.

9. Kuilman T, Michaloglou C, Vredeveld LC, Douma S, van Doorn R, Desmet CJ, Aarden LA, Mooi WJ, Peeper DS. Oncogene-induced senescence relayed by an interleukin-dependent inflammatory network. Cell. 2008;133(6):1019-31.

10. Acosta JC, O'Loghlen A, Banito A, Guijarro MV, Augert A, Raguz S, Fumagalli M, Da Costa M, Brown C, Popov N, Takatsu Y, Melamed J, d'Adda di Fagagna F, Bernard D, Hernando E, Gil J. Chemokine signaling via the CXCR2 receptor reinforces senescence. Cell. 2008;133(6):1006-18.

11. Rangaswami H, Bulbule A, Kundu GC. Osteopontin: role in cell signaling and cancer progression. Trends Cell Biol. 2006;16(2):79-87.

12. Senger DR, Wirth DF, Hynes RO. Transformed mammalian cells secrete specific proteins and phosphoproteins. Cell. 1979;16(4):885-93.

13. Rittling SR, Denhardt DT. Osteopontin function in pathology: lessons from osteopontin-deficient mice. Exp Nephrol. 1999;7(2):103-13.

14. Fedarko NS, Jain A, Karadag A, Van Eman MR, Fisher LW. Elevated serum bone sialoprotein and osteopontin in colon, breast, prostate, and lung cancer. Clinical cancer research : an official journal of the American Association for Cancer Research. 2001;7(12):4060-6.

15. Pazolli E, Luo X, Brehm S, Carbery K, Chung JJ, Prior JL, Doherty J, Demehri S, Salavaggione L, Piwnica-Worms D, Stewart SA. Senescent Stromal-Derived Osteopontin Promotes Preneoplastic Cell Growth. Cancer research. 2009.

16. Luo X, Ruhland MK, Pazolli E, Lind AC, Stewart SA. Osteopontin stimulates preneoplastic cellular proliferation through activation of the MAPK pathway. Molecular cancer research : MCR. 2011;9(8):1018-29. Epub 2011/06/16.

17. Coppe JP, Patil CK, Rodier F, Sun Y, Munoz DP, Goldstein J, Nelson PS, Desprez PY, Campisi J. Senescence-associated secretory phenotypes reveal cell-nonautonomous functions of oncogenic RAS and the p53 tumor suppressor. PLoS biology. 2008;6(12):2853-68.

18. Hahn WC, Dessain SK, Brooks MW, King JE, Elenbaas B, Sabatini DM, DeCaprio JA, Weinberg RA. Enumeration of the simian virus 40 early region elements necessary for human cell transformation. Molecular and cellular biology. 2002;22(7):2111-23.

19. Boehm JS, Zhao JJ, Yao J, Kim SY, Firestein R, Dunn IF, Sjostrom SK, Garraway LA, Weremowicz S, Richardson AL, Greulich H, Stewart CJ, Mulvey LA, Shen RR, Ambrogio L, Hirozane-Kishikawa T, Hill DE, Vidal M, Meyerson M, Grenier JK, Hinkle G, Root DE, Roberts TM, Lander ES, Polyak K, Hahn WC. Integrative genomic approaches identify IKBKE as a breast cancer oncogene. Cell. 2007;129(6):1065-79.

20. Ito K, Adcock IM. Histone acetylation and histone deacetylation. Mol Biotechnol. 2002;20(1):99-106.

21. Yang WM, Tsai SC, Wen YD, Fejer G, Seto E. Functional domains of histone deacetylase-3. The Journal of biological chemistry. 2002;277(11):9447-54.

22. Livak KJ, Schmittgen TD. Analysis of relative gene expression data using real-time quantitative PCR and the 2(-Delta Delta C(T)) Method. Methods. 2001;25(4):402-8. Epub 2002/02/16.

23. Rhodes DR, Kalyana-Sundaram S, Mahavisno V, Varambally R, Yu J, Briggs BB, Barrette TR, Anstet MJ, Kincead-Beal C, Kulkarni P, Varambally S, Ghosh D, Chinnaiyan AM. Oncomine 3.0: genes, pathways, and networks in a collection of 18,000 cancer gene expression profiles. Neoplasia. 2007;9(2):166-80.

24. Finak G, Bertos N, Pepin F, Sadekova S, Souleimanova M, Zhao H, Chen H, Omeroglu G, Meterissian S, Omeroglu A, Hallett M, Park M. Stromal gene expression predicts clinical outcome in breast cancer. Nat Med. 2008;14(5):518-27.

25. Shay JW, Pereira-Smith OM, Wright WE. A role for both RB and p53 in the regulation of human cellular senescence. Experimental cell research. 1991;196(1):33-9.

26. Morimoto I, Sasaki Y, Ishida S, Imai K, Tokino T. Identification of the osteopontin gene as a direct target of TP53. Genes Chromosomes Cancer. 2002;33(3):270-8.

27. Karin M. NF-kappaB as a critical link between inflammation and cancer. Cold Spring Harbor perspectives in biology. 2009;1(5):a000141.

28. Orjalo AV, Bhaumik D, Gengler BK, Scott GK, Campisi J. Cell surface-bound IL-1alpha is an upstream regulator of the senescence-associated IL-6/IL-8 cytokine network. Proceedings of the National Academy of Sciences of the United States of America. 2009;106(40):17031-6.

29. Renault MA, Jalvy S, Potier M, Belloc I, Genot E, Dekker LV, Desgranges C, Gadeau AP. UTP induces osteopontin expression through a coordinate action of NFkappaB, activator protein-1, and upstream stimulatory factor in arterial smooth muscle cells. The Journal of biological chemistry. 2005;280(4):2708-13.

30. Di Micco R, Fumagalli M, Cicalese A, Piccinin S, Gasparini P, Luise C, Schurra C, Garre M, Nuciforo PG, Bensimon A, Maestro R, Pelicci PG, d'Adda di Fagagna F. Oncogene-induced senescence is a DNA damage response triggered by DNA hyper-replication. Nature. 2006;444(7119):638-42.

31. Paull TT, Rogakou EP, Yamazaki V, Kirchgessner CU, Gellert M, Bonner WM. A critical role for histone H2AX in recruitment of repair factors to nuclear foci after DNA damage. Curr Biol. 2000;10(15):886-95.

32. Singh NP, McCoy MT, Tice RR, Schneider EL. A simple technique for quantitation of low levels of DNA damage in individual cells. Experimental cell research. 1988;175(1):184-91.

33. Wagner JM, Hackanson B, Lubbert M, Jung M. Histone deacetylase (HDAC) inhibitors in recent clinical trials for cancer therapy. Clin Epigenetics.1(3-4):117-36.

34. Grant S, Dent P. Simultaneous interruption of signal transduction and cell cycle regulatory pathways: implications for new approaches to the treatment of childhood leukemias. Current drug targets. 2007;8(6):751-9.

35. Bakkenist CJ, Kastan MB. DNA damage activates ATM through intermolecular autophosphorylation and dimer dissociation. Nature. 2003;421(6922):499-506.

36. Lagger G, O'Carroll D, Rembold M, Khier H, Tischler J, Weitzer G, Schuettengruber B, Hauser C, Brunmeir R, Jenuwein T, Seiser C. Essential function of histone deacetylase 1 in proliferation control and CDK inhibitor repression. The EMBO journal. 2002;21(11):2672-81.

37. Krtolica A, Parrinello S, Lockett S, Desprez PY, Campisi J. Senescent fibroblasts promote epithelial cell growth and tumorigenesis: a link between cancer and aging. Proceedings of the National Academy of Sciences of the United States of America. 2001;98(21):12072-7.

38. Parrinello S, Coppe JP, Krtolica A, Campisi J. Stromal-epithelial interactions in aging and cancer: senescent fibroblasts alter epithelial cell differentiation. Journal of cell science. 2005;118(Pt 3):485-96.

39. Wu L, Multani AS, He H, Cosme-Blanco W, Deng Y, Deng JM, Bachilo O, Pathak S, Tahara H, Bailey SM, Behringer RR, Chang S. Pot1 deficiency initiates DNA damage checkpoint activation and aberrant homologous recombination at telomeres. Cell. 2006;126(1):49-62.

40. Elkon R, Rashi-Elkeles S, Lerenthal Y, Linhart C, Tenne T, Amariglio N, Rechavi G, Shamir R, Shiloh Y. Dissection of a DNA-damage-induced transcriptional network using a combination of microarrays, RNA interference and computational promoter analysis. Genome Biol. 2005;6(5):R43.

41. Olumi AF, Grossfeld GD, Hayward SW, Carroll PR, Tlsty TD, Cunha GR. Carcinoma-associated fibroblasts direct tumor progression of initiated human prostatic epithelium. Cancer research. 1999;59(19):5002-11.

42. Buchwald M, Kramer OH, Heinzel T. HDACi--targets beyond chromatin. Cancer letters. 2009;280(2):160-7.

43. van Attikum H, Gasser S. Crosstalk between histone modifications during the DNA damage response. Trends Cell Biol. 2009;19(5):207-17.

44. Oberdoerffer P, Michan S, McVay M, Mostoslavsky R, Vann J, Park SK, Hartlerode A, Stegmuller J, Hafner A, Loerch P, Wright SM, Mills KD, Bonni A, Yankner BA, Scully R, Prolla TA, Alt FW, Sinclair DA. SIRT1 redistribution on chromatin promotes genomic stability but alters gene expression during aging. Cell. 2008;135(5):907-18.

45. Magnaghi-Jaulin L, Groisman R, Naguibneva I, Robin P, Lorain S, Le Villain JP, Troalen F, Trouche D, Harel-Bellan A. Retinoblastoma protein represses transcription by recruiting a histone deacetylase. Nature. 1998;391(6667):601-5.

46. Dokmanovic M, Clarke C, Marks PA. Histone deacetylase inhibitors: overview and perspectives. Molecular cancer research : MCR. 2007;5(10):981-9.

47. Tan J, Cang S, Ma Y, Petrillo RL, Liu D. Novel histone deacetylase inhibitors in clinical trials as anti-cancer agents. J Hematol Oncol.3:5.

48. Qiu L, Burgess A, Fairlie DP, Leonard H, Parsons PG, Gabrielli BG. Histone deacetylase inhibitors trigger a G2 checkpoint in normal cells that is defective in tumor cells. Molecular biology of the cell. 2000;11(6):2069-83.

49. Ungerstedt JS, Sowa Y, Xu WS, Shao Y, Dokmanovic M, Perez G, Ngo L, Holmgren A, Jiang X, Marks PA. Role of thioredoxin in the response of normal and

transformed cells to histone deacetylase inhibitors. Proceedings of the National Academy of Sciences of the United States of America. 2005;102(3):673-8.

50. Kelly WK, O'Connor OA, Krug LM, Chiao JH, Heaney M, Curley T, MacGregore-Cortelli B, Tong W, Secrist JP, Schwartz L, Richardson S, Chu E, Olgac S, Marks PA, Scher H, Richon VM. Phase I study of an oral histone deacetylase inhibitor, suberoylanilide hydroxamic acid, in patients with advanced cancer. Journal of clinical oncology : official journal of the American Society of Clinical Oncology. 2005;23(17):3923-31.

51. Munster PN, Thurn KT, Thomas S, Raha P, Lacevic M, Miller A, Melisko M, Ismail-Khan R, Rugo H, Moasser M, Minton SE. A phase II study of the histone deacetylase inhibitor vorinostat combined with tamoxifen for the treatment of patients with hormone therapy-resistant breast cancer. British journal of cancer.104(12):1828-35.

CHAPTER 3

The transcription factor c-myb is a novel regulator of SASP expression

Elise Alspach*, Kevin Flanagan*, Ermira Pazolli* and Sheila A. Stewart

*E. Alspach, K. Flanagan and E. Pazolli contributed equally to this work

INTRODUCTION

In the past decade, the microenvironment's role in tumorigenesis has become well established. Indeed, in xenograft models, preneoplastic cells from a variety of tissues fail to grow in the absence of associated stroma (1, 2). Senescent fibroblasts, which accumulate with age (3, 4), are hypothesized to contribute to stroma-mediated tumor support. Interestingly, senescent fibroblasts stimulate preneoplastic cell growth in co-culture and xenograft settings (5-7). The induction of senescence results in an altered gene expression profile known as the senescence-associated secretory phenotype (SASP) (8). The SASP is enriched in proteins involved in extracellular-matrix remodeling, promotion of proliferation, immune cell recruitment and angiogenesis--processes that are critical for the establishment and progression of tumors (9, 10). Because senescent cells accumulate in tissues with age and have a pro-tumorigenic secretory profile, the presence of senescent cells in the tumor microenvironment is hypothesized to contribute to age-related increases in cancer risk.

The SASP factor osteopontin (OPN) is a secreted phospho-protein with multiple cell-signaling roles. We have documented the pro-tumorigenic nature of OPN secreted from senescent cells (10). Indeed, depletion of OPN from senescent cells through expression of short hairpin RNA (shRNA) molecules results in an inability of senescent fibroblasts to promote the growth of preneoplastic keratinocytes *in vivo* (10). Furthermore, treatment of preneoplastic keratinocytes with recombinant OPN is sufficient to promote

their growth (10). These data indicate that senescent fibroblast-derived OPN is an important driver of SASP-mediated tumorigenesis.

Given the pro-tumorigenic nature of OPN, understanding its regulation is important in elucidating therapeutic targets that will be utilized to inhibit its expression. IL6, IL8, and many other SASP factors are regulated by a pathway involving the transcription factor NFκB and the DNA damage response protein ATM (11-14). In contrast, little is known about how OPN is activated in response to senescence. Previous work by our laboratory has implicated the histone deacetylase complex 1 (HDAC1) in OPN expression in senescent cells (13). Treatment of fibroblasts with HDAC inhibitors like sodium butyrate is sufficient to induce the expression of OPN and other SASP factors (13). Furthermore, expression of an HDAC1 dominant negative construct in young fibroblasts is sufficient to drive the upregulation of OPN (13). This effect is specific to HDAC1, as expression of an HDAC3 dominant negative construct does not increase OPN expression (13). These data indicate that HDAC1 is a negative regulator of OPN regulation and must be inactivated to achieve OPN upregulation. Positive regulators of OPN in senescent cells, however, remain to be elucidated.

The transcription factor c-myb has well characterized roles in hematopoietic cells, where it regulates growth and differentiation (15). C-myb has also been implicated in oncogenesis in various tissues including breast and colon (16, 17). The transcriptional activation of targets by c-myb can occur in both DNA binding-dependent and

independent mechanisms (18, 19). C-myb activity often requires the cooperation of co-activators, the most characterized of which is C/EBPβ (20, 15). Interestingly, c-myb has been shown to transcriptionally activate OPN in other settings (21, 22), although a role for c-myb in activating OPN in response to senescence has not been investigated.

Here, through analysis of the OPN promoter, we find that c-myb plays a key role in OPN regulation in response to senescence.

METHODS

Cells and reagents

BJ skin fibroblasts were grown under standard culture conditions in DMEM supplemented with 15% FBS, 15% M199 and penicillin/streptomycin. 293T kidney epithelial cells were cultured in DMEM supplemented with 10% FBS and penicillin/streptomycin. WI38 lung fibroblasts were cultured in DMEM supplemented with 10% FBS and penicillin/streptomycin. The OPN promoter reporter constructs were a gift from Dr. Paul Kuo (Duke University, Durham, NC). The pCDNA-myb overexpression construct was a gift from Dr. Robert Rosenberg (Harvard Medical School, Boston, MA). The pLXSN-mybENER construct was a gift from Dr. Linda Wolff (National Cancer Institute, Bethesda, MD). Senescence was induced with a 24 hour treatment of bleomycin (100 μg/mL, Sigma Aldrich, St. Louis, MO). For c-myb dominant negative studies, cells were treated with tamoxifen for 24 hours (20μM, Sigma Aldrich, St. Louis, MO). shmyb #1 (5'-GAAATACGGTCCGAAAC-3, (23)) was subcloned in to pLKO using

the AgeI and EcoRI sites. shmyb #2 was purchased from Addgene (plasmid #25790, Cambridge, MA).

Luciferase Assay

Cells were transiently transfected with OPN promoter constructs and pGL3 *Renilla* plasmid control using Lipofectamine2000 following manufacturers protocols (Life Technologies, Carlsbad, CA). Luciferase activity was measured with the Dual-Luciferase Reporter Assay (Promega, Madison, WI).

qRT-PCR

Total RNA was isolated using the Ribopure RNA isolation kit (Life Technologies, Carlsbad, CA). cDNA was synthesized using previously published protocols (10). OPN mRNA was amplified with the following primers: F- TTGCAGCCTTCTCAGCCAA and R-AAGCAAATCACTGCAATTCTC. GAPDH mRNA was amplified with the following primers: F- GCATGGCCTTCCGTGTCC and R- ATGCCAGCCCCAGCGTCAAA. The endogenous OPN promoter was amplified with a custom Taqman probe designed to sit at the transcription start site (Assay ID AJRR84A, Life Technologies, Carlsbad, CA). c-myb mRNA was amplified using a Taqman probe (Hs00920556_m1, Life Technologies, Carlsbad, CA).

Virus Production

Virus was produced as previously published (10).

Chromatin Immunoprecipitation (ChIP)

Cells were fixed 48 hours after transfection using 1% formaldehyde in PBS for 10 minutes. Fixation was quenched with 125mM glycine for 5 minutes with gentle rotation.

Cells were lysed in lysis buffer (1% SDS, 10 mM EDTA, 50 mM Tris pH 8.1) for 15 minutes. The lysate was sonicated at 50 Amps with 30 s on, 30 s off for 6 rounds to achieve DNA fragments approximately 300-500 bp in length. 1 mg protein was used for each immunoprecipitation. Immunoprecipitation was performed with rabbit anti human c-myb (sc517, Santa Cruz Biotechnology, Dallas, TX) or normal rabbit IgG (Cell Signaling Technologies, Danvers, MA). OPN190 and OPN190mut were amplified by PCR with the following primers: F- CTTTATGTTTTTGCGTCTTCCA and R- CTAGCAAAATAGGCTGTCCC.

Immunofluorescence

Cells were fixed with 4% paraformaldehyde for 20 minutes. Cells were blocked and permeabilized with 8% BSA/0.1% triton-X for 20 minutes. Visualization of mybENER was done with rabbit anti engrailed (sc28640, Santa Cruz Biotechnology, Dallas, TX).

Site-directed mutagenesis of OPN190

The OPN190 luciferase reporter was mutagenized to remove the c-myb binding site using the QuikChange site-directed mutagenesis kit (Agilent Technologies, Santa Clara, CA). The sequence of the OPN promoter was changed from ATGTTTTAACTGTAGATTGTGTG to ATGTTTT**GCTA**GTAGA**C**TGTGTG (the c-myb binding site is shaded and the changed nucleotides are in bold).

RESULTS

The senescence-responsive region of the OPN promoter contains a c-myb binding site

To identify senescence-specific transcriptional regulators of OPN, we first sought to identify the region of the OPN promoter that was activated in response to senescence induction. To do so, regions of the OPN promoter ranging from 80 base pairs upstream of the transcriptional start site (TSS) to 2 kb upstream of the TSS were used to drive expression of a luciferase reporter. These OPN reporter constructs were then transiently transfected into young fibroblasts or fibroblasts made senescent though treatment with the DNA damaging agent bleomycin (referred to as stress-induced premature senescence or SIPS). Following transduction luciferase activity was measured to assess the transcriptional activity of the OPN promoter. We observed that a region 190 base pairs upstream of the TSS (OPN190) was consistently activated in response to senescence compared to the level of activity observed in young fibroblasts (**Fig 3.1A**). We then subjected OPN190 to transcription factor binding site analysis using Transfac®. A perfectly conserved binding site for the c-myb transcription factor (TAACTGT) was identified in this region (**Fig 3.1B**). These results suggest that the transcription factor c-myb is responsible for activation of the OPN promoter in response to senescence.

c-myb is required for activation of OPN in response to senescence

The presence of a c-myb binding site within the senescence-responsive region of the OPN promoter implicated c-myb in OPN activation. To determine if c-myb is required for

the transcriptional activation of OPN in response to senescence, BJ fibroblasts were depleted of c-myb using two independent shRNA (shmyb #1 and shmyb #2). Depletion of c-myb was verified by quantitative real-time PCR (qRT-PCR) (**Fig 3.2A**). In response to c-myb depletion, senescence-dependent OPN expression was significantly reduced (**Fig 3.2B**), indicating that c-myb activity is required for the activation of OPN in the senescent context.

To further verify the results of c-myb depletion using shRNA, we used a c-myb dominant negative construct consisting of the c-myb DNA binding domain fused to the *engrailed* trans-repressor domain and the estrogen receptor (mybENER). When cells are treated with tamoxifen, the mybENER construct translocates to the nucleus, binds c-myb binding sequences and represses gene expression (24). Senescent WI38 lung fibroblasts stably expressing mybENER were treated with vehicle or tamoxifen to induce translocation of the construct (**Fig 3.2C**) and OPN levels were analyzed by qRT-PCR. In contrast to vehicle treated senescent fibroblasts, activation of mybENER in senescent fibroblasts resulted in a significant decrease in OPN expression (**Fig 3.2D**), recapitulating the results observed in response to depletion of c-myb through the expression of shRNA. These data further indicate that transcriptional activation by c-myb is required for the activation of OPN in response to senescence.

c-myb DNA binding is required for OPN activation

C-myb can activate its transcriptional targets through both DNA binding-dependent and independent mechanisms (18, 19). To determine if c-myb directly controlled OPN expression in response to senescence, we utilized site-directed mutagenesis to mutate the c-myb binding region of the OPN190 reporter (OPN190mut). Senescent BJ fibroblasts were transiently transfected with either the wild-type OPN190 or OPN190mut construct and luciferase activity was used to measure the transcriptional activity of the OPN promoter. Compared to senescent fibroblasts transfected with wild-type OPN190, senescent fibroblasts transfected with OPN190mut displayed significantly reduced luciferase activity (**Fig 3.3A**) indicating that the c-myb binding site is required for OPN promoter responsiveness to senescence induction.

To further verify that the putative c-myb binding site identified in the OPN promoter was bound by c-myb we performed chromatin immunoprecipitation (ChIP) of c-myb from wild-type OPN190 or OPN190mut. Briefly, 293T kidney epithelial cells were transfected with a c-myb overexpression construct and either OPN190 or OPN190mut. 293T cell lysates were used for ChIP using a c-myb specific antibody or IgG control, and PCR was used to visualize the presence of either OPN190 or OPN190mut in the immunoprecipitations. We observed that while c-myb was capable of binding the OPN190 construct over the IgG control, it was unable to bind the OPN190mut construct (**Fig 3.3B**). This data indicates that c-myb binds directly to the OPN promoter and

suggests that the inability of the OPN190mut reporter to activate in response to senescence is due to the absence of c-myb binding.

Finally, we wanted to verify that c-myb binds the endogenous OPN promoter. 293T cells were transiently transfected with a c-myb expression construct followed by ChIP with an antibody specific for c-myb or an IgG control. qPCR using primers spanning the c-myb binding site was used to measure levels of the endogenous OPN promoter present in the immunoprecipitations. Compared to the IgG control, there was significantly more OPN promoter present in the c-myb immunoprecipitations (**Fig 3.3B**). These data indicate that c-myb binds directly to the endogenous OPN promoter.

DISCUSSION

Through expression of SASP, senescent cells promote the growth and progression of cancerous lesions (5-7). Previous work in our laboratory has demonstrated that the SASP factor OPN is a critical driver of senescent-stroma driven preneoplastic keratinocyte cell growth (10). The transcriptional regulators that activate OPN expression in response to senescence have, however, remained elusive. Our work demonstrates that the transcription factor c-myb is required for the activation of OPN in response to senescence. Using an OPN promoter-reporter, we show that mutation of the c-myb binding site and inhibition of c-myb binding to the OPN promoter prevents promoter activation in senescent cells (**Fig 3.3**). We further show that depletion of c-myb through expression of c-myb-specfic shRNA or a dominant-negative c-myb construct

prevents OPN expression in response to senescence (**Fig 3.2**). These data indicate that c-myb is a direct transcriptional activator of OPN in the senescent context.

What activates c-myb in response to senescence remains to be elucidated. Preliminary work in our laboratory to uncover the mechanism that drives c-myb activation has shown that neither protein levels nor localization of c-myb change in response to senescence (data not shown). Ongoing work is focused on the roles of c-myb co-activators, specifically C/EBPβ plays in OPN expression in response to senescence. Elucidation of a more complete pathway that results in OPN activation in senescent cells will provide further therapeutic targets that can be used to inhibit its expression. Furthermore, we are interested in investigating if other SASP factors are regulated by c-myb. As mentioned previously, OPN is not regulated via the ATM-NFκB pathway that regulates SASP factors like IL6 and IL8 (13). It will be interesting to see how pervasive c-myb regulation of SASP expression is because the ideal therapeutic target against SASP expression is one that inhibits the expression of a wide variety of SASP factors, thereby inhibiting multiple different tumor-promoting factors at once.

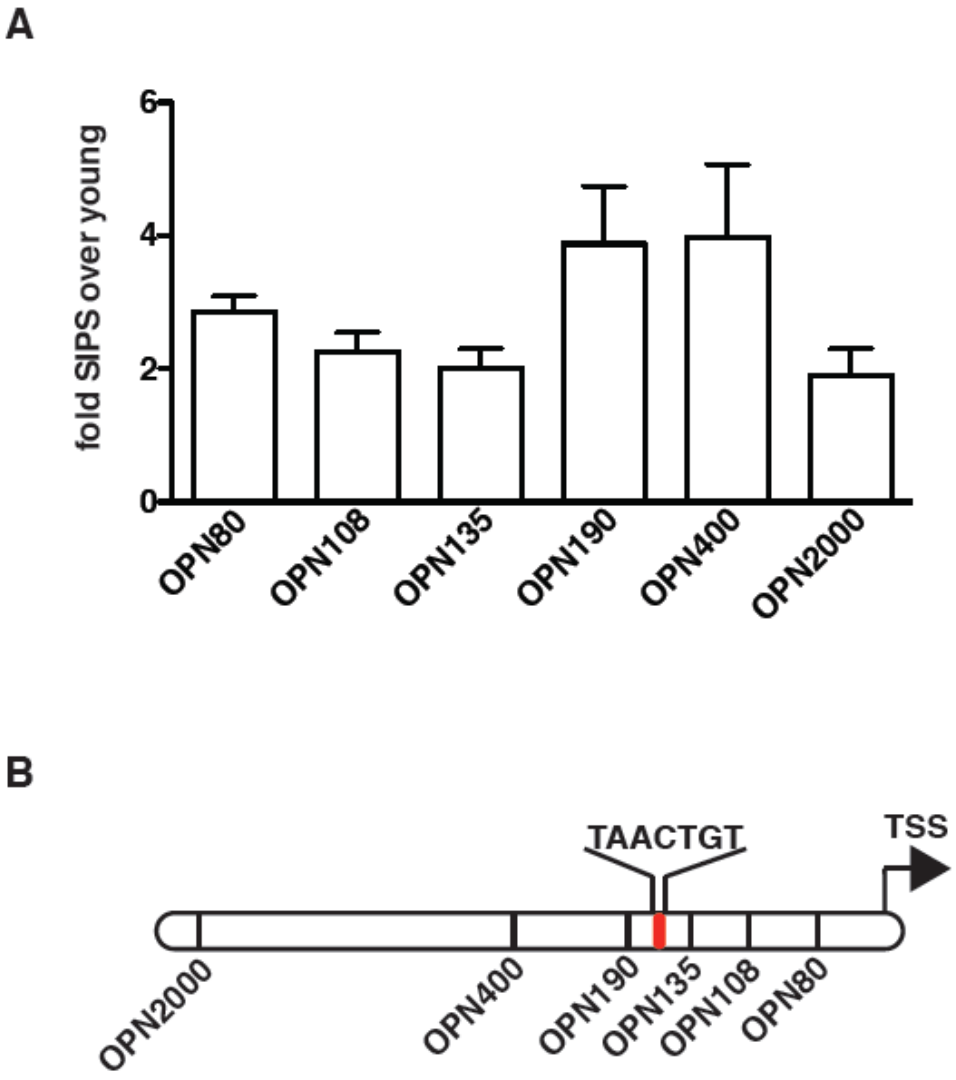

Fig 3.1: The senescence-responsive region of the OPN promoter contains a c-myb binding site. A) Young or senescent BJ fibroblasts were transiently transfected with OPN promoter-luciferase reporters. Luciferase activity was measured to analyze OPN promoter activity. Data represent mean + SEM, n=3. B) Transcription factor binding site analysis performed on the OPN190 region identified a putative c-myb binding site, denoted in red. The sequence of the c-myb binding site is shown. SIPS: stress-induced premature senescence.

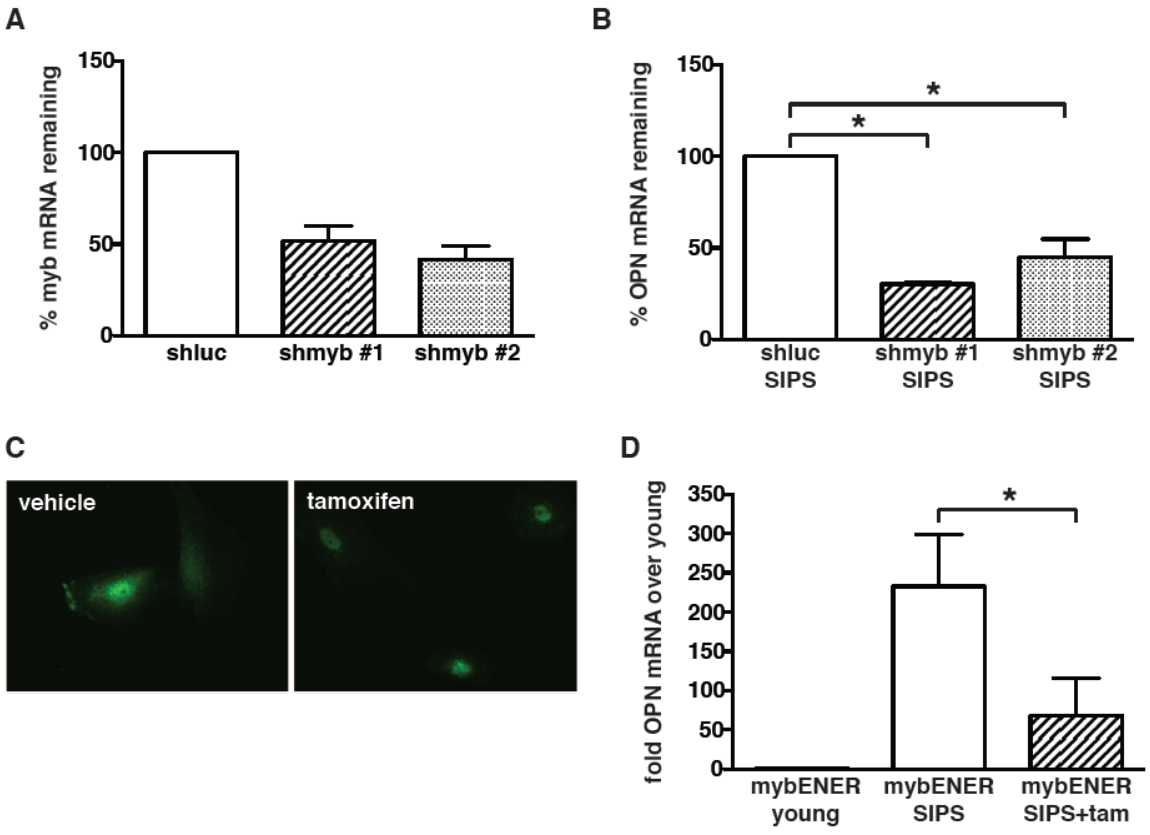

Fig 3.2: c-myb is required for activation of OPN in response to senescence. A) BJ fibroblasts were transduced with shmyb #1, shmyb #2 or a control hairpin (shluc) and c-myb levels were analyzed using qRT-PCR, n=2. B) qRT-PCR was used to measure OPN expression level in senescent BJ fibroblasts transduced with the indicated hairpin, n=2. C) WI38 fibroblasts were transduced with myb ENER and immunofluorescence imaging was used to detect translocation of the construct in to the nucleus following treatment with tamoxifen. D) qRT-PCR was used to measure OPN expression level in young WI38 fibroblasts or senescent WI38 fibroblasts treated with vehicle or tamoxifen, n=3. Data represent mean + SD. SIPS: stress-induced premature senescence, tam: tamoxifen. * indicates $p<0.05$.

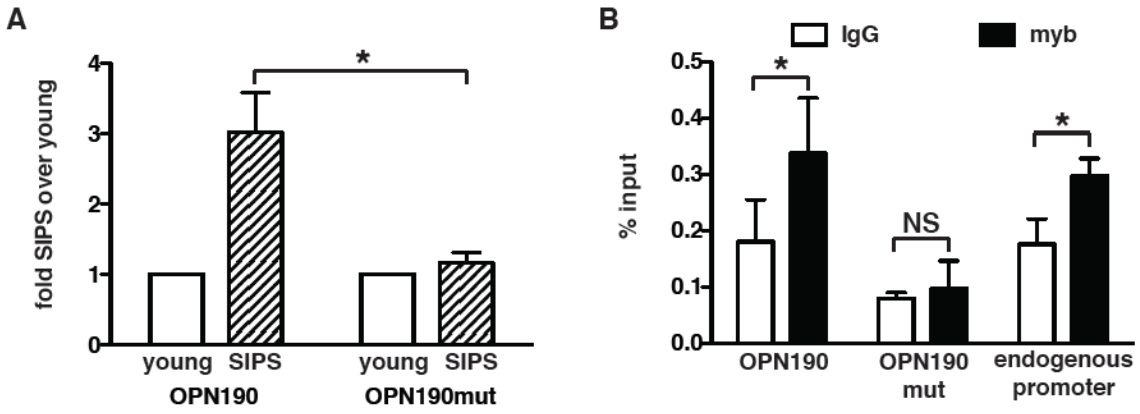

Fig 3.3: c-myb DNA binding is required for activation of OPN. A) Young or senescent BJ fibroblasts were transiently transfected with OPN190 or OPN190mut and luciferase activity was used to measure OPN promoter activation. n=4. B) 293T kidney epithelial cells were transiently transfected with a c-myb overexpression construct and either OPN190 or OPN190mut. ChIP was performed using a c-myb specific antibody or IgG control. PCR was used to measure the amount of OPN190 or OPN190mut in the immunoprecipitations. qRT-PCR was used to measure the presence of the endogenous OPN promoter in the immunoprecipitations. n=3. Data represent mean + SEM. SIPS: stress-induced premature senescence. * indicates $p<0.05$.

REFERENCES

1. Olumi AF, Grossfeld GD, Hayward SW, Carroll PR, Tlsty TD, Cunha GR. Carcinoma-associated fibroblasts direct tumor progression of initiated human prostatic epithelium. Cancer research. 1999;59(19):5002-11.

2. Kuperwasser C, Chavarria T, Wu M, Magrane G, Gray JW, Carey L, Richardson A, Weinberg RA. Reconstruction of functionally normal and malignant human breast tissues in mice. Proceedings of the National Academy of Sciences of the United States of America. 2004;101(14):4966-71.

3. Dimri GP, Lee X, Basile G, Acosta M, Scott G, Roskelley C, Medrano EE, Linskens M, Rubelj I, Pereira-Smith O, et al. A biomarker that identifies senescent human cells in culture and in aging skin in vivo. Proceedings of the National Academy of Sciences of the United States of America. 1995;92(20):9363-7.

4. Jeyapalan JC, Ferreira M, Sedivy JM, Herbig U. Accumulation of senescent cells in mitotic tissue of aging primates. Mechanisms of ageing and development. 2007;128(1):36-44.

5. Bavik C, Coleman I, Dean JP, Knudsen B, Plymate S, Nelson PS. The gene expression program of prostate fibroblast senescence modulates neoplastic epithelial cell proliferation through paracrine mechanisms. Cancer research. 2006;66(2):794-802.

6. Krtolica A, Parrinello S, Lockett S, Desprez PY, Campisi J. Senescent fibroblasts promote epithelial cell growth and tumorigenesis: a link between cancer and aging. Proceedings of the National Academy of Sciences of the United States of America. 2001;98(21):12072-7.

7. Parrinello S, Coppe JP, Krtolica A, Campisi J. Stromal-epithelial interactions in aging and cancer: senescent fibroblasts alter epithelial cell differentiation. Journal of cell science. 2005;118(Pt 3):485-96.

8. Coppe JP, Patil CK, Rodier F, Sun Y, Munoz DP, Goldstein J, Nelson PS, Desprez PY, Campisi J. Senescence-associated secretory phenotypes reveal cell-nonautonomous functions of oncogenic RAS and the p53 tumor suppressor. PLoS biology. 2008;6(12):2853-68.

9. Coppe JP, Desprez PY, Krtolica A, Campisi J. The senescence-associated secretory phenotype: the dark side of tumor suppression. Annu Rev Pathol.5:99-118.

10. Pazolli E, Luo X, Brehm S, Carbery K, Chung JJ, Prior JL, Doherty J, Demehri S, Salavaggione L, Piwnica-Worms D, Stewart SA. Senescent Stromal-Derived Osteopontin Promotes Preneoplastic Cell Growth. Cancer research. 2009.

11. Rodier F, Coppe JP, Patil CK, Hoeijmakers WA, Munoz DP, Raza SR, Freund A, Campeau E, Davalos AR, Campisi J. Persistent DNA damage signalling triggers senescence-associated inflammatory cytokine secretion. Nature cell biology. 2009;11(8):973-9.

12. Chien Y, Scuoppo C, Wang X, Fang X, Balgley B, Bolden JE, Premsrirut P, Luo W, Chicas A, Lee CS, Kogan SC, Lowe SW. Control of the senescence-associated secretory phenotype by NF-kappaB promotes senescence and enhances chemosensitivity. Genes & development. 2011;25(20):2125-36. Epub 2011/10/08.

13. Pazolli E, Alspach E, Milczarek A, Prior J, Piwnica-Worms D, Stewart SA. Chromatin remodeling underlies the senescence-associated secretory phenotype of

tumor stromal fibroblasts that supports cancer progression. Cancer research. 2012;72(9):2251-61. Epub 2012/03/17.

14. Freund A, Patil CK, Campisi J. p38MAPK is a novel DNA damage response-independent regulator of the senescence-associated secretory phenotype. The EMBO journal. 2011;30(8):1536-48. Epub 2011/03/15.

15. Ramsay RG, Gonda TJ. MYB function in normal and cancer cells. Nature reviews Cancer. 2008;8(7):523-34. Epub 2008/06/25.

16. Kauraniemi P, Hedenfalk I, Persson K, Duggan DJ, Tanner M, Johannsson O, Olsson H, Trent JM, Isola J, Borg A. MYB oncogene amplification in hereditary BRCA1 breast cancer. Cancer research. 2000;60(19):5323-8. Epub 2000/10/18.

17. Torelli G, Venturelli D, Colo A, Zanni C, Selleri L, Moretti L, Calabretta B, Torelli U. Expression of c-myb protooncogene and other cell cycle-related genes in normal and neoplastic human colonic mucosa. Cancer research. 1987;47(20):5266-9. Epub 1987/10/15.

18. Kanei-Ishii C, Yasukawa T, Morimoto RI, Ishii S. c-Myb-induced trans-activation mediated by heat shock elements without sequence-specific DNA binding of c-Myb. The Journal of biological chemistry. 1994;269(22):15768-75. Epub 1994/06/03.

19. Lutwyche JK, Keough RA, Hunter J, Coles LS, Gonda TJ. DNA binding-independent transcriptional activation of the vascular endothelial growth factor gene (VEGF) by the Myb oncoprotein. Biochemical and biophysical research communications. 2006;344(4):1300-7. Epub 2006/05/03.

20. Tahirov TH, Sato K, Ichikawa-Iwata E, Sasaki M, Inoue-Bungo T, Shiina M, Kimura K, Takata S, Fujikawa A, Morii H, Kumasaka T, Yamamoto M, Ishii S, Ogata K. Mechanism of c-Myb-C/EBP beta cooperation from separated sites on a promoter. Cell. 2002;108(1):57-70. Epub 2002/01/17.

21. Schultz J, Lorenz P, Ibrahim SM, Kundt G, Gross G, Kunz M. The functional -443T/C osteopontin promoter polymorphism influences osteopontin gene expression in melanoma cells via binding of c-Myb transcription factor. Molecular carcinogenesis. 2009;48(1):14-23. Epub 2008/05/07.

22. Chen RX, Xia YH, Xue TC, Ye SL. Transcription factor c-Myb promotes the invasion of hepatocellular carcinoma cells via increasing osteopontin expression. Journal of experimental & clinical cancer research : CR. 2010;29:172. Epub 2010/12/31.

23. Berge T, Matre V, Brendeford EM, Saether T, Luscher B, Gabrielsen OS. Revisiting a selection of target genes for the hematopoietic transcription factor c-Myb using chromatin immunoprecipitation and c-Myb knockdown. Blood cells, molecules & diseases. 2007;39(3):278-86. Epub 2007/06/26.

24. Schmidt M, Nazarov V, Stevens L, Watson R, Wolff L. Regulation of the resident chromosomal copy of c-myc by c-Myb is involved in myeloid leukemogenesis. Molecular and cellular biology. 2000;20(6):1970-81. Epub 2000/02/25.

CHAPTER 4

p38MAPK plays a crucial role in stromal mediated tumorigenesis

Elise Alspach, Kevin C. Flanagan, Xianmin Luo, Megan K. Ruhland, Hui Huang, Ermira Pazolli, Maureen J. Donlin, Timothy Marsh, David Piwnica-Worms, Joseph Monahan, Deborah V. Novack, Sandra S. McAllister, and Sheila A. Stewart

This chapter was published in 2014 in *Cancer Discovery* 4(6): 716-29

INTRODUCTION

The critical role the tumor microenvironment (TME) plays in disease is underscored by findings that changes within stromal cells can predict clinical outcome (1-3). For this reason, many groups have focused on how various stromal cell types impact tumorigenesis. For example, activated fibroblasts isolated from carcinomas (cancer-associated fibroblasts or CAFs) promote preneoplastic cell growth and increase tumor cell migration, invasion, and angiogenesis (4). Likewise, senescent fibroblasts, which are also found in human tissue (5), support tumorigenesis through the promotion of growth, invasion, and angiogenesis (6-8). Intriguingly, both senescent fibroblasts and CAFs express a plethora of pro-tumorigenic factors and in senescent cells this is referred to as the senescence-associated secretory phenotype (SASP) (6, 9).

There is significant overlap between the pro-tumorigenic factors expressed in CAFs and senescent cells. Expression array analyses of human fibroblasts treated with granulin, which renders a CAF-like phenotype (10), and fibroblasts isolated from human tumors reveal that both populations express SASP factors ((11, 12) and reviewed in (13)). In addition, CAFs isolated by laser capture micro-dissection (LCM) or via cell surface marker expression similarly display SASP factor expression (1-4, 14). Finally, cells that fail to enter senescence following exposure to a senescence-inducing stress robustly express SASP factors (15, 16), indicating that entrance into senescence is not a prerequisite for SASP expression. Together, these observations raise the possibility that the mechanisms that govern SASP expression are conserved in many tumor-

promoting fibroblasts and are not dependent upon the induction of senescence. Thus, identifying mechanisms that activate and sustain SASP expression will have a profound impact on our understanding of the development of a pro-tumorigenic TME and the identification of novel therapeutic targets.

Despite the profound impact the pro-tumorigenic SASP has on tumor cell growth and progression, the mechanisms that lead to its activation and maintenance remain poorly understood. The majority of regulatory pathways elucidated thus far have focused on SASP factor transcription, specifically by NFκB and C/EBPβ (15-19). NFκB's transcriptional activation of the SASP is dependent on the mitogen-activated protein kinase p38 (p38MAPK) and the DNA-damage response protein ATM (19). However, in other systems p38MAPK facilitates expression of cytokines including IL6 by impacting post-transcriptional mRNA stability, possibly through the RNA binding-protein AUF1 (20-22). Post-transcriptional regulation of the SASP by p38MAPK has yet to be investigated.

Given the importance of the SASP on stromal-supported tumorigenesis, we investigated the impact of p38MAPK on SASP-mediated tumor promotion. We demonstrate that inhibition of p38MAPK activity abrogates the tumor promoting capacity of senescent fibroblasts. Furthermore, inhibiting p38MAPK in CAFs inhibits their tumor promoting abilities, demonstrating for the first time that regulatory mechanisms elucidated in senescent stroma are applicable in CAFs. Finally, we elucidate a p38MAPK-dependent

post-transcriptional SASP regulatory pathway that modulates RNA-binding protein activity.

METHODS

Cell lines and treatments

BJ human foreskin fibroblasts were obtained from Dr. Robert Weinberg (Massachusetts Institute of Technology, Cambridge, MA) and were cultured as previously described (23). IMR90 human lung fibroblasts were purchased from ATCC (Manassas, VA) and were cultured in Dulbecco's Modified Eagle's Medium (DMEM) supplemented with 10% FBS (Sigma, St. Louis, MO) and 1% penicillin/streptomycin. Patient-derived breast cancer-associated fibroblasts were purchased from Asterand (Detroit, MI) and cultured in DMEM supplemented with 10% FBS, 1 μg/mL hydrocortisone, 5 μg/mL transferrin, 5 μg/mL insulin, and 1% penicillin/streptomycin. Fibroblasts were treated with bleomycin sulfate (100 μg/mL, Sigma, St. Louis, MO) for 24 hours, followed by incubation in normal culture medium for the time points indicated. Fibroblasts were treated with actinomycin D (10 μg/mL, Sigma, St. Louis, MO) for 24 hours, SB203580 (10 μM, Millipore, Billerica, MA) for 48 hours, or CDD-111 (also referred to as SP-006, 1 μM, Confluence Life Sciences, St. Louis, MO) for 48 hours unless indicated otherwise. SB203580 and CDD-111 were replenished daily. Fibroblasts were treated with 2 fresh changes of 4 mM sodium butyrate (NaB, Sigma, St. Louis, MO) for 72 or 120 hours. RNA was isolated using TRI Reagent (Life Technologies, Carlsbad, CA) at the time points indicated. HaCaT preneoplastic keratinocyte cells (obtained from Dr. Norbert E. Fusenig, German

Cancer Research Center, Heidelberg, Germany) stably expressing click beetle red (CBR) luciferase (HaCat-CBR) (16) were grown in DMEM supplemented with 10% heat-inactivated FBS and 1% penicillin/streptomycin (Sigma, St. Louis, MO). BPH1 preneoplastic prostate epithelial cells (obtained from Dr. Robert Weinberg, Massachusetts Institute of Technology, Cambridge, MA) stably expressing CBR luciferase (BPH1-CBR) were growth in DMEM supplemented with 10% non-heat inactivated FBS and 1% penicillin/streptomycin. All cells were cultured at 37 °C in 5% carbon dioxide and 5% oxygen. No cell lines used were authenticated.

Plasmids

The luciferase reporter construct fused to the 3' UTR of IL6 (lucIL6) was a gift from Dr. Nicholas Davidson (Washington University School of Medicine, St. Louis, MO) and was subcloned into the *Eco*RI site of pBABE-hygro. Luciferase reporter constructs fused to the 3' UTR of GMCSF or GAPDH were purchased from Switch Gear Genomics (Menlo Park, CA) and were subcloned in to pBABE-hygro using the *Sna*bI and *Sal*I restriction sites. Short hairpin RNA sequences targeting human AUF1 (shAUF1A: 5'-AGAGTGGTTATGGGAAGGTAT-3', shAUF1B: 5'-AGTAAGAACGAGGAGGATGAA-3'), p38 (5'-GCCGTATAGGATGTCAGACAA-3') and Hsp27 (5-CCCGGACGAGCTGACGGTCAA-3') were obtained from the Children's Discovery Institute's viral vector-based RNAi core at Washington University in St. Louis, and were supplied in the pLKO.1-puro backbone. Luciferase reporter assays were performed using a plasmid containing an NFκB-responsive promoter driving expression of firefly luciferase (NFκB-luc) and a plasmid encoding *Renilla* luciferase driven by the thymidine

kinase promoter, obtained from Dr. David Piwnica-Worms (Washington University School of Medicine, St. Louis, MO).

Senescence-associated β-galactosidase (SA-β-gal) staining

SA-β-gal staining was carried out as described previously (23).

Quantitative PCR

cDNA synthesis and quantitative PCR was performed using previously published protocols and manufacturers' instructions (42) (SYBR Green, Life Technologies, Carlsbad, CA). Primers for GAPDH (F: 5'-GCATGGCCTTCGGTGTCC-3', R: 5'-AATGCCAGCCCCAGCGTCAAA-3'), IL6 (F: 5'-ACATCCTCGACGGCATCTCA-3', R: 5'-TCACCAGGCAAGTCTCCTCA-3'), IL8 (F: 5'-GCTCTGTGTGAAGGTGCAGT-3', R: 5'-TGCACCCAGTTTTCCTTGGG-3'), MMP3 (F: 5'-GTTTTGGCCCATGCCTATGCCCC-3', R: 5'-GGAGTCAGGGGGAGGTCCATAGAGG-3'), CCL20 (F: 5'-CTGCGGCGAATCAGAAGCAGC-3', R: 5'-CCTTCATTGGCCAGCTGCCGT-3'), lucIL6 (F: 5'-CGGGCGCGGTCGGTAAAGTT-3', R: 5'-AAACAACAACGGCGGCGGGA-3'), and lucGMCSF and lucGAP (F: 5'-GAGAAACATGCGGAGAACGC-3', R: 5'-AGCATGCACGATAGCCTTGA-3') were purchased from IDT. GMCSF cDNA was amplified using a Taqman probe/primer set (catalog number Hs00929873_m1, Life Technologies, Carlsbad, CA).

ELISA

Conditioned medium was generated by incubating cells for 24 hours in serum-free medium. Following collection, secreted IL6 protein levels were measured using the

human IL6 Quantikine ELISA kit (catalog number D6050, R&D Systems, Minneapolis, MN).

Western blot analysis

Cell pellets were lysed in buffer containing 50 mM Tris pH 8.0, 5 mM EDTA, 0.5% NP40 and 100 mM sodium chloride for 20 minutes at 4 °C. Protein concentration was quantified using the Bradford Protein Assay (Bio-Rad, Berkeley, CA). The primary antibodies used were: polyclonal AUF1 (Millipore, Billerica, MA, catalog number 07260MI) at 1:3000, polyclonal p-p38 (PhosphoSolutions, Aurora, CO, catalog number p190-1802) at 1:1000, polyclonal p38 (Cell Signaling, Boston, MA, catalog number 9218) at 1:1000, monoclonal β-catenin (BD Biosciences, San Jose, CA, catalog number 610153) at 1:5000, and monoclonal α-tubulin (Abcam, Cambridge, MA, product number ab6160) at 1:1000. All secondary antibodies from the appropriate species were horseradish peroxidase-conjugated (Jackson Laboratories, Bar Harbor, ME) and diluted 1:10000.

Virus Production

Virus was produced as described previously (23).

RNA-binding protein immunoprecipitation (RIP)

Cell pellets from $7x10^7$ BJ fibroblasts were lysed in the same buffer used for western blot analysis. Protein concentration was analyzed using the Bradford Protein Assay (Bio-Rad, Berkeley, CA). 3 mg of protein was used for each immunoprecipitation. The following primary antibody was used: 30 µg of polyclonal AUF1 (Millipore, Billerica, MA, catalog number 07260MI). Equivalent amounts of normal IgG antibody (Cell Signaling,

Boston, MA) were used to control for specific immunoprecipitation. Cell lysates were pre-cleared with 20 µL protein A Dynabeads (Life Technologies, Carlsbad, CA) for 30 minutes at 4 °C prior to immunoprecipitation. 100 µL Protein A Dynabeads were used for each immunoprecipitation. Beads were washed 3 times in 0.1 M monosodium phosphate and then incubated in 0.1 M monosodium phosphate with the appropriate antibody for at least 1 hour at room temperature. Beads were then washed 3 times in Buffer A (1x PBS, 0.1% SDS, 0.3% sodium deoxycholate, 0.3% NP40), followed by incubation for 30 minutes at room temperature in NT2 buffer (50 mM Tris pH 7.4, 150 mM sodium chloride, 1 mM magnesium chloride). Antibody-bound beads were then added to pre-cleared cell lysates, and immunoprecipitated overnight at 4 °C. 100 µL of cell lysate was removed from the IgG immunoprecipitation to be used for input controls. Immunoprecipitated beads were washed 2 times with each of the following buffers: Buffer A, Buffer B (5x PBS, 0.1% SDS, 0.5% sodium deoxycholate, 0.5% NP40) and Buffer C (50 mM Tris pH 7.4, 10 mM magnesium chloride, 0.5% NP40). Beads were then resuspended in NT2 containing 0.1% SDS, 80 U RNase OUT (Life Technologies, Carlsbad, CA), and 30 µg Proteinase K and incubated at 55 °C for 30 minutes. RNA was isolated from the beads by adding 1 mL of TRI Reagent (Life Technologies, Carlsbad, CA). Following cDNA synthesis, mRNA levels of SASP factors were analyzed by qPCR using the primers and procedures described above.

Luciferase reporter assay

BJ fibroblasts were transiently transfected with plasmids encoding NFκB-luc and *Renilla* luciferase. *Renilla* luciferase expression was used to standardize for transfection

efficiency. Transfection was performed using manufacturer's protocol for the Lipofectamine 2000 reagent (Life Technologies, Carlsbad, CA). Luciferase activities were measured 48 hours post-transfection using live cell imaging as described (43).

Co-culture

Co-culture experiments were performed as previously described with the following modifications (23). 1.3×10^4 fibroblasts were plated in black-walled 96 well plates (Fisher Scientific, Pittsburgh, PA). Cells were incubated in starve medium (DMEM + 1% penicllin/streptomycin) for 3 days before the addition of HaCat-CBR cells. SB203580 was refreshed daily until HaCaT-CBR plating. HaCat-CBR cells were cultured in starve medium for 24 hours prior to plating on fibroblasts. 1.0×10^3 HaCat-CBR cells were plated on fibroblasts and incubated for the indicated length of time. At the times indicated, D-luciferin (Biosynth, Naperville, IL) was added to a final concentration of 150 µg/mL. After ten minutes, plates were imaged using an IVIS 100 camera (PerkinElmer, Downers Grove, IL) using the following settings: exposure=10 s–5 min, field of view=15, binning=16, f/stop=1, open filter.

Xenografts

$1x10^6$ BPH1-CBR preneoplastic prostate epithelial cells were co-injected with $1x10^6$ BJ human foreskin fibroblasts. Cells were injected subcutaneously in a 50:50 mixture of DMEM:growth factor-reduced Matrigel (BD Biosciences, San Jose, CA) into the rear flanks of female NcR nude mice (Taconic, Germantown, NY). In vivo bioluminescence imaging was performed on the days indicated on an IVIS 100 (PerkinElmer, Downers Grove, IL; Living Image 3.2, 1–60 s exposures, binning 4, 8 or, 16, FOV 15 cm, f/stop 1,

open filter) following IP injection of D-luciferin (150 mg/kg; Biosynth, Naperville, IL). For analysis, total photon flux (photons/sec) was measured from a fixed region of interest over the xenografts using Living Image 2.6 (PerkinElmer, Downers Grove, IL).

RNA Sequence Analysis

Total RNA was isolated using TRI Reagent (Life Technologies, Carlsbad, CA) and the RiboPure RNA isolation kit (Life Technologies, Carlsbad, CA) following the manufacturer's instructions. Ribosomal RNA was removed by poly-A selection using oligo-dT beads. mRNA was then fragmented and reverse transcribed to yield double stranded cDNA using random hexamers. cDNA was blunt ended, had an A base added to the 3' ends, and then had Illumina sequencing adapters ligated to the ends. Ligated fragments were then amplified for 12 cycles using primers incorporating unique index tags. Fragments were sequenced on an Illumina HiSeq-2000 (San Diego, CA) using single reads extending 50 bases. Raw data was de-multiplexed and aligned to the reference genome using TopHat. Transcript abundances were then estimated from the alignment files using Cufflinks. EdgeR was used for differential expression analysis.

Generation of CAFs

Primary breast tissue was collected without patient identifiers in compliance with a protocol approved by the Brigham and Women's Hospital (Institutional Review Board 93-085). Fibroblasts were isolated (10, 11) and immortalized through expression of hTERT-GFP (44) as previously described.

To generate cancer-associated fibroblasts (CAFs), $3x10^6$ human mammary fibroblasts were co-injected with $1x10^6$ MCF7-Ras tumor cells subcutaneously into nude mice. After tumors reached 1 cm, mice were euthanized and CAFs were re-isolated by digesting tissues in 1 mg/ml collagenase A for 1-4 hours at 37 °C with continuous rotation. Resulting cell suspensions were dispersed with an 18-gauge needle, washed 2 times with resuspension buffer (2% heat-inactivated fetal calf serum in sterile Hank's Balanced Salt Solution (HBSS)), and filtered through 70 mm nylon mesh. GFP+ CAFs were then isolated by fluorescence-activated cell sorting and maintained under their standard culture conditions. CAFs were confirmed to be human by staining with human specific mitochondrial DNA (data not shown).

Oral dosage of p38MAPK inhibitor

The p38MAPK small molecule inhibitor CDD-111 (Confluence Life Sciences, Inc, St. Louis, MO) was compounded at 516 ppm with Purina Rodent Chow #5001 (St. Louis, MO) to generate a daily exposure of 80 mg/kg/day. Female NcR nude mice (Taconic, Germantown, NY) were fed ad libitum.

LPS challenge and TNFα ELISA

Female NcR nude mice (Taconic, Germantown, NY) were fed ad libitum for 3 days. 100 ng lipopolysaccharide (LPS) (Sigma, St. Louis, MO) was then administered by IP injection. Serum was collected 1 hour after LPS dosage. TNFα levels were analyzed by ELISA (R&D Systems, Minneapolis, MN)

Staining of xenograft tumors

Following excision, tumors were fixed in 10% formalin and embedded in paraffin for sectioning. Standard H&E technique was used for all sections. Serial sections were stained for Ki67 (1:50, catalog number 550609, BD Bioscience, San Jose, CA), p16 (1:100, catalog number sc-1661, Santa Cruz Biotechnology, Dallas, TX) and vimentin (1:700, catalog number ab45939, Abcam, Cambridge, MA).

Statistical Analysis

Data is presented as the mean ± SEM. Statistical significance was determined using the Student's *t* test, with a p value < 0.05 considered significant. Percent mRNA remaining was calculated as the fold mRNA in ActD-treated SIPS cells over untreated SIPS cells. Overrepresented gene ontology terms in the expression data were identified using a Fisher's exact test, with a significance threshold of $p < 0.05$ as implemented in GOstat (45).

RESULTS

p38MAPK activity controls the pro-tumorigenic properties of the SASP

SASP factors promote preneoplastic cell growth (6-8, 23, 24) and p38MAPK contributes significantly to the initiation of SASP factor expression (25). To confirm this, senescent fibroblasts (fibroblasts staining positive for senescence-associated β-gal, **Supplemental Fig. 4.1A**) were treated with a highly specific small-molecule inhibitor of p38MAPK (SB203580) (26). Hsp27 is a direct downstream target of p38MAPK. Therefore, to confirm that our treatment inhibited the kinase activity of p38MAPK, we

measured Hsp27 phosphorylation by western blot analysis. We found that SB203580 treatment led to a reduction in Hsp27 phosphorylation, indicating successful inhibition of p38MAPK activity (**Fig. 4.1A**). As expected, SB203580 treatment of senescent fibroblasts resulted in a significant reduction in the expression of SASP factors IL6, IL8, and GMCSF (**Fig. 4.1B**). To determine if p38MAPK activity was responsible for the tumor-promoting activities of senescent cells, we performed co-culture experiments with normal human fibroblasts induced to senesce by treatment with bleomycin (referred to throughout as stress-induced premature senescence, SIPS) and preneoplastic HaCaT keratinocyte cells expressing click beetle red (CBR) luciferase (HaCaT-CBR) (23). Prior to the addition of HaCAT-CBR cells, fibroblasts were treated with vehicle or SB203580 as indicated in **Fig. 4.1C**. Senescent fibroblasts treated with vehicle increased the growth of HaCaT-CBR cells compared to HaCaT-CBR cells cultured with young fibroblasts (**Fig. 4.1D**), recapitulating our previously published observations (15, 23). However, while inhibition of p38MAPK had no effect on HaCAT-CBR cells grown in the absence of fibroblasts (**Supplemental Fig. 4.1B**), we found that p38MAPK inhibition reduced the pro-tumorigenic activity of senescent fibroblasts by significantly reducing HaCaT-CBR cell growth (**Fig. 4.1D**).

Given the potent impact of p38MAPK inhibition in co-culture experiments, we next examined the impact of p38MAPK depletion on preneoplastic cell growth in xenograft experiments. p38MAPK was depleted from senescent fibroblasts (**Fig. 4.1E**), resulting in a significant reduction in the level of p38MAPK-dependent SASP factor IL8 (**Fig.**

4.1F). To assess the impact of p38MAPK loss in vivo, young, senescent, or p38MAPK-depleted senescent fibroblasts were admixed with the preneoplastic epithelial cell line BPH1 expressing CBR luciferase (BPH1-CBR) and injected subcutaneously into nude mice. Tumor growth was analyzed by bioluminescence imaging. As expected, senescent fibroblasts increased BPH1-CBR cell growth relative to young fibroblasts (**Fig. 4.1G**). However, depletion of p38MAPK and subsequent reduction in p38MAPK-dependent SASP factor expression reduced tumor growth to the level observed when BPH1-CBR cells were co-injected with young fibroblasts (**Fig. 4.1G**). These results indicate that expression of p38MAPK-dependent SASP factors within the TME plays a pivotal role in preneoplastic cell growth in vivo.

The pro-tumorigenic SASP is subject to post-transcriptional regulation

We next sought to elucidate the mechanism by which p38MAPK regulates pro-tumorigenic SASP factor expression. Previous work demonstrated that p38MAPK modulates NFκB-driven transcription of SASP factors including IL6 and IL8 (19). To determine that the effects of p38MAPK inhibition were transcriptionally based, senescent fibroblasts were treated with the transcription inhibitor actinomycin D (ActD) at several time points following bleomycin treatment. SASP factor expression was significantly inhibited when cells were treated with ActD 24 hours after bleomycin treatment (**Fig. 4.2A**), a time point at which SASP factor mRNA was increased (**Supplemental Fig. 4.2A**) but cells were not yet senescent (**Supplemental Fig. 4.1A**). These results indicate that at this time point SASP factor expression is dependent on

transcription. Surprisingly, at 96 hours after bleomycin treatment, when cells displayed morphological features characteristic of senescence including staining positive for SA-β-gal (**Supplemental Fig. 4.1A**), treatment with ActD failed to reduce SASP factor mRNA levels (**Fig. 4.2A**). These changes in mRNA were also reflected at the protein level. Indeed, we found that IL6 protein levels in conditioned medium collected from cells treated with ActD at 24 hours fell drastically compared to untreated cells. In contrast, when cells were treated with ActD at 96 hours, IL6 protein levels remained high (**Fig. 4.2B**). Given p38MAPK inhibition at the later time point significantly reduced SASP expression (**Fig. 4.1B**), these findings raised the possibility that p38MAPK impacts SASP factor mRNA stability rather than NFκB-driven transcriptional activation upon the acquisition of senescence. To confirm that p38MAPK had no effect on NFκB-driven transcription at the later time point, normal human fibroblasts were transduced with an NFκB transcription reporter plasmid driving expression of luciferase (NFκB-luc). Transduced cells were treated with bleomycin, and 72 hours later senescent cells were treated with the p38MAPK inhibitor SB203580 for an additional 48 hours. As expected, when SB203580 treatment was initiated 72 hours after bleomycin treatment, there was no significant effect on NFκB transcriptional activity (**Fig. 4.2C).** These results indicate that after the establishment of senescence, p38MAPK has a profound effect on SASP factor mRNA stability.

To address whether SASP factor mRNA stability was affected in cells undergoing replicative senescence or other types of stress-induced senescence, normal human

fibroblasts were induced to senesce through telomere dysfunction (replicative senescence, RS) or treatment with the histone deacetylase inhibitor sodium butyrate (NaB). Cells undergoing RS or NaB-induced senescence robustly induced expression of SASP factors, including IL6 and IL8 (**Supplemental Fig 4.2B and Supplemental Fig 4.2C, respectively**). Further, we found that SASP factor mRNAs were significantly stabilized in cells that had undergone RS or NaB-induced senescence (**Fig. 4.2D and Supplemental Fig. 4.2D, respectively**). Significantly, SASP factor mRNA stabilization was not limited to skin fibroblasts; when IMR90 human lung fibroblasts were treated with bleomycin, they displayed a similar increase in SASP factor mRNA stability 96 hours post-bleomycin treatment (**Supplemental Fig. 4.2E**). Together, these data indicate that SASP factor mRNAs are stabilized by a post-transcriptional regulatory program that is active in fibroblasts from diverse tissues, regardless of the mechanism through which senescence is induced.

p38MAPK post-transcriptionally regulates the SASP

Our results indicate that p38MAPK inhibition reduces SASP expression and TME-dependent promotion of tumorigenesis but does not affect the activity of the primary transcriptional regulator of the SASP, NFκB, following induction of senescence. Interestingly, p38MAPK post-transcriptionally regulates IL6 and IL8 in other contexts (20, 21). Thus, we investigated p38MAPK's role in stabilizing SASP factor mRNA. We first examined whether p38MAPK was active throughout the time course under investigation. To assess p38MAPK activation, lysates were prepared from cells 24 or

96 hours after bleomycin treatment and examined for phosphorylated p38MAPK (p-p38) by western blot analysis. In agreement with previous findings (19), we observed that phosphorylated p38MAPK increased from 24 to 96 hours following bleomycin treatment (**Supplemental Fig. 4.2F**). These kinetics were consistent with SASP factor mRNA stabilization, suggesting that p38MAPK activation regulates SASP factor mRNA stability.

To elucidate p38MAPK's role in regulating SASP factor mRNA stabilization, normal human fibroblasts depleted of p38MAPK (shp38) were treated with ActD 24 or 96 hours after bleomycin treatment (**Fig.** 4.**2E**). When treated with ActD 24 hours after bleomycin treatment, cells expressing shSCR or shp38 displayed decreased SASP mRNA stability, indicating that p38MAPK does not post-transcriptionally regulate SASP mRNAs at this time point. As expected, both IL6 and IL8 mRNA stability increased when shSCR control cells were treated with ActD 96 hours after bleomycin treatment, although not to the same extent as that observed in non-transduced fibroblasts. In contrast, when shp38 cells were treated with ActD 96 hours post-bleomycin treatment, they displayed significantly reduced IL6 and IL8 mRNA stability when compared to cells expressing the control hairpin (shSCR) (**Fig. 4.2E**). Similar results were obtained with a second independent shRNA targeting p38MAPK (data not shown).

The 3' UTRs of SASP factor transcripts control mRNA stabilization in stromal cells

We next examined the mechanisms by which SASP factor mRNA was stabilized. The 3' untranslated region (UTR) of many mRNAs contains protein binding motifs that alter mRNA stability under diverse biological stimuli (27). To determine whether the 3' UTRs of SASP factor mRNAs govern post-transcriptional regulation, we utilized a luciferase reporter cDNA fused to the 3' UTR of IL6 (lucIL6) or GMCSF (lucGMCSF). A luciferase reporter cDNA fused to the 3' UTR of GAPDH (lucGAP) was used as a control. Normal human fibroblasts were stably transduced with the luciferase reporter constructs and luciferase mRNA levels were monitored in response to ActD at the time points indicated (**Fig. 4.3A**). Similar to our observations with the endogenous IL6 and GMCSF transcripts, we observed that the stability of the lucIL6 and lucGMCSF transcripts increased significantly when treated with ActD 96 hours compared to 24 hours after bleomycin treatment (**Fig. 4.3A**). As expected, there was no significant change in the stability of the lucGAP transcript (**Fig. 4.3A**), indicating that 3' UTR-dependent mRNA stabilization was specific for SASP factor mRNA and did not extend to all mRNAs in response to senescence. These results indicate that the 3' UTR of SASP factor transcripts mediates increases in mRNA stability.

AUF1 directly binds to SASP factor mRNA and modulates their stabilization

AUF1 is a protein that binds the 3' UTRs of many mRNAs including IL6, IL8, and GMCSF and reduces their stability (28-30). Furthermore, p38MAPK is known to impact

AUF1 activity in other settings (22), although a link between AUF1 and p38MAPK in the post-transcriptional regulation of IL6 and IL8 has not been demonstrated. To examine AUF1 binding to SASP factor mRNA in response to senescence, we utilized RNA-binding protein immunoprecipitation (RIP) to examine AUF1 binding to SASP factor mRNAs in response to senescence. Cell lysates were collected 24 and 96 hours after bleomycin treatment and subjected to immunoprecipitation with either an AUF1-specific antibody or a nonspecific IgG; mRNA levels were normalized to the levels of each transcript measured in the input fractions. We observed that AUF1 occupancy on IL6 and IL8 mRNAs significantly decreased from 24 to 96 hours after bleomycin treatment (**Fig. 4.3B**), corresponding with the increase in mRNA stability observed in **Fig. 4.2**. We observed similar results for GMCSF and CCL20 mRNA, indicating that this mechanism impacts many SASP factor mRNAs (**Fig. 4.3B**). This observation suggests that decreased AUF1 binding leads to increased mRNA stability once senescence is established.

We next sought to determine whether AUF1 was required to destabilize SASP mRNAs. To address this question, we stably transduced normal human fibroblasts with two independent short-hairpin RNA (shRNA) constructs targeting AUF1 (shAUF1a and shAUF1b) (**Fig. 4.3C**). AUF1-depleted cells were treated with bleomycin and 24 hours later treated with ActD, a time at which AUF1 is bound to SASP factor mRNAs displaying reduced stability (**Fig. 4.3B**). In contrast to control cells, we found that AUF1 depletion significantly increased the stability of IL6 and IL8 mRNA at the early time point

when these mRNAs are normally unstable (**Fig. 4.3D**). These data demonstrate that before senescence is established, AUF1 destabilizes SASP mRNAs by binding to their 3' UTRs.

To address whether the impact of p38MAPK on SASP mRNA stabilization was due to modulation of AUF1–SASP mRNA binding, we carried out RIP analysis. Following bleomycin treatment, normal human fibroblasts were treated with SB203580 or vehicle control as described in **Fig. 4.3E**. In contrast to control cells in which AUF1 occupancy decreased at the late time point, there was no decrease in AUF1 occupancy on IL8 mRNA in p38MAPK-inhibited cells collected 96 hours after bleomycin treatment (**Fig. 4.3E**). Similar results were obtained for IL6 (data not shown). These observations indicate that p38MAPK activation is required to release AUF1 from SASP factor mRNA. Further, these studies suggest that loss of SASP factor mRNA stabilization in p38MAPK inhibited cells (**Fig. 4.2**) is the result of a failure to remove AUF1 from SASP factor transcripts.

p38MAPK-dependent factors are expressed in the TME of breast cancer lesions

The TME plays a pivotal role in tumor progression, and recent expression analyses indicate that TME-specific expression changes are predictive of clinical outcome (1-3). Both senescent fibroblasts and CAFs express pro-tumorigenic SASP factors, raising the intriguing possibility that the regulatory mechanisms that control SASP expression in senescent cells also operate in cancer-associated stroma. Given the importance of

p38MAPK in SASP factor expression**,** we carried out a meta-analysis to establish a list of p38MAPK-regulated genes in senescent fibroblasts and evaluated their expression in the TME of human breast cancers (**Fig. 4.4A**). We performed RNA sequence analysis (RNA-seq) of young, senescent, and p38MAPK-inhibited senescent human fibroblasts and observed that IL6 and IL8 expression was p38MAPK-dependent. Along with previously identified factors, we found that 50 additional SASP factors were p38MAPK-dependent, including GMCSF, GCSF, IL1α, IL1β, CXCL1, CXCL2, CXCL5, CCL20, MMP1, and MMP7 (**Supplemental Table 4.1, Fig. 4.4A**). A subset of these factors was validated by qRT-PCR (**Supplemental Fig. 4.3A**). Gene ontology (GO) process analysis performed on the p38MAPK-dependent factors demonstrated that genes related to the regulation of inflammation, chemotaxis, cell adhesion, angiogenesis, and proliferation were significantly enriched in this gene set (**Fig. 4.4B**).

We next compared our p38MAPK-dependent SASP list to factors significantly over-expressed in the TME of breast cancer (BC) lesions. We examined three data sets generated from microarray analyses of normal stroma versus cancer-associated stroma that had been obtained by laser capture micro-dissection of breast tissue (1-3) (**Fig. 4.4A**). Of the 50 p38MAPK-dependent factors identified in senescent fibroblasts, we found that 29 were expressed in the stroma of the Finak breast cancer dataset (1), including CXCL2 and IL24. Seventeen factors were expressed in the TME of the Ma breast cancer data set (2), including IL1β. Finally, 7 factors overlapped with the Karnoub breast cancer data set (3), including CCL20 (**Supplemental Table 4.1)**.

Furthermore, CCL20, CXCL5, IL11, IL1β, IRAK3, MMP1, MPP7, and SOD2 were expressed in the BC-associated stromal compartment of at least two studies (**Fig. 4.4C**). Of note, CCL20, CXCL5, IL11, IL1β, and MMP1 are factors with known pro-tumorigenic activities (31-35). We observed that BC-associated stromal genes compose a large percentage of the total number of p38MAPK-dependent SASP factors involved in the regulation of inflammation, chemotaxis, angiogenesis, and cell adhesion based on GO process analyses (**Fig. 4.4B**). Given that these factors are associated with disease progression, our findings raise the possibility that anti-p38MAPK therapy could significantly impact tumor progression in humans.

Inhibition of p38MAPK abrogates the pro-tumorigenic activities of CAFs

Expression of p38MAPK-dependent factors within the stroma of breast cancer lesions raised the possibility that they contribute to the tumor promoting activities of CAFs. Therefore, we examined whether inhibition of p38MAPK would abrogate the tumor-promoting activities of CAFs as it did for senescent fibroblasts. To generate CAFs, we obtained normal human mammary fibroblasts from reduction mammoplasty (NMF), admixed them with MCF7-Ras breast carcinoma cells and injected the cell mixture into immunocompromised mice and allowed tumors to grow. Human CAFs were isolated from these tumors and we assessed their tumor-promoting potential by co-culturing them with preneoplastic HaCaT skin keratinocytes expressing CBR luciferase (HaCaT-CBR). As expected, CAFs significantly stimulated HaCaT-CBR cell growth compared to HaCaT-CBR cells cultured with parental NMF fibroblasts (**Fig. 4.4D**). To investigate the

importance of p38MAPK-dependent CAF factors, we inhibited p38MAPK in CAFs with SB203580 and assessed their ability to promote preneoplastic cell growth. Similar to what we observed when senescent fibroblasts were treated with the p38MAPK inhibitor SB203580 (**Fig. 4.1C**), CAFs treated with SB203580 failed to promote HaCaT-CBR cell growth (**Fig. 4.4D**). These results indicate that p38MAPK regulates the tumor-promoting activity of CAFs. Together with our meta-analysis and expression of p38MAPK-dependent genes in the stromal compartment of human breast cancer lesions, these observations suggest that p38MAPK plays a central role in sustaining the expression of tumor-promoting factors. Thus, stromal p38MAPK represents a novel therapeutic target for senescent and non-senescent cancer-associated stromal compartments in breast cancer.

p38MAPK inhibition compromises the tumor-promoting capacity of the microenvironment

The critical importance of SASP factor expression in our tumor models and our work to uncover the mechanisms that sustain SASP factor expression identified p38MAPK as a central player in SASP expression in senescent cells as well as in CAFs. Given our findings that p38MAPK-dependent factors are expressed in human breast cancer lesions, we evaluated the feasibility of targeting p38MAPK in a preventative and therapeutic setting. Several p38MAPK inhibitors have entered phase II clinical trails for rheumatoid arthritis and thus have proven safe in a nonlethal disease (36, 37). We obtained a p38MAPK inhibitor (CDD-111, also referred to as SD-0006 (38), Confluence

Life Sciences) and compounded it into mouse chow. CDD-111 was chosen because it can be orally administered and shows high specificity for the p38MAPK α subunit (38). Indeed, extensive analysis of CDD-111 revealed that it is selective for p38MAPK α over fifty other kinases including p38MAPK β, γ, and δ. Furthermore, the IC_{50} for inhibiting tumor necrosis factor-α (TNFα) release in vitro and in vivo was less than 200 nM (38). Treatment of senescent cells with CDD-111 in vitro revealed that it effectively reduced SASP expression as evidenced by a significant reduction in IL6 and IL8 levels (data not shown).

To establish the impact of orally administered CDD-111 on p38MAPK activity in our system, mice were placed on CDD-111 (p38i) or control chow for three days, challenged with LPS, and serum TNFα levels were measured. We found that mice receiving oral p38i failed to mount a robust TNFα response following an LPS challenge compared to animals receiving control chow (**Supplemental Fig. 4.3B**). We also verified that p38i inhibited SASP expression in vivo. Senescent normal human fibroblasts were injected subcutaneously into the rear flanks of nude mice maintained on control or p38i chow. Ten days after injection the cells were removed, RNA was isolated, and the levels of human IL8 were analyzed by qRT-PCR. Senescent fibroblasts isolated from mice on p38i had significantly less IL8 mRNA than senescent fibroblasts isolated from mice on control chow (**Fig. 4E**), demonstrating that CDD-111 inhibited SASP expression in vivo.

We next evaluated the p38MAPK inhibitor's efficacy in a xenograft setting. BPH1-CBR cells admixed with young or senescent fibroblasts were subcutaneously injected into mice maintained on control or p38i chow (**Fig. 4.4F**). Bioluminescence analysis of tumor growth revealed that p38i significantly reduced the growth of BPH1-CBR cells co-injected with senescent fibroblasts (**Fig. 4.4G & H**). Analysis of cellular proliferation (Ki67 staining) revealed that senescent fibroblasts significantly increased BPH1 cell proliferation compared to when BPH1 cells were co-injected with young fibroblasts (**Fig. 4.5A**). Importantly, the increase BPH1 proliferation that was noted in the presence of senescent fibroblasts was markedly reduced when mice were maintained on p38i versus control chow (**Fig. 4.5A**). These data demonstrate that the reduced tumor size observed in response to p38i administration was a result of decreased epithelial cell proliferation. Importantly, the difference in epithelial cell proliferation between tumors containing senescent stroma from p38i- and control-fed mice was not due to differences in stromal composition between these tumor types, as staining for a senescence marker, p16, and a fibroblast marker, vimentin, demonstrated that 1) senescent fibroblasts persisted throughout the time course of the experiment regardless of p38MAPK inhibition and 2) the stromal composition of treated and untreated tumors was similar. Vascularity and myeloid infiltration were also investigated in these tumors. No significant differences in either vascularity or leukocyte infiltration were noted (data not shown). Administration of CDD-111 to mice injected with BPH1 cells admixed with young fibroblasts also resulted in a decrease in epithelial cell growth, although not to the same extent as that observed in tumors containing senescent fibroblasts. Oral

administration of CDD-111 had no significant impact on BPH1-CBR cells injected alone (data not shown).

To address the effectiveness of p38MAPK inhibition in a therapeutic setting, mice were injected with BPH1-CBR cells admixed with senescent fibroblasts and tumors were allowed to grow for one week until the average tumor volume reached 74 mm^3. Mice were then administered control or p38i chow and bioluminescence imaging was used to monitor tumor growth. Significantly, tumor growth was arrested in mice receiving p38i. In contrast, tumors in mice receiving control chow continued to show significant growth (**Fig. 4.5B**).

To investigate the applicability of orally administered p38i in CAF-containing microenvironments, we obtained primary CAFs (pCAFs) from a lesion removed from a patient with invasive breast cancer. We subcutaneously injected BPH1 cells alone or BPH1 cells admixed with pCAFs into nude mice fed either control or p38i chow as described for the experiments in **Fig 4.4F**. As expected, there was no difference in BPH1 cell growth whether mice were fed control or p38i chow (**Fig. 4.5C**). Importantly, in mice receiving control chow, BPH1 cells admixed with pCAFs grew significantly more than BPH1 cells injected alone, verifying that our patient-derived fibroblasts were *bona fide* CAFs (**Fig. 4.5C**). pCAF-mediated BPH1 growth was significantly inhibited in mice receiving p38i (**Fig. 4.5C**), similar to what was observed with senescent fibroblast-mediated BPH1 growth (**Fig 4.4G and H**). These findings, combined with those from

p38MAPK inhibition of senescent-fibroblast driven tumors, suggest that p38MAPK is a viable, stromal specific therapeutic target that may show efficacy in diverse tumor microenvironments and diverse tumor types

DISCUSSION

The regulation of SASP expression is complex, involving the DNA damage response (16), HDAC1 activity (15), and transcriptional regulation by NFκB and C/EBPβ (17-19). p38MAPK perhaps best exemplifies the complexity of SASP regulation. Previous reports have shown that p38MAPK impacts NFκB-driven transcriptional control of SASP expression immediately following exposure to a senescence-inducing signal (19). In our system, p38MAPK inhibition had no effect on NFκB transcriptional activity when it was initiated after cells acquired the senescent phenotype as evidenced by SA-β-gal staining. However, p38MAPK inhibition did have a significant impact on SASP factor mRNA stability. Our data are consistent with p38MAPK playing a dual role in SASP factor expression. We hypothesize that SASP factor expression is achieved through early rounds of transcription followed by post-transcriptional mRNA stabilization, both of which require distinct p38MAPK functions.

Inhibiting the SASP represents a novel stromal-specific therapeutic cancer modality that could be beneficial at multiple stages of tumorigenesis. We have demonstrated that senescent cells are present in the microenvironment before the formation of preneoplastic lesions and that SASP factors promote preneoplastic cell growth (15, 23).

The SASP also promotes more aggressive malignancies by increasing angiogenesis and invasion (9, 39). Finally, the SASP is hypothesized to promote later events in cancer progression including metastasis and recurrence through its promotion of cancer stem cell formation and chemo-resistant niches (7, 40, 41). Together, these findings suggest that inhibition of the SASP will prevent the development and/or progression of malignancies. p38MAPK could provide an ideal target as it impacts both the transcriptional and post-transcriptional regulation of SASP (19) and may be particularly effective because it can inhibit SASP expression after the stabilization of SASP mRNAs has already occurred.

Our findings that oral administration of a p38MAPK inhibitor dramatically inhibits SASP-mediated tumor growth driven by senescent fibroblasts and CAFs indicates for the first time that the tumor-promoting capabilities of senescent and cancer-associated fibroblasts are mediated through similar signaling pathways. Furthermore, these findings suggest that p38MAPK is an important therapeutic target with wide applicability in a variety of tumor-promoting microenvironments. This is strengthened by our in silico analysis of the stromal compartment of breast cancer lesions, which we show express many p38MAPK-dependent genes. These data are intriguing in light of the fact that p38MAPK inhibitors have moved into phase II and III clinical trials for inflammatory diseases including rheumatoid arthritis, Crohn's disease, and psoriasis, demonstrating their tolerability in patients (36, 37). Given our findings, we suggest that p38MAPK inhibitors warrant investigation for use as anti-neoplastic therapy.

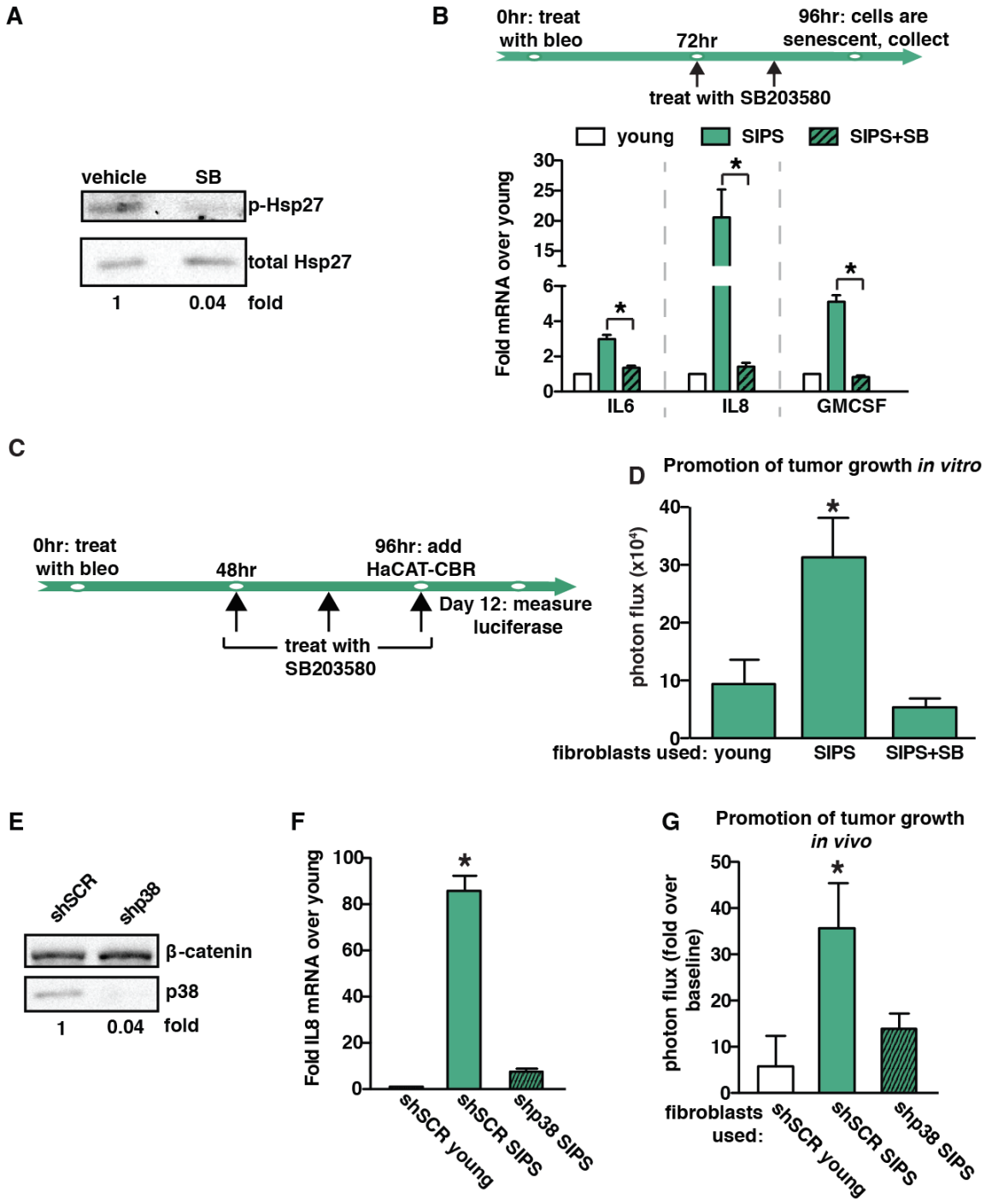

Fig 4.1: p38MAPK activity controls the pro-tumorigenic properties of the SASP A) Western blot analysis demonstrating that SB203580 treatment inhibits p38MAPK activity. SB203580 treatment significantly impacts phosphorylation of p38MAPK's direct downstream target, Hsp27. B) Schematic of protocol to generate SIPS in BJ fibroblasts.

Cells were treated with bleomycin for 24 hours. SB203580 (SB) treatment or vehicle control was initiated 48 hours after removal of bleomycin (bleo). 96 hours after bleomycin treatment, cells were collected for expression analysis of IL6, IL8, and GMCSF by qRT-PCR. Representative experiment, n=4. C) Timeline of bleomycin (bleo) and SB203580 treatment of BJ fibroblasts in (D). SB203580 was replenished daily until co-culture with HaCAT-CBR cells was initiated. D) Growth of human keratinocytes expressing click beetle red (HaCaT-CBR) measured 8 days following initiation of co-culture with indicated fibroblast populations. Representative experiment, n=3. E) BJ fibroblasts were depleted of p38MAPK through the expression of shRNA (shp38) or control shRNA (shSCR). p38 depletion was verified by western blot analysis. F) Expression of IL8 was analyzed by qRT-PCR 96 hours following bleomycin treatment in p38MAPK-depleted (shp38) or control (shSCR) fibroblasts and represented relative to young fibroblasts expressing shSCR control. Representative experiment, n=3. G) BJ fibroblasts expressing shp38 or shSCR were treated with bleomycin for 72 hours prior to injection. Indicated fibroblast populations were admixed with preneoplastic epithelial cells expressing click beetle red (BPH1-CBR cells) and injected subcutaneously into the rear flanks of female NcR nude mice. Luciferase activity was measured using live, whole-animal imaging to monitor BPH1 cell growth relative to baseline signal. Data represents mean + SEM, n=8. Data represents mean + SD unless otherwise stated. * indicates $p<0.05$. SIPS: stress induced premature senescence.

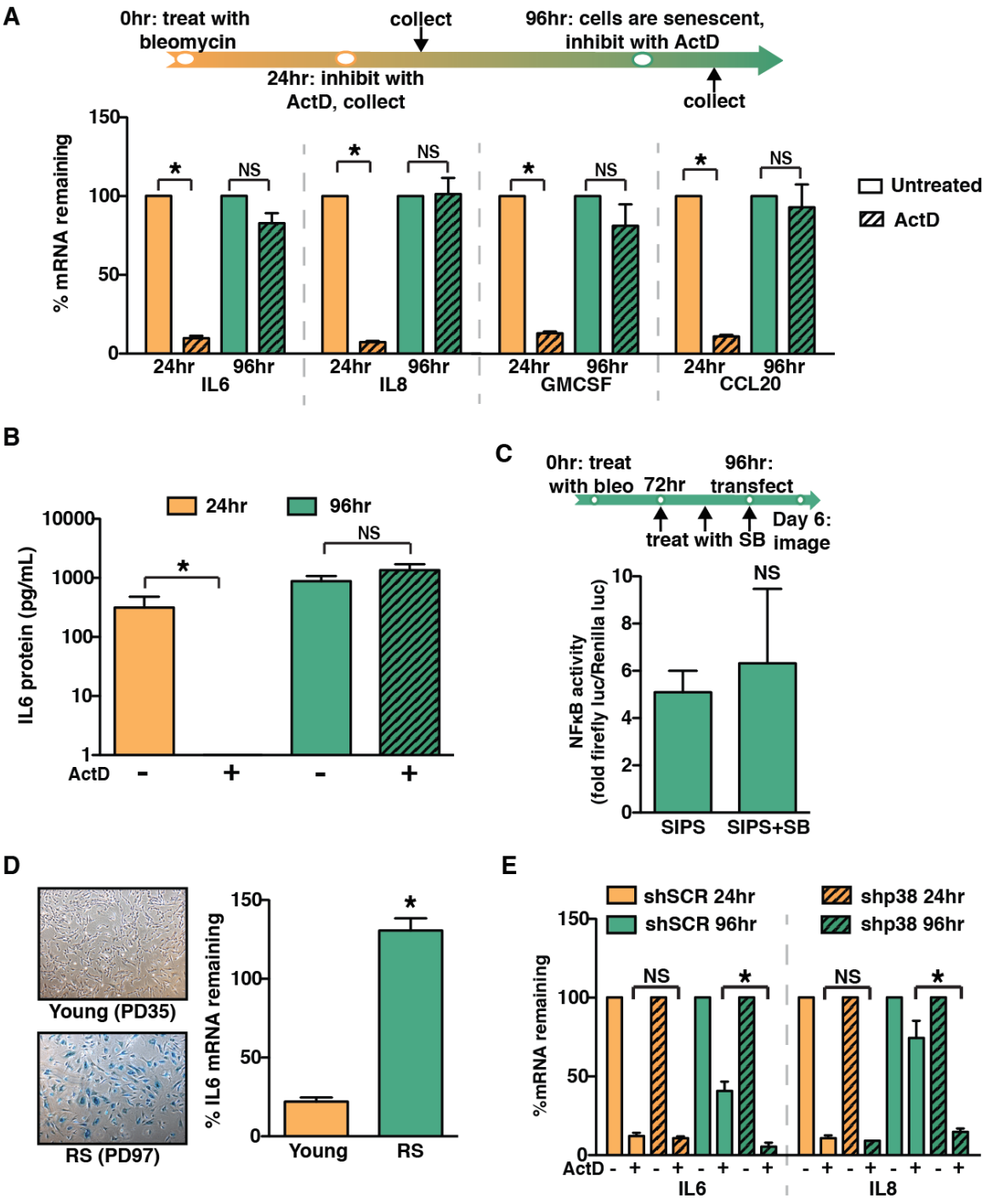

Fig 4.2: p38MAPK post-transcriptionally regulates the SASP A) Schematic of protocol to generate SIPS in BJ fibroblasts. Cells were treated with bleomycin for 24 hours. Cells were subsequently treated with actinomycin D (ActD) for 24 hours. The

ActD treatment was initiated 24 or 96 hours after the completion of bleomycin treatment. IL6, IL8, GMCSF, and CCL20 mRNA levels were analyzed by qRT-PCR. To account for changes in gene expression, levels mRNA in ActD-treated cells were normalized to the levels observed in untreated cells from the respective time points (% mRNA remaining). Representative experiment, n=3. B) ELISA analysis of IL6 protein levels in conditioned media from cells treated as in (A). Representative experiment, n=4. C) BJ fibroblasts were treated with bleomycin (bleo) for 24 hours and with SB203580 (SB) as indicated. 96 hours post bleomycin treatment cells were transiently transfected with an NFκB activity luciferase reporter. Luciferase activity was measured by live-cell imaging 48 hours post transfection. Representative experiment, n=2. D) Young BJ fibroblasts (35 population doublings, PD) or replicatively senescent BJ fibroblasts (PD97) were stained for senescence-associated β-galactosidase to confirm senescent phenotype (left). Cells were treated with ActD and IL6 mRNA levels were analyzed by qRT-PCR. Representative experiment, n=3. E) BJ fibroblasts expressing a control hairpin (shSCR) or shp38 were treated for 24 hours with ActD at 24 or 96 hours after the completion of bleomycin treatment. IL6 and IL8 mRNA levels were analyzed by qRT-PCR. Representative experiment, n=2.

Data represent mean + SD. * indicates $p<0.05$. SIPS: stress-induced premature senescence.

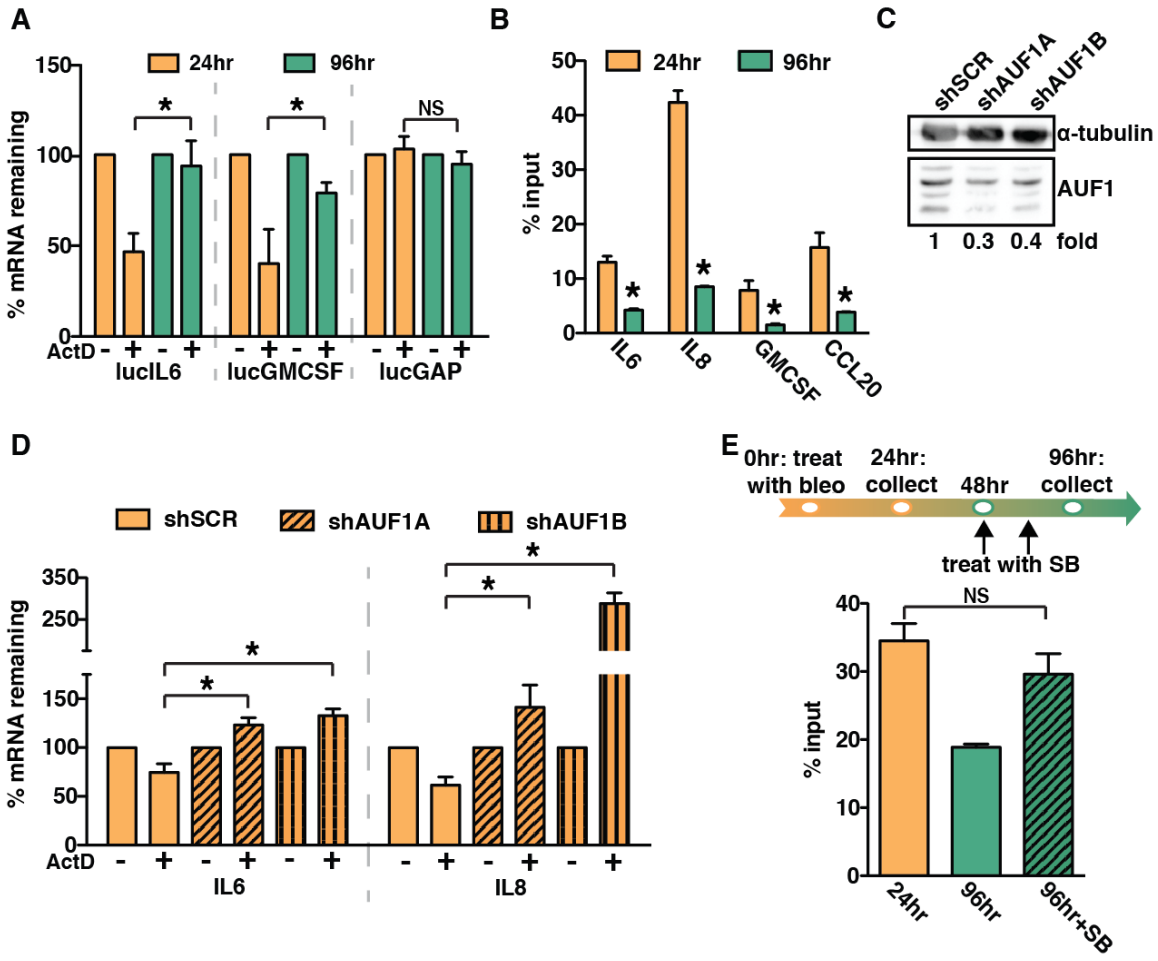

Fig 4.3: AUF1 directly binds to SASP factor mRNA and modulates SASP factor stabilization A) BJ fibroblasts were stably transduced with luciferase constructs fused to the 3' untranslated regions (UTR) of IL6, GMCSF, and GAPDH (lucIL6, lucGMCSF, and lucGAP). Cells were treated with ActD at 24 or 96 hours following bleomycin treatment. Luciferase mRNA levels were analyzed by qRT-PCR. Representative experiment, n=3. B) RNA immunoprecipitation was performed for AUF1 using BJ fibroblast cell lysates collected 24 or 96 hours after bleomycin treatment. IL6, IL8, GMCSF, and CCL20 mRNA levels in immunoprecipitations were analyzed by qRT-PCR. Representative experiment, n=4. C) BJ fibroblasts were transduced with shRNAs to deplete AUF1 (shAUF1A and shAUF1B) or a control shRNA (shSCR). Protein levels

were analyzed by western blot analysis. Note: there are four AUF1 isoforms present and α-tubulin was used as a loading control. D) 24 hours following bleomycin treatment, BJ fibroblasts expressing a control hairpin shSCR, shAUF1A, or shAUF1B were treated with ActD for 1 hour. IL6 and IL8 mRNA levels were analyzed by qRT-PCR. Representative experiment, n=2. E) RNA immunoprecipitation for AUF1 was performed on BJ fibroblasts treated with bleomycin (bleo) and SB203580 (SB) as indicated. The level of IL8 mRNA in the AUF1 immunoprecipitation was measured by qRT-PCR. Representative experiment, n=3. Data represent mean + SD. * indicates $p<0.05$.

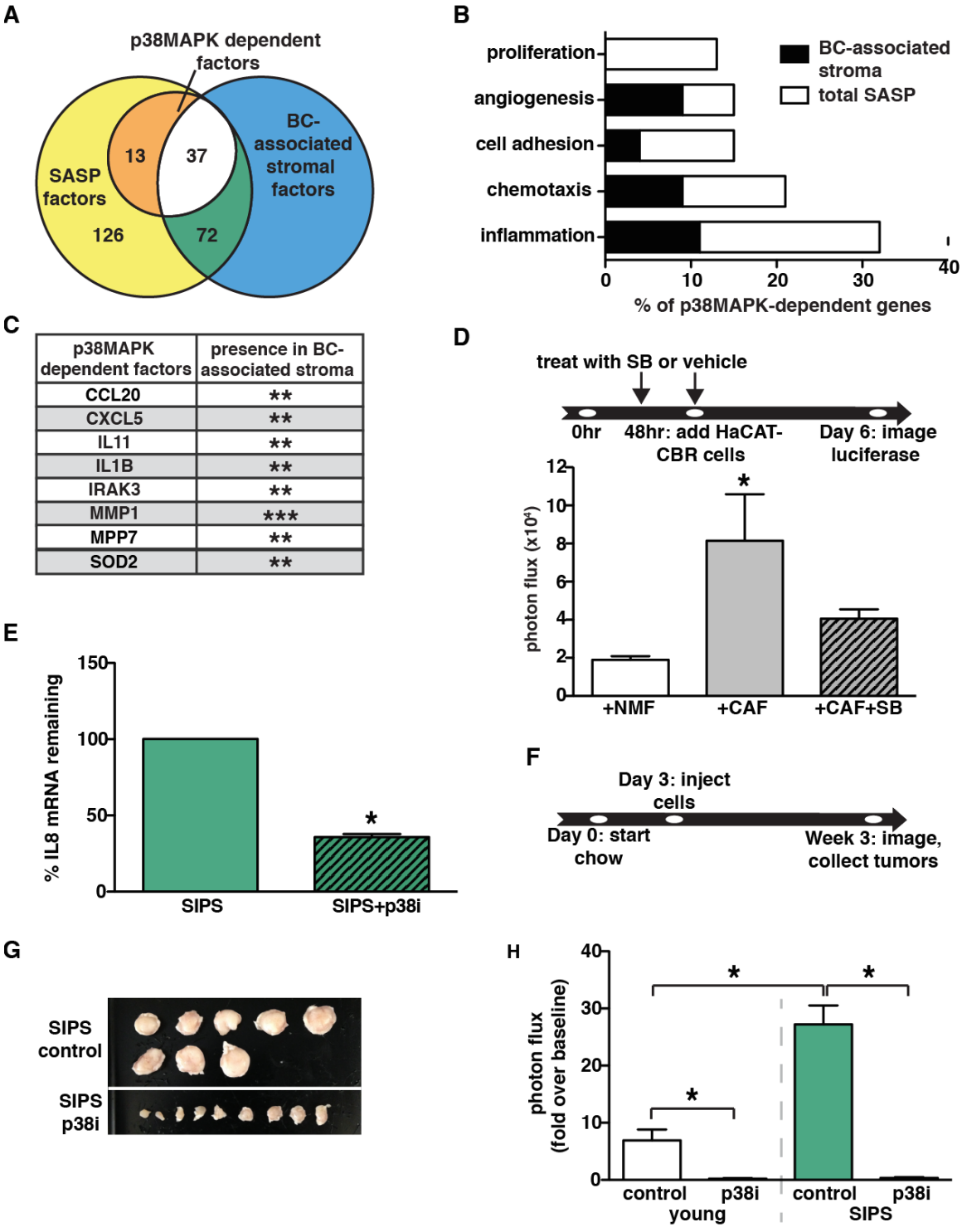

Fig 4.4: p38MAPK-dependent factors are expressed in the TME of breast cancer lesions A) RNA-seq analysis was performed on young fibroblasts, senescent fibroblasts, and senescent fibroblasts treated with SB203580. RNA-seq results were

analyzed to determine the number of factors upregulated in response to senescence (SASP factors) and the number of p38MAPK-dependent factors. These results were also analyzed for overlap with the expression profiles of breast cancer (BC)-associated stroma. B) GO processes analysis was performed on p38MAPK-dependent SASP factors. Results are presented as the percent of p38MAPK-depenedent genes assigned to the processes shown. Black regions of the bars represent the percent of p38MAPK-dependent SASP factors assigned to each process that are also expressed in BC-associated stroma. The significance threshold was set at $p < 0.05$. C) p38MAPK-dependent SASP factors that are expressed in more than one BC-associated stroma data set. **indicates expression in 2 BC-associated stroma datasets, ***indicates expression in 3 BC-associated stroma datasets. D) Tumor-educated human CAFs and their normal isogenic counterparts (NMF) were treated with SB203580 (SB) or vehicle as indicated and replenished daily until co-culture with HaCAT-CBR preneoplastic keratinocytes was initiated. Luciferase activity was measured using live-cell imaging 4 days following initiation of co-culture to monitor HaCaT cell growth. Representative experiment, n=2. E) Senescent BJ fibroblasts in matrigel were injected subcutaneously into the rear flanks of nude mice fed either control or p38i chow. Cells were removed 10 days after injection and IL8 mRNA levels were measured using qRT-PCR. Representative experiment, n=4. F,G and H) Xenografts of BPH1-CBR cells co-injected with senescent BJ fibroblasts (SIPS) into female NcR nude mice. Control or the p38i compounded chow were performed as outlined in (F). Tumor are shown in (G). Tumor

growth was analyzed by bioluminescence imaging (H). Data represent mean + SEM, n=8.

Data represent mean + SD unless otherwise stated. * indicates $p<0.05$. SIPS: stress induced premature senescence.

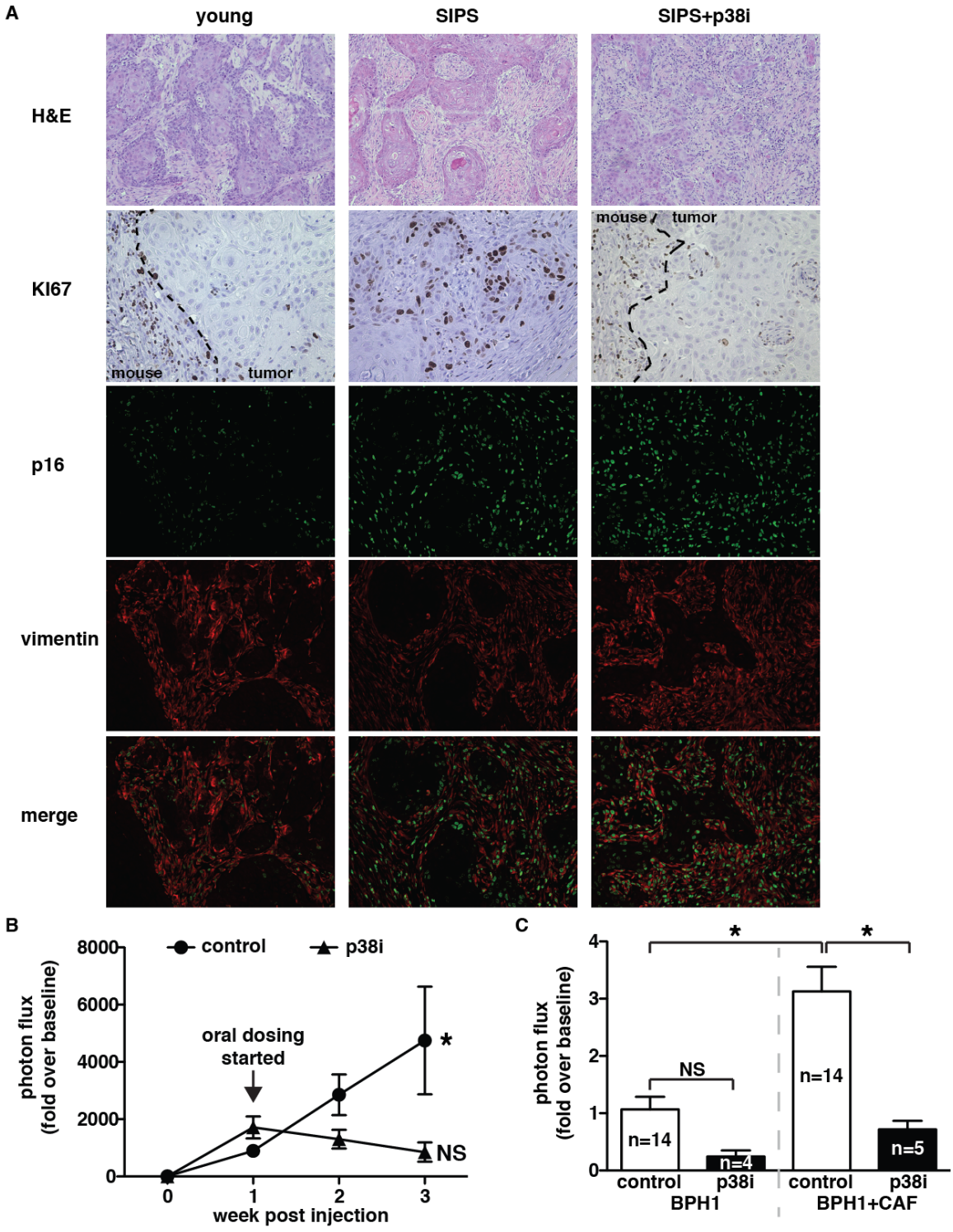

Fig 4.5: p38MAPK inhibition is effective in both senescent fibroblast and CAF-driven tumors A) Tumors were removed at the endpoint of the experiment described in (Fig 4.4F) and stained for Ki67 (dashed line demarks the margin between the mouse

and xenograft), p16, and vimentin. H&E images were captured with a 10X objective, all other images were captured with a 20X objective. Representative images, n=2. B) Xenograft growth of BPH1-CBR cells co-injected with senescent BJ fibroblasts (SIPS) into female NcR nude mice. Tumors were allowed to grow for 1 week after injection, at which time mice were placed on control or p38i-compounded chow. Tumor growth was analyzed by bioluminescence imaging. Data represent mean + SEM, n=16. * indicates significance between 1 and 3 weeks post-injection in mice fed control chow. C) Xenografts of BPH1-CBR cells co-injected with pCAFs into female NcR nude mice. Mice were fed control or p38i chow as outlined for the experiment in Fig 4.4F. Tumor growth was analyzed by bioluminescence imaging. Data represent mean + SEM, n is indicated for each sample. * indicates $p<0.05$. NS: not significant.

Supplemental Table 4.1: p38MAPK dependent SASP factors and their overlap with BC-associated stroma

p38MAPK-dependent SASP	overlap with Finak	overlap with Ma	overlap with Karnoub
ABCA6	ABCA6	AKR1B1	AKR1B1
AKR1B1	BDKRB2	C1QTNF1	CCL20
ANKRD30BL	C1QTNF1	CCL20	GMCSF
BDKRB2	C8orf4	CXCL 5	IRAK3
C1QTNF1	CARD6	FOXE1	MMP1
C8orf4	CD36	IL11	MPP7
CARD6	CH25H	IL1A	NAMPT
CCL20	CXCL 2	IL1B	
CD36	CXCL 5	IL8	
CH25H	CYP26B1	LACC1	
CXCL 1	CYP7B1	LPXN	
CXCL 2	FOXE1	MMP1	
CXCL 5	FRMD6	MMP3	
CYP26B1	GCSF	NAMPT	
CYP7B1	GDNF	NEK10	
ERRFI1	GREM2	PSG1	
FAM43A	IL11	SFRP1	
FOXE1	IL13RA2	SOD2	
FRMD6	IL1B		
GCSF	IL24		
GDF15	IRAK3		
GDNF	KCNJ2		
GMCSF	MMP1		
GREM2	MPP7		
HAS2	MYEOV		
IL11	PLCH1		
IL13RA2	PSG1		
IL1A	SOD2		
IL1B	XDH		
IL24			
IL6			
IL8			
IRAK3			
KCNJ2			
LACC1			
LPXN			
MMP1			
MMP3			
MPP7			
MYEOV			
NAMPT			
NAMPTL			
NEK10			
PLA2G4A			
PLCH1			
PSG1			
SFRP1			
SOD2			
TFPI2			
TNFSF18			
USP53			
XDH			

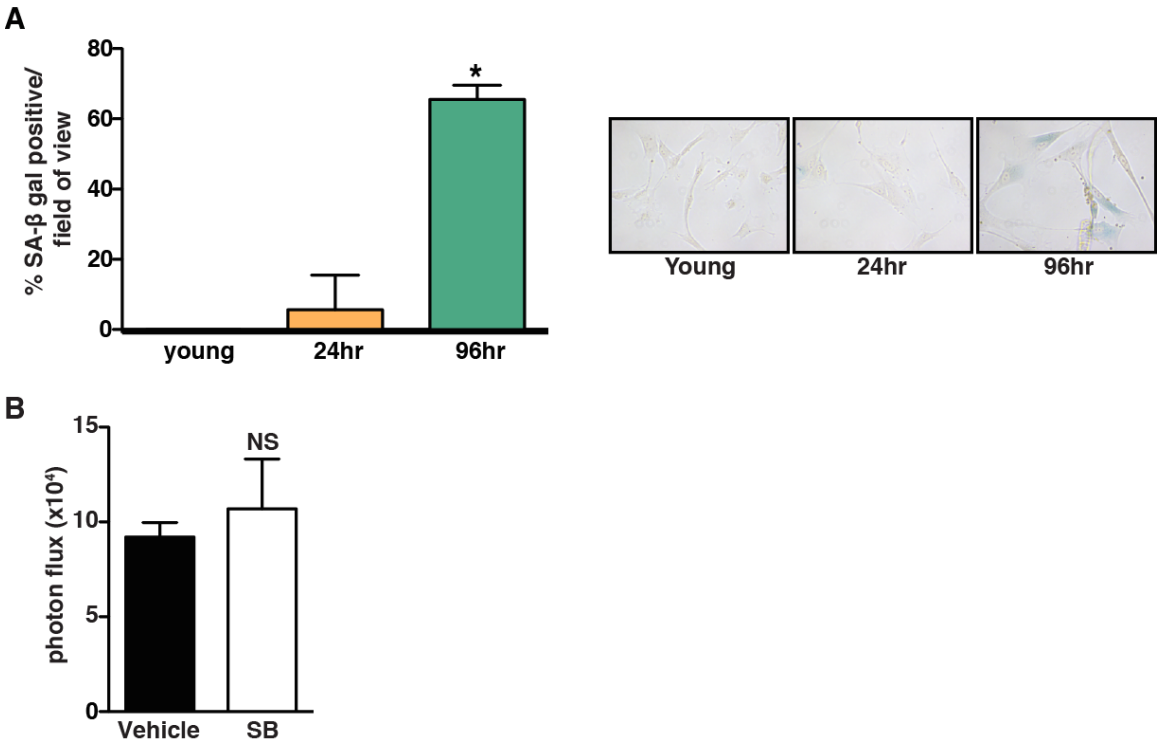

Supplemental Fig. 4.1: p38MAPK activity controls the pro-tumorigenic properties of the SASP A) BJ fibroblasts were fixed for senescence-associated β-galactosidase 24 or 96 hours after treatment with bleomycin. n=3. B) HaCAT-CBR preneoplastic skin keratinocytes were treated with SB203580 or vehicle for 72 hours. Representative experiment, n=3. Data is presented as mean ± SD. * indicates $p \leq 0.05$.

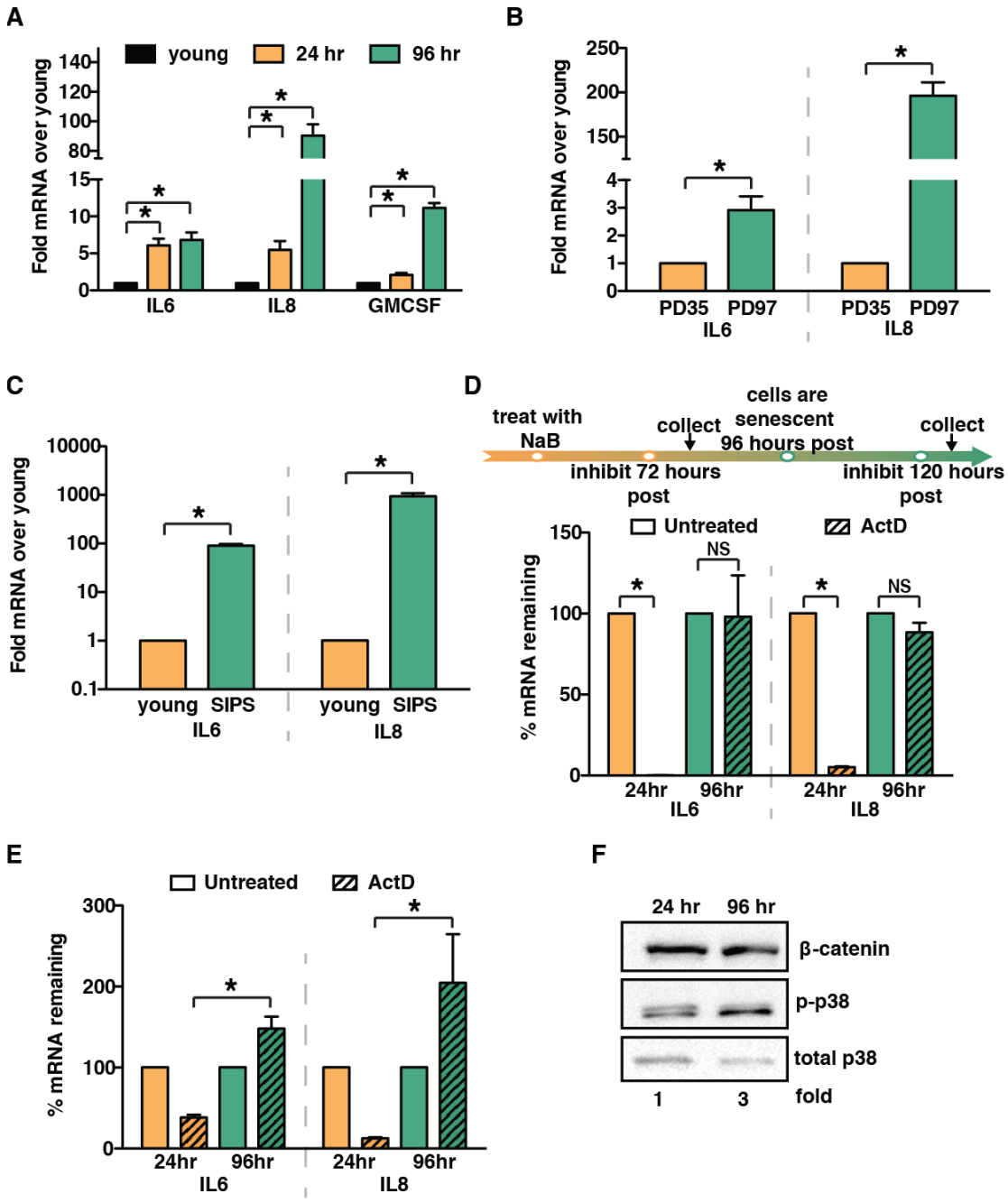

Supplemental Fig. 4.2: p38MAPK post-transcriptionally regulates the SASP A) BJ fibroblasts were treated with bleomycin for 24 hours. Cells were collected either 24 or 96 hours after treatment with bleomycin and upregulation of SASP factors IL6, IL8 and GMCSF was verified by qRT-PCR. Representative experiment, n=3. B) BJ fibroblasts

were induced to senesce through telomere attrition (replicative senescence, RS). Upregulation of SASP factors IL6 and IL8 was verified by qRT-PCR. Representative experiment, n=3. C) BJ fibroblasts were treated with sodium butyrate (NaB) for 120 hours. Upregulation of SASP factors IL6 and IL8 was verified by qRT-PCR. Representative experiment, n=3. D) BJ fibroblasts were treated with NaB for 72 or 120 hours followed by actinomycin D (ActD) at the time points indicated. IL6 and IL8 expression was quantified by qRT-PCR. Representative experiment, n=3. E) IMR90 human lung fibroblasts were treated with bleomycin and ActD as described in **Fig. 4.2B**. IL6 and IL8 expression was quantified by qRT-PCR. Representative experiment, n=2. F) BJ fibroblast cell lysates 24 or 96 hours post bleomycin treatment were analyzed for phosphorylation of p38MAPK (p-p38). Total p38MAPK was used as a loading control. Representative experiment, n=3. Data is presented as mean + SD. * indicates $p \leq 0.05$. SIPS: stress-induced premature senescence.

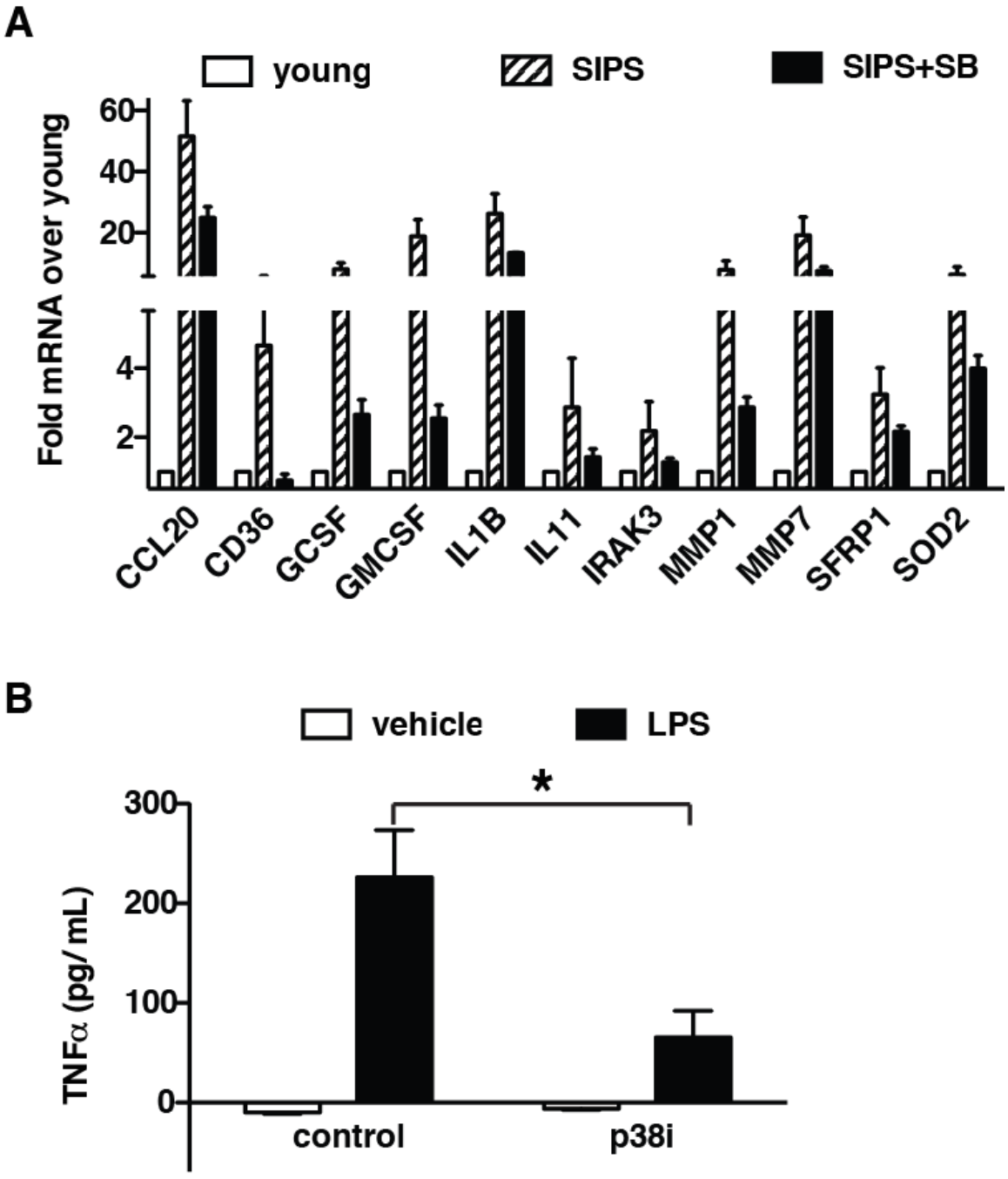

Supplemental Fig. 4.3: p38MAPK-dependent factors are expressed in the stromal compartment of breast cancer lesions A) A subset of p38MAPK-dependent SASP factors was validated by qRT-PCR in young, senescent or senescent fibroblasts treated with SB203580. Data represent mean + SD. B) Female NcR nude mice were given

control or p38i chow for 3 days prior to challenging with 100ng LPS. 1 hour post LPS injection, mice were sacrificed and serum was collected for analysis by TNFα ELISA. Data represent mean + SEM, n=3. * indicates $p \leq 0.05$. SIPS: stress-induced premature senescence.

REFERENCES

1. Finak G, Bertos N, Pepin F, Sadekova S, Souleimanova M, Zhao H, Chen H, Omeroglu G, Meterissian S, Omeroglu A, Hallett M, Park M. Stromal gene expression predicts clinical outcome in breast cancer. Nat Med. 2008;14(5):518-27.

2. Ma XJ, Dahiya S, Richardson E, Erlander M, Sgroi DC. Gene expression profiling of the tumor microenvironment during breast cancer progression. Breast Cancer Res. 2009;11(1):R7.

3. Karnoub AE, Dash AB, Vo AP, Sullivan A, Brooks MW, Bell GW, Richardson AL, Polyak K, Tubo R, Weinberg RA. Mesenchymal stem cells within tumour stroma promote breast cancer metastasis. Nature. 2007;449(7162):557-63. Epub 2007/10/05.

4. Olumi AF, Grossfeld GD, Hayward SW, Carroll PR, Tlsty TD, Cunha GR. Carcinoma-associated fibroblasts direct tumor progression of initiated human prostatic epithelium. Cancer research. 1999;59(19):5002-11.

5. Dimri GP, Lee X, Basile G, Acosta M, Scott G, Roskelley C, Medrano EE, Linskens M, Rubelj I, Pereira-Smith O, et al. A biomarker that identifies senescent human cells in culture and in aging skin in vivo. Proceedings of the National Academy of Sciences of the United States of America. 1995;92(20):9363-7.

6. Bavik C, Coleman I, Dean JP, Knudsen B, Plymate S, Nelson PS. The gene expression program of prostate fibroblast senescence modulates neoplastic epithelial cell proliferation through paracrine mechanisms. Cancer research. 2006;66(2):794-802.

7. Parrinello S, Coppe JP, Krtolica A, Campisi J. Stromal-epithelial interactions in aging and cancer: senescent fibroblasts alter epithelial cell differentiation. Journal of cell science. 2005;118(Pt 3):485-96.

8. Krtolica A, Parrinello S, Lockett S, Desprez PY, Campisi J. Senescent fibroblasts promote epithelial cell growth and tumorigenesis: a link between cancer and aging. Proceedings of the National Academy of Sciences of the United States of America. 2001;98(21):12072-7.

9. Coppe JP, Patil CK, Rodier F, Sun Y, Munoz DP, Goldstein J, Nelson PS, Desprez PY, Campisi J. Senescence-associated secretory phenotypes reveal cell-nonautonomous functions of oncogenic RAS and the p53 tumor suppressor. PLoS biology. 2008;6(12):2853-68.

10. Elkabets M, Gifford AM, Scheel C, Nilsson B, Reinhardt F, Bray MA, Carpenter AE, Jirstrom K, Magnusson K, Ebert BL, Ponten F, Weinberg RA, McAllister SS. Human tumors instigate granulin-expressing hematopoietic cells that promote malignancy by activating stromal fibroblasts in mice. The Journal of clinical investigation. 2011;121(2):784-99. Epub 2011/01/27.

11. Orimo A, Gupta PB, Sgroi DC, Arenzana-Seisdedos F, Delaunay T, Naeem R, Carey VJ, Richardson AL, Weinberg RA. Stromal fibroblasts present in invasive human breast carcinomas promote tumor growth and angiogenesis through elevated SDF-1/CXCL12 secretion. Cell. 2005;121(3):335-48.

12. Erez N, Truitt M, Olson P, Arron ST, Hanahan D. Cancer-Associated Fibroblasts Are Activated in Incipient Neoplasia to Orchestrate Tumor-Promoting Inflammation in an NF-kappaB-Dependent Manner. Cancer cell. 2010;17(2):135-47. Epub 2010/02/09.

13. Hu M, Polyak K. Microenvironmental regulation of cancer development. Current opinion in genetics & development. 2008;18(1):27-34. Epub 2008/02/20.

14. Allinen M, Beroukhim R, Cai L, Brennan C, Lahti-Domenici J, Huang H, Porter D, Hu M, Chin L, Richardson A, Schnitt S, Sellers wR, Polyak K. Molecular characterization of the tumor microenvironment in breast cancer. Cancer cell. 2004;6(1):17-32.

15. Pazolli E, Alspach E, Milczarek A, Prior J, Piwnica-Worms D, Stewart SA. Chromatin remodeling underlies the senescence-associated secretory phenotype of tumor stromal fibroblasts that supports cancer progression. Cancer research. 2012;72(9):2251-61. Epub 2012/03/17.

16. Rodier F, Coppe JP, Patil CK, Hoeijmakers WA, Munoz DP, Raza SR, Freund A, Campeau E, Davalos AR, Campisi J. Persistent DNA damage signalling triggers senescence-associated inflammatory cytokine secretion. Nature cell biology. 2009;11(8):973-9.

17. Kuilman T, Michaloglou C, Vredeveld LC, Douma S, van Doorn R, Desmet CJ, Aarden LA, Mooi WJ, Peeper DS. Oncogene-induced senescence relayed by an interleukin-dependent inflammatory network. Cell. 2008;133(6):1019-31.

18. Chien Y, Scuoppo C, Wang X, Fang X, Balgley B, Bolden JE, Premsrirut P, Luo W, Chicas A, Lee CS, Kogan SC, Lowe SW. Control of the senescence-associated

secretory phenotype by NF-kappaB promotes senescence and enhances chemosensitivity. Genes & development. 2011;25(20):2125-36. Epub 2011/10/08.

19. Freund A, Patil CK, Campisi J. p38MAPK is a novel DNA damage response-independent regulator of the senescence-associated secretory phenotype. Embo J.

20. Winzen R, Kracht M, Ritter B, Wilhelm A, Chen CY, Shyu AB, Muller M, Gaestel M, Resch K, Holtmann H. The p38 MAP kinase pathway signals for cytokine-induced mRNA stabilization via MAP kinase-activated protein kinase 2 and an AU-rich region-targeted mechanism. The EMBO journal. 1999;18(18):4969-80. Epub 1999/09/16.

21. Zhao W, Liu M, Kirkwood KL. p38alpha stabilizes interleukin-6 mRNA via multiple AU-rich elements. The Journal of biological chemistry. 2008;283(4):1778-85. Epub 2007/11/29.

22. Knapinska AM, Gratacos FM, Krause CD, Hernandez K, Jensen AG, Bradley JJ, Wu X, Pestka S, Brewer G. Chaperone Hsp27 modulates AUF1 proteolysis and AU-rich element-mediated mRNA degradation. Molecular and cellular biology. 2011;31(7):1419-31. Epub 2011/01/20.

23. Pazolli E, Luo X, Brehm S, Carbery K, Chung JJ, Prior JL, Doherty J, Demehri S, Salavaggione L, Piwnica-Worms D, Stewart SA. Senescent Stromal-Derived Osteopontin Promotes Preneoplastic Cell Growth. Cancer research. 2009.

24. Liu D, Hornsby PJ. Senescent human fibroblasts increase the early growth of xenograft tumors via matrix metalloproteinase secretion. Cancer research. 2007;67(7):3117-26.

25. Freund A, Patil CK, Campisi J. p38MAPK is a novel DNA damage response-independent regulator of the senescence-associated secretory phenotype. The EMBO journal. 2011;30(8):1536-48. Epub 2011/03/15.

26. Cuenda A, Rouse J, Doza YN, Meier R, Cohen P, Gallagher TF, Young PR, Lee JC. SB 203580 is a specific inhibitor of a MAP kinase homologue which is stimulated by cellular stresses and interleukin-1. FEBS letters. 1995;364(2):229-33. Epub 1995/05/08.

27. Guhaniyogi J, Brewer G. Regulation of mRNA stability in mammalian cells. Gene. 2001;265(1-2):11-23. Epub 2001/03/20.

28. Paschoud S, Dogar AM, Kuntz C, Grisoni-Neupert B, Richman L, Kuhn LC. Destabilization of interleukin-6 mRNA requires a putative RNA stem-loop structure, an AU-rich element, and the RNA-binding protein AUF1. Molecular and cellular biology. 2006;26(22):8228-41. Epub 2006/09/07.

29. Raineri I, Wegmueller D, Gross B, Certa U, Moroni C. Roles of AUF1 isoforms, HuR and BRF1 in ARE-dependent mRNA turnover studied by RNA interference. Nucleic acids research. 2004;32(4):1279-88. Epub 2004/02/21.

30. Sarkar S, Han J, Sinsimer KS, Liao B, Foster RL, Brewer G, Pestka S. RNA-binding protein AUF1 regulates lipopolysaccharide-induced IL10 expression by activating IkappaB kinase complex in monocytes. Molecular and cellular biology. 2011;31(4):602-15. Epub 2010/12/08.

31. Strieter RM, Burdick MD, Gomperts BN, Belperio JA, Keane MP. CXC chemokines in angiogenesis. Cytokine & growth factor reviews. 2005;16(6):593-609. Epub 2005/07/28.

32. Liu J, Zhang N, Li Q, Zhang W, Ke F, Leng Q, Wang H, Chen J, Wang H. Tumor-associated macrophages recruit CCR6+ regulatory T cells and promote the development of colorectal cancer via enhancing CCL20 production in mice. PloS one. 2011;6(4):e19495. Epub 2011/05/12.

33. Ernst M, Najdovska M, Grail D, Lundgren-May T, Buchert M, Tye H, Matthews VB, Armes J, Bhathal PS, Hughes NR, Marcusson EG, Karras JG, Na S, Sedgwick JD, Hertzog PJ, Jenkins BJ. STAT3 and STAT1 mediate IL-11-dependent and inflammation-associated gastric tumorigenesis in gp130 receptor mutant mice. The Journal of clinical investigation. 2008;118(5):1727-38. Epub 2008/04/24.

34. Apte RN, Dotan S, Elkabets M, White MR, Reich E, Carmi Y, Song X, Dvozkin T, Krelin Y, Voronov E. The involvement of IL-1 in tumorigenesis, tumor invasiveness, metastasis and tumor-host interactions. Cancer metastasis reviews. 2006;25(3):387-408. Epub 2006/10/18.

35. Uhlirova M, Bohmann D. JNK- and Fos-regulated Mmp1 expression cooperates with Ras to induce invasive tumors in Drosophila. The EMBO journal. 2006;25(22):5294-304. Epub 2006/11/04.

36. Cohen P. Protein kinases--the major drug targets of the twenty-first century? Nature reviews Drug discovery. 2002;1(4):309-15. Epub 2002/07/18.

37. Saklatvala J. The p38 MAP kinase pathway as a therapeutic target in inflammatory disease. Curr Opin Pharmacol. 2004;4(4):372-7. Epub 2004/07/15.

38. Burnette BL, Selness S, Devraj R, Jungbluth G, Kurumbail R, Stillwell L, Anderson G, Mnich S, Hirsch J, Compton R, De Ciechi P, Hope H, Hepperle M, Keith

RH, Naing W, Shieh H, Portanova J, Zhang Y, Zhang J, Leimgruber RM, Monahan J. SD0006: a potent, selective and orally available inhibitor of p38 kinase. Pharmacology. 2009;84(1):42-60. Epub 2009/07/11.

39. Coppe JP, Kauser K, Campisi J, Beausejour CM. Secretion of vascular endothelial growth factor by primary human fibroblasts at senescence. The Journal of biological chemistry. 2006;281(40):29568-74.

40. Gilbert LA, Hemann MT. DNA damage-mediated induction of a chemoresistant niche. Cell. 2010;143(3):355-66. Epub 2010/10/30.

41. Cahu J, Bustany S, Sola B. Senescence-associated secretory phenotype favors the emergence of cancer stem-like cells. Cell death & disease. 2012;3:e446. Epub 2012/12/21.

42. Coppe JP, Boysen M, Sun CH, Wong BJ, Kang MK, Park NH, Desprez PY, Campisi J, Krtolica A. A role for fibroblasts in mediating the effects of tobacco-induced epithelial cell growth and invasion. Molecular cancer research : MCR. 2008;6(7):1085-98.

43. Moss BL, Gross S, Gammon ST, Vinjamoori A, Piwnica-Worms D. Identification of a ligand-induced transient refractory period in nuclear factor-kappaB signaling. The Journal of biological chemistry. 2008;283(13):8687-98. Epub 2008/01/22.

44. Hahn WC, Counter CM, Lundberg AS, Beijersbergen RL, Brooks MW, Weinberg RA. Creation of human tumour cells with defined genetic elements. Nature. 1999;400(6743):464-8.

45. Beissbarth T, Speed TP. GOstat: find statistically overrepresented Gene Ontologies within a group of genes. Bioinformatics. 2004;20(9):1464-5. Epub 2004/02/14.

CHAPTER 5

Conclusions and future directions

The role the tumor microenvironment plays in tumor progression has become well established (1, 2). Indeed, the tumor-promoting cell types within the microenvironment have been identified and how these different cellular compartments impact tumorigenesis is beginning to be well understood (3-6). The identification of the mechanisms through which the microenvironment facilitates tumor growth and progression is important for the development of stroma-targeting therapies. Such therapies are critical for the treatment of cancer because not only do they provide another treatment avenue in addition to a direct assault on the cancer cells themselves, but also because the genetically "normal" nature of the microenvironment is hypothesized to produce less resistance to therapies than those geared towards the genetically unstable, easily mutagenized (and therefore resistance-generating) nature of cancer cells. Finally, there is growing evidence that the TME provides chemo-protective niches that shelter incipient tumor cells during chemotherapy (7). Thus, if we are to access these protective shelters therapies are needed that directly target the stromal niche.

The work outlined in the previous chapters has investigated how two types of tumor-promoting fibroblasts (senescent fibroblasts and CAFs) impact tumorigenesis. These tumor-promoting fibroblasts can impact every step in the tumorigenic process including tumor cell growth, angiogenesis, inflammatory cell recruitment, remodeling of the extra-cellular matrix and invasion (1, 8, 9). Expression array analyses revealed that these cell types are remarkably similar (10, 11) and in senescent fibroblasts this expression profile

has become known as the senescence-associated secretory phenotype or SASP (10). My work suggests that similar mechanisms may be responsible for expression of many pro-tumorigenic factors in these two cell types. Indeed, the work described herein has elucidated several novel regulatory pathways that govern SASP expression, and demonstrate that one such regulatory pathway is also involved in tumor-promotion by CAFs. This investigation has also yielded at least one therapeutic target capable of preventing tumor-promotion by both senescent fibroblasts and CAFs.

CONCLUSIONS

The regulation of gene expression occurs on multiple levels, spanning from transcriptional control, to mRNA stability and translational control to protein stability. The previous chapters describe our investigation of SASP factor regulation on multiple levels. We have found that treatment of fibroblasts with histone deacetylase complex (HDAC) inhibitors results in activation of a variety of SASP factors including IL6, IL8 and OPN (12). Furthermore, expression of a dominant-negative HDAC1 construct was sufficient to increase OPN expression (and to a lesser extent IL6 and IL8) in the absence of senescence (12). This effect was specific to HDAC1 because an HDAC3 dominant-negative construct was unable to recapitulate SASP activation (12). Our observations suggest a central role for chromatin modulation in SASP factor expression, as inhibition of chromatin-remodeling proteins result in SASP activation even in the absence of senescence induction (12).

Despite the coordinated nature of SASP factor expression, there are very few regulatory pathways identified to date that effect the expression of all SASP components. For example, our work and that of others has demonstrated that inflammatory SASP components are regulated by a pathway involving the DNA damage response protein ATM (12, 13) and transcriptional activation by NFκB (14, 15). Our work has elucidated an additional transcriptional regulatory mechanism that regulates the SASP factor OPN. OPN regulation is independent of ATM and NFκB activity (12). Through promoter analysis, we identified the transcription factor c-myb as an important initiator of OPN expression in response to senescence. Indeed, inhibition of c-myb activity through expression of either shRNA targeting c-myb or a c-myb dominant-negative construct prevents OPN expression in senescent cells. Furthermore, we have shown that c-myb directly binds the endogenous OPN promoter, and that mutagenesis of the c-myb binding site prevents OPN upregulation. These results identify c-myb as a novel regulator of SASP factor expression.

Our work has also identified a novel post-transcriptional regulatory pathway involved in the expression of SASP factors such as IL6, IL8 and GMCSF. We have found that post-transcriptional stabilization of SASP factor mRNAs occurs after the full establishment of cellular senescence. Stabilization of SASP transcripts involves the activation of p38MAPK, and subsequent removal of the RNA-destabilizing protein AUF1 from SASP 3' UTRs. Interestingly, p38MAPK is also involved in the transcriptional activation of SASP factors through regulation of NFκB. Our work has demonstrated that p38MAPK

switches from transcriptional regulation of SASP factors to post-transcriptional regulation of SASP factors, as inhibition of p38MAPK after the full induction of senescence has no effect on NFκB transcriptional activity yet significantly effects the stabilization of SASP mRNAs.

Elucidating the regulatory mechanisms that govern SASP factor expression is necessary for the development of stroma-targeting therapies. Our work has identified p38MAPK as a potential therapeutic target and represents the first time that SASP factors have been suppressed *in vivo* through the inhibition of an upstream regulator in order to prevent tumor growth. We have demonstrated that depletion of p38MAPK specifically in senescent fibroblasts results in decreased preneoplastic epithelial cell growth. Furthermore, p38MAPK represents an effective treatment strategy in a therapeutic setting, as orally administered p38MAPK inhibitors prevent further growth of already established, senescent fibroblast-driven tumors.

Finally, we have demonstrated that p38MAPK is a target in CAF-driven microenvironments. CAFs function analogously to senescent fibroblasts in tumor-promotion and have a very similar expression profile (1, 11). Indeed, our RNA-seq analysis has revealed that cancer-associated stromas express a large number of p38MAPK-dependent SASP factors. We investigated the efficacy of p38MAPK inhibition in CAF-driven tumorigenesis in xenograft experiments using preneoplastic epithelial cells and CAFs derived from invasive breast cancer patients. We observed that an orally

administered p38MAPK inhibitor is effective in preventing CAF-mediated epithelial cell growth similar to what we observed with senescent fibroblasts. These results indicate that p38MAPK is a therapeutic target that is effective in a variety of tumor-promoting microenvironments. Furthermore, we have demonstrated that a regulatory pathway that controls the expression of pro-tumorigenic factors in senescent cells is also operative in CAFs.

FUTURE DIRECTIONS

p38MAPK regulates SASP factor expression both transcriptionally through its involvement in NFκB activation (14) and post-transcriptionally by regulating the occupancy of AUF1 on SASP factor mRNAs. These different regulatory roles are temporally separate. Depletion of p38MAPK during the transcriptional phase of SASP factor expression has no effect on SASP mRNA stability, while inhibition of p38MAPK during the post-transcriptional phase of SASP factor expression has no effect on NFκB-driven transcription. What regulates these separate functions of p38MAPK remains to be elucidated. One hypothesis is that changes in p38MAPK sub-cellular localization govern its separate functions, with transcriptional activation taking place in the nucleus and mRNA stabilization taking place in the cytoplasm. Preliminary investigations using immunofluorescence to track p38MAPK localization, however, have given inconclusive results. Given that the time point at which p38MAPK transitions from transcriptional to post-transcriptional regulation is not thoroughly established it may be necessary to investigate changes in p38MAPK localization through live-cell imaging.

We have demonstrated that p38MAPK is an effective therapeutic target in both senescent fibroblast and CAF-driven microenvironments. Our xenograft experiments used a prostate preneoplastic cell line. Future experiments are aimed at utilizing patient-derived cancer cells in order to more thoroughly establish the applicability of p38MAPK inhibition in a patient setting. To this end, we have acquired triple negative patient-derived cancer cells (TNBC) from breast cancer patients that have been expanded and carried exclusively in mice to maintain genetic similarity to the parent tumor. Indeed, expression analysis and genotypic analysis of these cells indicate that they retain their patient characteristics after many passages in the mouse. These patient-derived cancer cells will be used in xenograft experiments with both senescent fibroblasts and CAFs. It is also of interest to investigate p38MAPK inhibition in the context of genetic mouse models of a variety of cancer types, which would help to establish the efficacy of p38MPAK inhibition in an immune competent and spontaneous tumor setting, as well as investigate p38MAPK's role in a variety of tissues. All of these experiments would aid in the generation of preclinical data for the ultimate movement of p38MAPK inhibitors to clinical trials for the treatment of human disease.

REFERENCES

1. Olumi AF, Grossfeld GD, Hayward SW, Carroll PR, Tlsty TD, Cunha GR. Carcinoma-associated fibroblasts direct tumor progression of initiated human prostatic epithelium. Cancer research. 1999;59:5002-11.

2. Kuperwasser C, Chavarria T, Wu M, Magrane G, Gray JW, Carey L, et al. Reconstruction of functionally normal and malignant human breast tissues in mice. Proceedings of the National Academy of Sciences of the United States of America. 2004;101:4966-71.

3. Hanahan D, Folkman J. Patterns and emerging mechanisms of the angiogenic switch during tumorigenesis. Cell. 1996;86:353-64.

4. Ruffell B, Affara NI, Coussens LM. Differential macrophage programming in the tumor microenvironment. Trends in immunology. 2012;33:119-26.

5. Orimo A, Gupta PB, Sgroi DC, Arenzana-Seisdedos F, Delaunay T, Naeem R, et al. Stromal fibroblasts present in invasive human breast carcinomas promote tumor growth and angiogenesis through elevated SDF-1/CXCL12 secretion. Cell. 2005;121:335-48.

6. Sato T, Sakai T, Noguchi Y, Takita M, Hirakawa S, Ito A. Tumor-stromal cell contact promotes invasion of human uterine cervical carcinoma cells by augmenting the expression and activation of stromal matrix metalloproteinases. Gynecologic oncology. 2004;92:47-56.

7. Gilbert LA, Hemann MT. DNA damage-mediated induction of a chemoresistant niche. Cell. 2010;143:355-66.

8. Bavik C, Coleman I, Dean JP, Knudsen B, Plymate S, Nelson PS. The gene expression program of prostate fibroblast senescence modulates neoplastic epithelial cell proliferation through paracrine mechanisms. Cancer research. 2006;66:794-802.

9. Coppe JP, Kauser K, Campisi J, Beausejour CM. Secretion of vascular endothelial growth factor by primary human fibroblasts at senescence. The Journal of biological chemistry. 2006;281:29568-74.

10. Coppe JP, Patil CK, Rodier F, Sun Y, Munoz DP, Goldstein J, et al. Senescence-associated secretory phenotypes reveal cell-nonautonomous functions of oncogenic RAS and the p53 tumor suppressor. PLoS biology. 2008;6:2853-68.

11. Finak G, Bertos N, Pepin F, Sadekova S, Souleimanova M, Zhao H, et al. Stromal gene expression predicts clinical outcome in breast cancer. Nat Med. 2008;14:518-27.

12. Pazolli E, Alspach E, Milczarek A, Prior J, Piwnica-Worms D, Stewart SA. Chromatin remodeling underlies the senescence-associated secretory phenotype of tumor stromal fibroblasts that supports cancer progression. Cancer research. 2012;72:2251-61.

13. Rodier F, Coppe JP, Patil CK, Hoeijmakers WA, Munoz DP, Raza SR, et al. Persistent DNA damage signalling triggers senescence-associated inflammatory cytokine secretion. Nature cell biology. 2009;11:973-9.

14. Freund A, Patil CK, Campisi J. p38MAPK is a novel DNA damage response-independent regulator of the senescence-associated secretory phenotype. The EMBO journal. 2011;30:1536-48.

15. Chien Y, Scuoppo C, Wang X, Fang X, Balgley B, Bolden JE, et al. Control of the senescence-associated secretory phenotype by NF-kappaB promotes senescence and enhances chemosensitivity. Genes & development. 2011;25:2125-36.

APPENDIX 1

The small heat shock protein Hsp27 regulates SASP mRNA stability

INTRODUCTION

As shown in the previous chapter, the RNA-destabilizing protein AUF1 post-transcriptionally regulates the stability of senescence-associated secretory phenotype (SASP) factor mRNAs. We have shown that AUF1 binds to SASP factor transcripts prior to senescence induction, resulting in low SASP mRNA stability. After senescence is fully established and in response to activation of p38MAPK, AUF1 is removed from SASP mRNAs, resulting in increased mRNA stability. It is not known how AUF1 is removed from SASP factor transcripts. It is also not clear how p38MAPK results in changes in AUF1 occupancy because AUF1 is not a known target for phosphorylation by p38MAPK (1, 2).

One of p38MAPK's down-stream targets is the small heat-shock protein Hsp27. In addition to its activities as a heat-shock protein, Hsp27 plays a role in mRNA stability in response to activation by p38MAPK. Indeed, depletion of Hsp27 results in the stabilization of mRNAs containing AU-rich 3' UTRs (3). Intriguingly, Hsp27 is part of some AUF1-containing complexes, and activation of Hsp27 through p38MAPK-mediated phosphorylation results in proteolytic decay of AUF1 (1, 3). This work from other laboratories led to the hypothesis that Hsp27 was responsible for mediating AUF1 removal from SASP mRNAs in response to p38MAPK activation.

METHODS

Cells and reagents

BJ skin fibroblasts were grown under standard culture conditions in DMEM supplemented with 15% FBS, 15% M199 and penicillin/streptomycin. Fibroblasts were treated with bleomycin sulfate (100μg/mL, Sigma) as previously described (4). Fibroblasts were treated with actinomycin D (10μg/mL, Sigma) and for 24 hours. RNA was isolated using the Tri Reagent (Life Technologies) at the time points indicated. Short hairpin RNA sequences in the pLKO.1 backbone were obtained from the Children's Discovery Institute's viral-vector-based RNAi core at Washington University in St. Louis. The FLAG-tagged Hsp27 phosphomimetic (Hsp27 TriD) was a gift from Dr. Gary Brewer (1), and was subcloned into pBABE-hygro.

Virus production

Virus was produced as described previously (5).

Western blot analysis

Cells were lysed in 50mM Tris pH 8.0, 5mM EDTA, 0.5% NP40 and 100mM sodium chloride for 20 minutes at 4°C. Primary antibodies used were mouse-anti-human Hsp27 (catalog number 2402, Cell Signaling) and mouse-anti-FLAG (catalog number F1804, Sigma Aldrich).

cDNA synthesis and quantitative real-time PCR (qRT-PCR)

cDNA synthesis and quantitative PCR was performed using previously published protocols and manufacturer's instructions (6) (SYBR Green, Life Technologies, Carlsbad, CA). Primers for GAPDH (F: 5'-GCATGGCCTTCGGTGTCC-3', R: 5'-

AATGCCAGCCCCAGCGTCAAA-3'), IL6 (F: 5'-ACATCCTCGACGGCATCTCA-3', R: 5'-TCACCAGGCAAGTCTCCTCA-3'), and IL8 (F: 5'-GCTCTGTGTGAAGGTGCAGT-3', R: 5'-TGCACCCAGTTTTCCTTGGG-3') were purchased from IDT.

RNA-binding protein immunoprecipitation (RIP)

RIP was performed as described in **CHAPTER 4**. The primary antibody used for Hsp27 immunoprecipitation was mouse-anti-human Hsp27 (catalog number 2402, Cell Signaling).

NOTE: These experiments have been repeated with the first TriD cell line generated. Subsequent generation of Hsp27-TriD cells did not recapitulate the phenotypes

RESULTS

Hsp27 depletion increases SASP mRNA stability

As mentioned previously, Hsp27 is an RNA-destabilizing factor (3). To investigate if Hsp27 destabilizes SASP factors, BJ fibroblasts were stably transduced with an shRNA targeting Hsp27 or a control shRNA (shSCR). Hsp27 depletion was assessed by western blot analysis (**Fig A1A**). Hsp27-depleated cells were treated with actinomycin D (ActD) 24 hours after treatment with bleomycin, a time point when SASP factors are unstable. We observed increased IL6 and IL8 factor mRNA stability in cells expressing shRNA compared to cells expressing shSCR (**Fig A1B**), indicating that the presence of Hsp27 destabilizes SASP factors at this time point. Given the similarities between Hsp27 and AUF1 depletion in cells 24 hours-post bleomycin treatment (**Fig A1B and**

Fig 4.3C respectively), these observations suggest that AUF1 and Hsp27 cooperate in destabilizing SASP mRNAs prior to senescence induction.

Phosphorylation of Hsp27 by p38MAPK increases SASP mRNA stability

A previous report indicated that phosphorylation of Hsp27 by p38MAPK results in stabilization of Hsp27 target mRNAs and reduces the affinity of Hsp27 for its targets (1). Our previous work demonstrated that p38MAPK promotes stabilization of SASP factor mRNAs through modulating the occupancy of AUF1 (**CHAPTER 4**), yet AUF1 is not a known target of p38MAPK (2). Therefore, we next investigated if p38MAPK's mRNA-stabilization activities were mediated through Hsp27. To do so, we obtained a phosphomimetic mutant of Hsp27 on all residues phosphorylated by p38MAPK (Hsp27-TriD) (1). BJ fibroblasts were stably transduced with Hsp27-TriD or a vector control (**Fig A1C**) and the mRNA stability of SASP factors was measured by treating the cells with ActD 24 hours-post bleomycin treatment, a time point at which SASP mRNAs are unstable (**CHAPTER 4**). We observed a significant increase in IL6 and IL8 mRNA stability in response to expression of constitutively phosphorylated Hsp27 compared to the mRNA stability observed in vector control cells (**Fig A1D**). This data indicates that phosphorylation of Hsp27 by p38MAPK results in stabilization of SASP transcripts and further implicates Hsp27 in the previously reported p38MAPK-AUF1 post-transcriptional regulatory mechanism that controls SASP expression.

Hsp27 binds to SASP factor mRNAs

To further support our hypothesis that Hsp27 mediates p38MAPK's regulation of AUF1 occupancy on SASP mRNAs, we investigated Hsp27's occupancy on SASP transcripts. To do so, we performed RNA immunoprecipitation (RIP) using an antibody specific to Hsp27 or an IgG control, and qRT-PCR was used to determine the level of IL6 and IL8 in the immunoprecipitations. RIP was performed in cells 24 hours-post bleomycin treatment, a time point at which SASP mRNAs display reduced stability, and in cells 96 hours-post bleomycin treatment, a time point at which SASP mRNAs display increased stability (discussed in **CHAPTER 4**). We observed significantly less Hsp27 binding to SASP factor mRNAs 96 hours-post bleomycin treatment compared to the level observed in cells 24 hours-post bleomycin treatment (**Fig A1E**). These results are strikingly similar to those observed for AUF1 occupancy (**Fig 4.3B**)**,** further suggesting that AUF1 and Hsp27 bind SASP mRNAs in a complex to regulate their stability.

DISCUSSION

Our work described in **CHAPTER 4** identified a post-transcriptional regulatory mechanism responsible for sustaining SASP expression that involves activation of p38MAPK and subsequent removal of the RNA-destabilizing protein AUF1 from SASP transcripts. Given that AUF1 is not a known target of p38MAPK (2), it remained unclear how p38MAPK was governing AUF1 binding capacity. The work described here suggests that p38MAPK activity is mediated through its downstream target Hsp27. We have demonstrated that depletion of Hsp27 phenocopies the effects of AUF1 depletion,

resulting in enhanced SASP mRNA stability prior to the induction of senescence (compare **Fig A1B** and **Fig 4.3C**). Furthermore, expression of an Hsp27 phosphomimetic construct at all residues known to be phosphorylated by p38MAPK results in SASP mRNA stabilization, indicating that p38MAPK activation inhibits the SASP mRNA destabilization mediated by Hsp27. Finally, RIP analysis of Hsp27 occupancy on SASP factor transcripts before and after the induction of senescence demonstrates that Hsp27 is removed from SASP transcripts after senescence is established. These results also phenocopy those seen in AUF1 RIP analysis (compare **Fig A1E** and **Fig 4.3B**). Taken together, or results from **CHAPTER 4** and **APPENDIX 1** suggest a model where SASP mRNAs are bound by AUF1 and Hsp27, resulting in their destabilization. After activation of p38MAPK in response to senescence induction, phosphorylation of Hsp27 results in the removal of Hsp27 and AUF1 from SASP mRNA and the subsequent stabilization of SASP transcripts (**Fig A1F**). Future work in the laboratory will focus on elucidating whether AUF1 occupancy on SASP mRNA depends on the phosphorylation status of Hsp27.

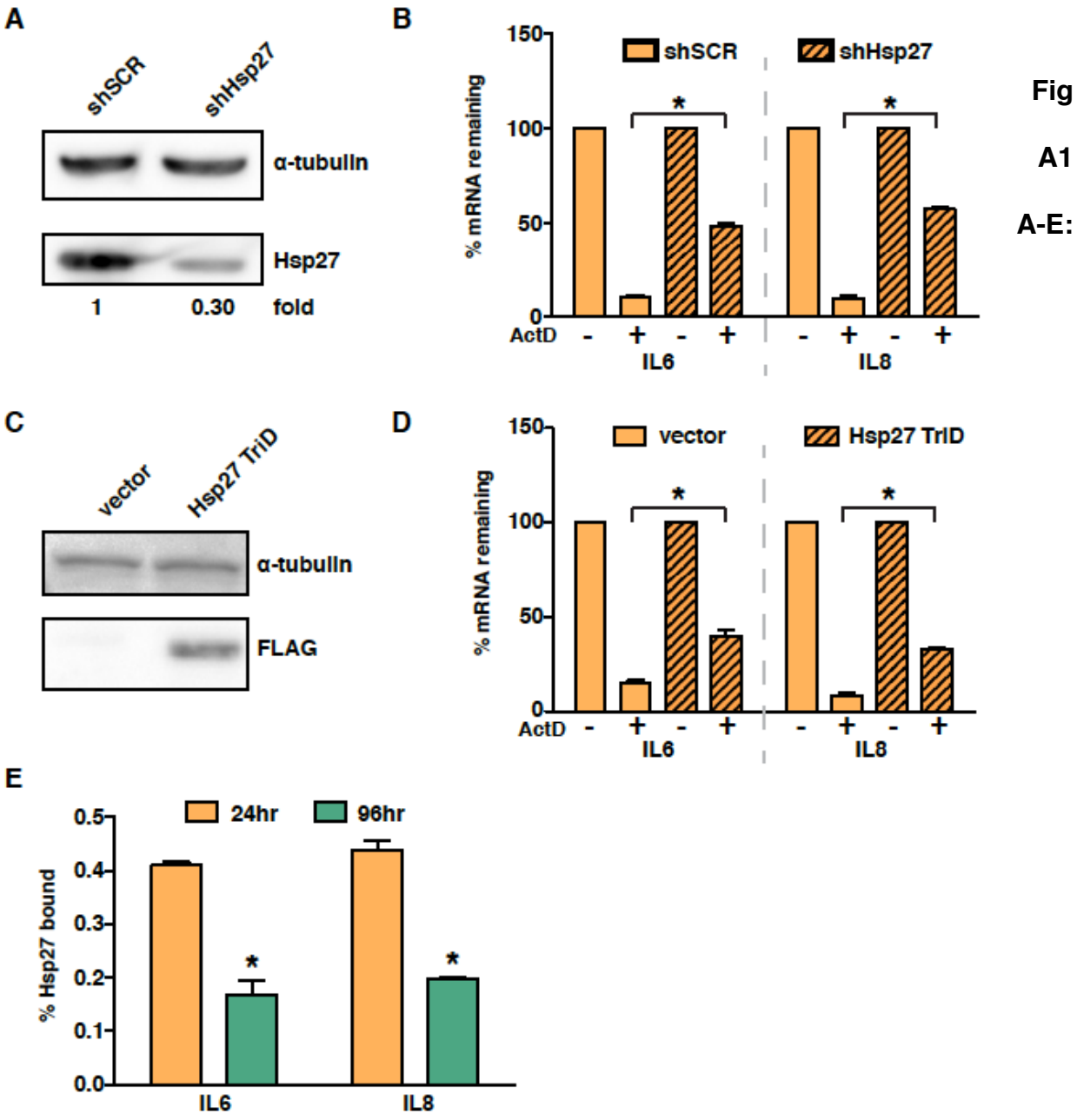

Fig A1 A-E:

Hsp27 regulates SASP mRNA stability. A) Western blot analysis to confirm depletion of Hsp27 in BJ fibroblasts transduced with shHsp27 or control hairpin (shSCR). B) BJ fibroblasts expressing either shHsp27 or shSCR were treated with ActD or vehicle control 24 hours-post treatment with bleomycin. qRT-PCR was used to measure the mRNA stability of IL6 and IL8. Representative experiment, n=3. C) Western blot

analysis to detect expression of FLAG- tagged Hsp27-TriD in stably transfected BJ fibroblasts. D) BJ fibroblasts expressing either vector control or Hsp27-TriD were treated with ActD or vehicle control 24 hours-post treatment with bleomycin. qRT-PCR was used to measure the mRNA stability of IL6 and IL8. Representative experiment, n=3. E) RIP analysis was performed for Hsp27 occupancy on IL6 and IL8 mRNA either 24 or 96 hours-post treatment with bleomycin. Representative experiment, n=2.

Data represents mean + SD. * indicates $p<0.05$.

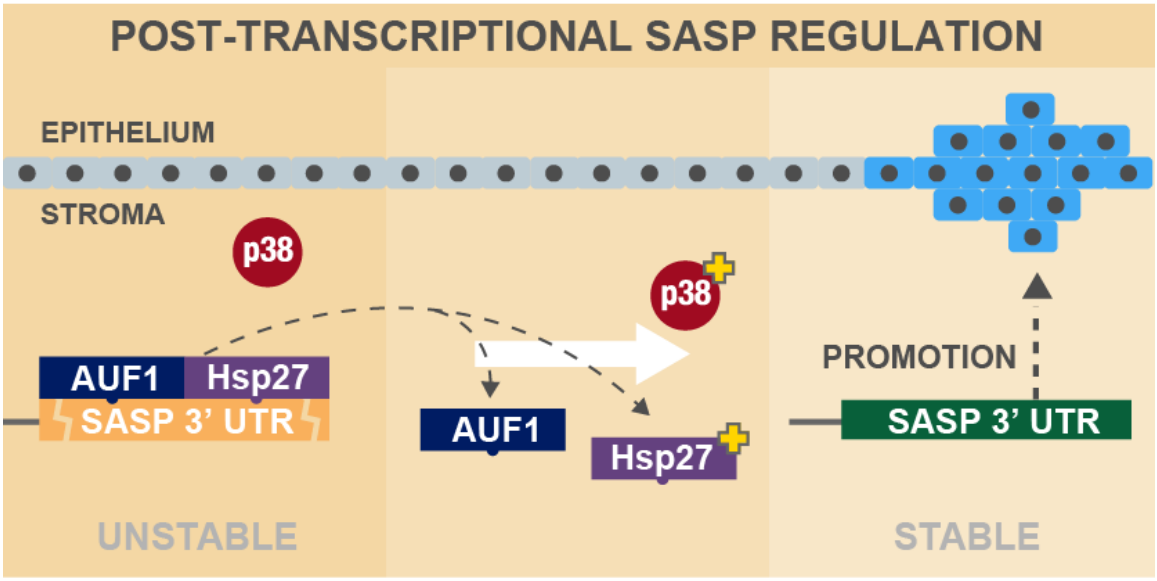

Fig A1F: Model of post-transcriptional SASP regulation. Prior to senescence induction, SASP mRNA are bound by AUF1 and Hsp27, resulting in their destabilization. In response to senescence and p38MAPK activation, Hsp27 is phosphorylated resulting in the release of both AUF1 and Hsp27 from SASP transcripts. This leads to SASP mRNA stabilization.

REFERENCES

1. Knapinska AM, Gratacos FM, Krause CD, Hernandez K, Jensen AG, Bradley JJ, Wu X, Pestka S, Brewer G. Chaperone Hsp27 modulates AUF1 proteolysis and AU-rich element-mediated mRNA degradation. Molecular and cellular biology. 2011;31(7):1419-31. Epub 2011/01/20.

2. Gratacos FM, Brewer G. The role of AUF1 in regulated mRNA decay. Wiley interdisciplinary reviews RNA. 2010;1(3):457-73. Epub 2011/10/01.

3. Sinsimer KS, Gratacos FM, Knapinska AM, Lu J, Krause CD, Wierzbowski AV, Maher LR, Scrudato S, Rivera YM, Gupta S, Turrin DK, De La Cruz MP, Pestka S, Brewer G. Chaperone Hsp27, a novel subunit of AUF1 protein complexes, functions in AU-rich element-mediated mRNA decay. Molecular and cellular biology. 2008;28(17):5223-37. Epub 2008/06/25.

4. Pazolli E, Alspach E, Milczarek A, Prior J, Piwnica-Worms D, Stewart SA. Chromatin remodeling underlies the senescence-associated secretory phenotype of tumor stromal fibroblasts that supports cancer progression. Cancer research. 2012;72(9):2251-61. Epub 2012/03/17.

5. Pazolli E, Luo X, Brehm S, Carbery K, Chung JJ, Prior JL, Doherty J, Demehri S, Salavaggione L, Piwnica-Worms D, Stewart SA. Senescent Stromal-Derived Osteopontin Promotes Preneoplastic Cell Growth. Cancer research. 2009.

6. Coppe JP, Boysen M, Sun CH, Wong BJ, Kang MK, Park NH, Desprez PY, Campisi J, Krtolica A. A role for fibroblasts in mediating the effects of tobacco-induced

epithelial cell growth and invasion. Molecular cancer research : MCR. 2008;6(7):1085-98.